Investigation of the therapeutic potential of the neuroprotective prion protein N1-fragment in cellular and mouse models of Alzheimer`s and prion disease

Dissertation zur Erlangung der Würde des Doktors der Naturwissenschaften der
Fakultät für Mathematik, Informatik und Naturwissenschaften
Fachbereich Biologie
der Universität Hamburg

Dissertation with the aim of achieving a doctoral degree at the Faculty of
Mathematics, Informatics and Natural Sciences
Department of Biology
University of Hamburg

Submitted by Behnam Mohammadi

Hamburg, 2019

Eidesstattliche Versicherung
Declaration on oath

Hiermit erkläre ich an Eides statt, dass ich die vorliegende Dissertationsschrift selbst verfasst und keine anderen als die angegebenen Quellen und Hilfsmittel benutzt habe.

I hereby declare, on oath, that I have written the present dissertation by my own and have not used other than the acknowledged resources and aids.

Hamburg, den
28.11.2019

Unterschrift

Behnam Mohammadi

Contents

iv

1 Introduction

1.1 Biology of the cellular prion protein (PrP^C)

1.1.1 The *Prnp* gene and its expression pattern

The human *Prnp* gene encodes for a prion protein containing 253 amino acids (aa) and is located on the short arm of chromosome 20. *Prnp* is a member of the *Prn* gene family that also includes *Prnd*, encoding the protein Doppel (Moore et al. 1999), and *Sprn*, encoding the protein Shadoo. Both proteins share some structural similarities with PrP^C (Schätzl et al. 1995; Watts and Westaway 2007).

Although in various species the *Prnp* gene comprises two to three exons, the PrP open reading frame itself is always encoded within a single exon (Basler et al. 1986; Gabriel et al. 1992; Hsiao et al. 1989; Westaway et al. 1987). The other exons contain non-coding sequences including the promoter and the transcription initiation site. The *Prnp* promoter is driving constitutive expression of PrP^C in many different tissues, with the highest levels being found in the central (CNS) and peripheral nervous system (PNS). In the CNS, expression of this gene is limited not only to neurons but is also present in astrocytes (Hartmann, Martins, and Lima 2013; Lima et al. 2007), in oligodendrocytes (Bribián et al. 2012; Moser et al. 1995), and in microglia (Adle-Biassette et al. 2006).

An alignment of the *Prnp* gene sequence of more than 40 various species shows that *Prnp* is remarkably conserved in vertebrates, indicating the evolutionary importance of PrP^C (Bendheim et al. 1992; Prusiner 2004).

In people with genetic/familial forms of prion disease, such as familial Creutzfeldt-Jakob disease (fCJD), Gerstmann-Sträussler-Scheinker (GSS) syndrome, and fatal familial insomnia (FFI), more than 30 mutations in the *Prnp* gene have been identified. Indeed, *Prnp* was established as the only causative gene for different prion diseases (reviewed in Takada et al., 2016). Importantly, some of these mutations may alter the structure of the prion protein (PrP) and favor misfolding into an abnormally shaped pathogenic isoform, known as PrP^{Sc}. Among those, the codon 129

polymorphism (M129V, rs1799990) is the most relevant genotypic variant, which is a recognized genetic marker for susceptibility to human prion diseases (Goldfarb et al. 1992).

1.1.2 Biogenesis, trafficking, localization, and structure of PrP^C

The PrP^C mRNA is initially translated by free ribosomes in the cytosol. The first 23 aa act as the N-terminal signal peptide which, once synthesized, is recognized and bound by signal recognition particles of the rough endoplasmic reticulum (ER). After binding to this receptor at the ER, protein synthesis continues and the PrP polypeptide chain translocates into the ER where the posttranslational modifications of immature PrP starts by addition of up to two N-linked glycans (at the Asn-181 and Asn-197 of human PrP) in its C-terminal region, attachment of a C-terminal glycosylphosphatidylinositol (GPI) anchor and proper folding of the protein before transport to the Golgi apparatus. Then PrP continues along the secretory pathway (Haraguchi et al. 1989; Stahl et al. 1987; TURK et al. 1988). Like other secretory proteins, before reaching the plasma membrane, PrP^C is subjected to different quality control steps to ensure its correct folding and posttranslational modifications. In case of a misfolded state, it may get retrotranslocated out of the ER into the cytosol, where it is degraded by proteasomes (Ma and Lindquist 2001; Yedidia et al. 2001).

After PrP^C transits to the cell surface, it is bound to the cell membrane via its GPI anchor. At the cell surface, the majority of PrP^C is found in detergent-resistant regions called lipid rafts (Gorodinsky and Harris 1995; Naslavsky et al. 1997; Vey et al. 1996). However, labeling of surface PrP^C molecules showed that not all PrP^C molecules remain on the cell surface (Shyng, Huber, and Harris 1993) but rather that a relevant fraction of all PrP^C molecules constitutively cycles between the plasma membrane and endocytic compartments. Indeed, endocytosis may have a large impact on the physiological functions of PrP^C (see 2.1.3). In this regard, clathrin-coated pits and vesicles have been shown to be the primary structures responsible for the endocytosis of PrP^C (Lainé et al. 2001; Shyng, Heuser, and Harris 1994). After its internalization via coated pits, PrP^C can be found associated with the transferrin receptor, indicating that it can recycle back to the cell surface by recycling endosomes (D'Souza-Schorey et al. 1998; Ghosh et al. 1998). PrP^C can also be alternatively endocytosed via the caveolin-mediated endocytic pathway. Caveolar vesicles containing endocytosed PrP^C do not contact compartments containing transferrin receptors, may originate from lipid rafts and are delivered to late endosomal/lysosomal compartments via endosomes (Madore 2002; Sunyach et al. 2003).

The mature cellular form of the prion protein is composed of a flexible and unstructured N-terminal half (aa 23-110) and a globular C-terminal domain that contains three α-helices, two short antiparallel β-sheets, and interconnecting loops (Cohen et al. 1994; Haire et al. 2004; Riek et al. 1996). In mammals, depending on the species, the N-terminus has a variable number of octapeptide repeats. Each octarepeat is able to bind divalent metals such as copper or zinc. Some of the suggested physiological functions of PrP^C have been related to its metal binding features (Millhauser 2007). There is also a disulfide bond between residues 179 and 214 (Zahn et al. 2000). In addition, PrP^C contains two N-glycosylation sites at residues 181 and 197 which are variably occupied. This results in three different glycoforms corresponding to un-, mono-, and diglycosylated PrP^C which are usually all found to varying degrees in a given biological sample (Williams, Stadtman, and Moskovitz 2004).
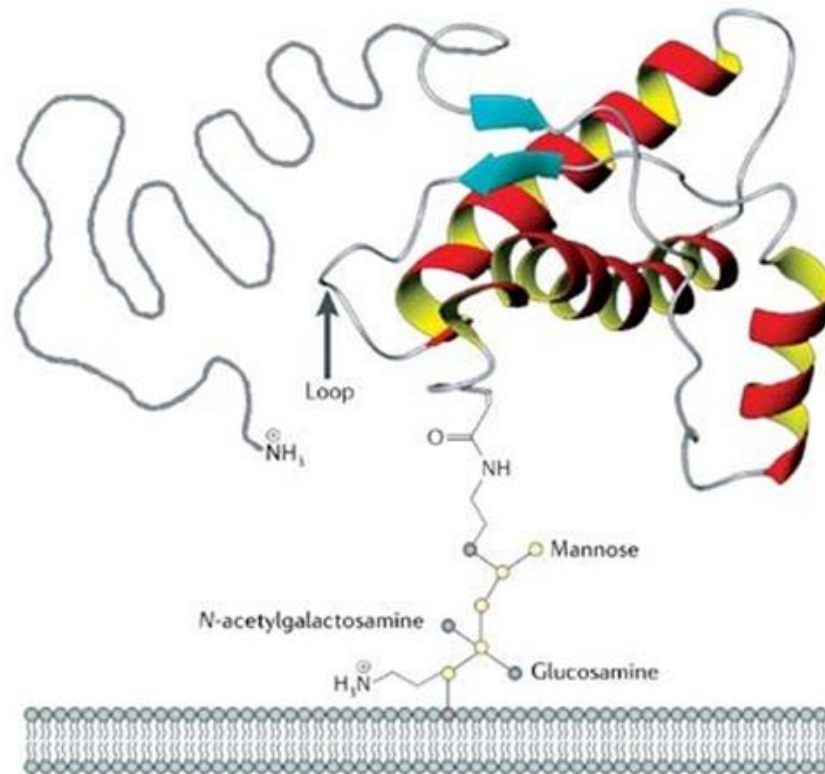

Figure 1: A schematic outline of the structure of the cellular prion protein including the 'unstructured' N-terminal half (grey) and the glycosylphosphatidylinositol (GPI) anchor. The loop connecting the second β-sheet and the third α-helix is indicated by the black arrow octarepeat region. Taken from (Aguzzi and Heikenwalder 2006).

1.1.3 A multitude of physiological functions suggested for PrP^C

In order to study the physiological roles of PrP^C, different *Prnp* knockout mouse lines (and knockouts in other species) have been generated, such as the mice models of Zurich I (Büeler et al. 1992) or the models of Edinburgh, also known as Npu (Manson et al. 1994). Surprisingly these mice develop and breed normally and do not have major abnormalities except for their absolute resistance to prion infection. Although they display subtle alterations in behavior and present with a peripheral neuropathy at late age, their normal appearance seems either to rule out that any physiological function for PrP^C is essential for life or gives the impression that it is redundant (Büeler et al. 1992); (Manson et al. 1994); (Bueler et al. 1993).

Despite many years of research investigating the physiological function of PrP^C in various cellular and animal models, the exact biological role of the protein still remains unclear. Several studies have suggested roles for PrP^C in numerous processes. Some of the potential functions are briefly described below:

Stress-protection: Several studies suggested a PrP^C-mediated protection of cells in serum-free conditions (Kim et al. 2004; Kuwahara et al. 1999; Wu et al. 2008), against staursporine-induced apoptosis (Lopes et al. 2005; Zanata et al. 2002), and in other conditions of oxidative stress, such as in the presence of high levels of reactive oxygen species (ROS) (W Rachidi et al. 2003; Zeng et al. 2003).Moreover, PrP^C expression in primary neurons, astrocytes, and cell lines has been associated with lower levels of damage following exposure to various oxidative toxins (Anantharam et al. 2008; Bertuchi et al. 2012; Brown et al. 1997; Dupiereux et al. 2008). A possible mechanism is that PrP^C modulates the activity of the antioxidant enzymes that convert ROS into less toxic products. PrP^C has also been implicated in the response to ER stress, which is caused by an accumulation of unfolded/misfolded proteins within the ER (Halliday and Mallucci 2014). The involvement of PrP^C in the cellular response to oxidative stress could explain the putative protective effect of PrP^C expression following stroke which results in reduced infarct volume (Shyu et al. 2005; Spudich et al. 2005; Weise et al. 2004, 2006).

Neurite outgrowth: Potential explanations for this suggested role include interactions of PrP^C with STI1 (Lopes et al. 2005), neural cell adhesion molecule 1 (NCAM1) (Santuccione et al. 2005), epidermal growth factor receptors (Llorens et al. 2013), integrins (Loubet et al. 2012), laminin (Graner et al. 2000), and metabotropic glutamate receptors (mGluRs) (Beraldo et al. 2011). The

proposed mechanism is that PrP^C prevents these partners from inhibiting the RhoA branch (ras homolog gene family, member A) of the ROCK pathway (Rho-associated protein kinase) (Loubet et al. 2012), consequently permitting RhoA's activation. The latter then stabilizes the actin cytoskeleton, which in turn develops neurites (O'Connor, Duerr, and Bentley 1990). Activation of the extracellular signal-regulated kinases 1 and 2 (ERK1/2), Akt, and protein kinase C (PKC) signaling pathways may also be involved in mediating PrP^C-dependent neurite outgrowth (Beraldo et al. 2011; Caetano et al. 2008; Llorens et al. 2013; Lopes et al. 2005).

Metal ion homeostasis: Among the more widely accepted functions of PrP^C is its role in the cellular homeostasis of divalent metal ions such as copper and zinc, which bind to the octapeptide repeat region of cell-surface PrP^C. This interaction has been implicated not only in the maintenance of the cellular Cu^{2+} homeostasis (Brown et al. 1997; Hornshaw, McDermott, Candy, et al. 1995; Hornshaw, McDermott, and Candy 1995), but also in the regulation of NMDA receptor activity (Gasperini et al. 2014), astrocytic glutamate uptake (Brown and Mohn 1999), as well as protection against oxidative stress (Walid Rachidi et al. 2003; Watt et al. 2007).

Roles in the immune system: Although prion diseases are primarily neurodegenerative disorders, there is also considerable interest in understanding the physiological functions of PrP^C in the immune system, since. PrP^C is highly expressed in different immune cells, including T-lymphocytes, natural killer cells, macrophages, and mast cells (Durig et al. 2000; Haddon et al. 2009). PrP^C has also been suggested to be involved in inflammatory responses (Haddon et al. 2009) and in regulating immunological quiescence (Bakkebo et al. 2015).

Myelin maintenance: It was previously shown that neuron-specific re-expression of PrP^C was sufficient to rescue the demyelination phenotype observed in aged Prnp0/0 mice (Bremer et al. 2010). More recent work from Aguzzi`s group on their new co-isogenic PrP-KO mice rather question all the other suggested functions, but the role in myelin maintenance seems to hold true. They have shown that PrP^C promotes myelin maintenance through an interaction between its extreme N-terminal region (residues 23–33) and the G-protein coupled receptor 126 (GPR126) on the surface of Schwann cells in the PNS (Küffer et al. 2016). However, the molecular mechanisms by which PrP^C affects myelin integrity need to be determined conclusively. It is conceivable, that the proteolytically released N-terminal part of PrP^C (termed N1 fragment.) is responsible for this effect.

1.2 Pathological conditions associated with the prion protein

1.2.1 Prion diseases are fatal and transmissible encephalopathies

1.2.1.1 Overview

Prion diseases, also known as transmissible spongiform encephalopathies (TSEs), are a group of rather rare, progressive, and fatal neurodegenerative disorders affecting a wide range of mammals, including Creutzfeldt-Jakob disease (CJD), fatal familial insomnia (FFI), Gerstmann-Sträussler-Scheinker (GSS) syndrome, and Kuru in humans, Scrapie in sheep and goats, bovine spongiform encephalopathy (BSE) in cattle, and chronic wasting disease (CWD) in cervids. Although the clinical symptoms vary among the different prion diseases, there are some similarities in the characteristic neuropathological hallmarks of brain damage between all of them including significant neuronal loss, widespread spongiform degeneration of the brain parenchyma, synaptic alterations, atypical brain inflammation, and the accumulation of prion aggregates (Budka 2003; Imran and Mahmood 2011b, 2011a). Prion diseases have different causes: (i) they can have sporadic/idiopathic origin, which accounts for most cases in humans or (ii) they can be due to a genetic mutation in the *Prnp* gene that destabilizes the physiological structure and tends to misfold the protein (genetic/familial cases). In addition, (iii) transmission of the disease can occur through exposure to the infectious agent (i.e. the "prion"), for instance by consuming contaminated meat products (Aguzzi and Calella 2009; Prusiner et al. 1998) or by environmental exposure, as prions can potentially persist in the environment for many years (Saunders, Bartelt-Hunt, and Bartz 2008).

1.2.1.2 Prion diseases in humans and animals

Sixteen different variants of prion disease have so far been reported, nine in humans and seven in animals. The etiology and host range for these disease variants are summarized in Table 1.1. CJD, the first prion disease described in humans, occurs in sporadic, familial or iatrogenic forms. Other TSEs in humans such as familial CJD, GSS, and FFI have been shown to be associated with specific *PRNP* gene mutations.

The degenerative tissue damage caused by prion diseases is characterized by four features, spongiform changes, which are due to vacuolization, severe neuronal loss, astrocytosis, and formation of synaptic aggregates or amyloid plaques (consisting primarily of the misfolded PrP^{Sc} isoform discussed below). Interestingly, these features are common with prion diseases found in

animals. These similarities encouraged the first attempts to transmit the human prion diseases "Kuru" and CJD to primates (Beck et al. 1973; Gajdusek, Gibbs, and Alpers 1966), followed by GSS transmission in 1981 (Masters, Gajdusek, and Gibbs 1981), and transmission of CJD to guinea pig in 1986 (Kim and Manuelidis 1986). These neuropathological features have formed the basis of the histological diagnosis of human prion diseases for many years, although it was recognized that prion diseases can be enormously variable between individual cases (Jeffrey, Goodbrand, and Goodsir 1995).

Human prion diseases		
Disease	**Distinctive clinical features**	**Etiology**
Kuru	Progressive cerebellar ataxia and (in contrast to most cases of sporadic CJD) dementia is a less prominent and usually late clinical feature	Ritualistic Cannibalism / "Transumption"
Sporadic CJD	Dementia, myoclonus, cerebellar dysfunction	Spontaneous PrP^C →PrP^{Sc} conversion or non-identified somatic mutation
Familial CJD	Depends on mutation petitions either resembles sporadic CJD, or personality change, dementia and Parkinsonism	Mutations in *PRNP*
GSS	Depends on mutation, patients either (i) have gait abnormalities and ataxia, (ii) Spastic paraparesis and dementia, or (iii) Ataxia, Parkinsonism, and dementia	Mutations in *PRNP*
FFI	Sleep disturbances and autonomic dysfunction	*Prnp* haplotype 178N-129M
New variant CJD	Onset with psychiatric symptoms and delayed development of neurologic signs	Infection with prions of BSE origin
Animal prion diseases		
Disease	**Host species**	**Causes**
Scrapie	Sheep, Goats, Mouflons	Infection with Prions of unknown origin
Transmissible mink encephalopathy (TME)	Mink	Infection with Prions of unknown origin
Chronic wasting disease (CWD)	Cervid	Infection with Prions of unknown origin
Bovine spongiform encephalopathy (BSE)	Cattle	Infection by feeding with meat-and-bone meal products containing mammalian prions
Exotic ungulate spongiform encephalopathy (EUE)	Nyala, Kudu	Infection by feeding with meat-and-bone meal products containing mammalian prions
Feline spongiform encephalopathy (FSE)	Cats	Infection with prions with BSE origin

Table 1.1: Overview of human and animal prion diseases. Modified from (Belay 1999; Imran and Mahmood 2011a, 2011b).

1.2.1.3 Features of pathogenic PrP^{Sc}

Strong evidence indicates that the infectious agent of prion diseases exclusively consists of PrP^{Sc} (with \`Sc\` referring to Scrapie, a prion disease of sheep), an abnormally folded and pathogenic isoform of the physiological PrP^{C} (Cohen and Prusiner 1998; Deleault et al. 2007). The misfolded conformation of PrP^{Sc} has distinct biological and physicochemical properties, including resistance to proteinase K (PK) digestion, increased hydrophobicity, and a strong tendency to aggregate formation which causes atypical brain inflammation (Cohen and Prusiner 1998; Taylor 2000). According to the seeding-nucleation model, preexisting or acquired PrP^{Sc} oligomers catalyze the conversion of PrP^{C} molecules into the growing PrP^{Sc} fibrils, with the breakage of the latter providing more templates (or "prion seeds") for the conversion process. This process of prion propagation and spread in the brain results in the pathogenesis of prion diseases (Collinge and Clarke 2007). Spectroscopic measurements of PrP^{C} from purified fractions of hamster brain showed that PrP^{C} has a high α-helix content (42%) and has almost no β-sheet content (3%) whereas PrP^{Sc} purified from hamster brain infected with the scrapie agent is composed of only 30% α-helix and 43% β-sheet (Pan et al. 1993).

1.2.2 Alzheimer's disease

Alzheimer's disease (AD) is the most common neurodegenerative disorder, responsible for 50 to 75% of cases of dementia in elderly persons above 60 years old, and according to the recent report from the European Institute of Women's Health it has prevalence of 10.5 million Europeans in 2015 and estimated to reach 18.5 million by 2050. The current prevalence in the U.S. is about 5.7 million Americans and it has been estimated that by 2025, the number of people over 65 with AD will reach 7.1 million in the U.S., which is an almost 29% increase from the current prevalence; by 2050, the population affected is expected to even grow further to 13.8 million, which is an enormous public health issue (Alzheimer's 2016; Prince M, Wimo A, Guerchet M 2015). AD is a multifactorial disease with involvement of environmental, dietary, and genetic factors, and is characterized by progressive impairment in short-term memory interfering with daily life activities as well as impairment in other cognitive aspects such as language, spatial orientation, decision-making abilities, behavioral changes, and ultimately, motor function difficulties.

The pathology of AD is characterized by two major protein abnormalities in the brain of affected individuals including (i) the extracellular accumulation of amyloid β (Aβ) plaques and (ii) intraneuronal deposits of neurofibrillary tangles (NFTs). Insoluble Aβ plaques are formed by aggregated Aβ peptides that derive from the abnormal "amyloidogenic" cleavage of the amyloid precursor protein (APP) into hydrophobic Aβ peptides, whereas NFTs are composed of hyper-phosphorylated tau protein aggregates accumulating in the neuronal cytoplasm, leading to destabilization of microtubules and axonal transport (Small and Duff 2008). Based on evidence from familial AD cases, Aβ is thought to be the trigger of the disease process (Selkoe and Hardy 2016). However, both of these two proteinopathies can trigger oxidative stress, microvascular dysfunction, blood-brain barrier (BBB) disruption, and may induce the activation of an inflammatory response within the brain, ultimately resulting in neuronal damage and neurodegeneration (Scheltens et al. 2016).

Interestingly, in addition to its essential role in prion diseases (Brandner et al. 1996; Büeler et al. 1993), PrP^C also plays important role in other neurodegenerative conditions such as AD (Fluharty et al. 2013; Scott-McKean et al. 2016). Some studies indicate an influence of PrP^C on the neurotoxicity of oligomeric species of Aβ (Laurén, David A. Gimbel, et al. 2009; You et al. 2012). The underlying mechanism of this interaction in AD is still under discussion (see 2.3.4).

It has also been shown that PrP^C negatively regulates the activity of beta-site APP-cleaving enzyme 1 (BACE1) thereby reducing the amyloidogenic processing of the amyloid precursor protein (APP) to Aβ (Griffiths et al. 2011; Parkin et al. 2007).

1.3 Proteolytic Processing of PrP^C

1.3.1 Conserved proteolytic cleavages generate various PrP fragments

It has already been known for decades that PrP^C undergoes endoproteolytic processing and many important physiological functions have been suggested for these cleavages and their resulting fragments. However, the physiological significance of PrP^C proteolytic cleavage has not yet been entirely elucidated. Under physiological conditions, PrP^C is subjected to at least four different evolutionary conserved proteolytic cleavage events that release biologically active PrP fragments. Here, I review the four cleavage events: α-cleavage as the major processing event with relevance to this thesis, β-cleavage, membrane-proximate shedding, and the recently discovered γ-cleavage.

The α-cleavage of PrP^C

On the route to the cell surface, α-cleavage occurs on a fraction of PrP^C molecules during the late secretory pathway (A R Walmsley et al. 2009; Zhao et al. 2006) and is performed by still unknown protease(s) cleaving between amino acids H110 and V111 (in the murine sequence) of PrP^C. This cleavage results in two biologically active PrP fragments possessing distinct functions: It releases the flexible N-terminus of PrP^C, a soluble fragment of approximately 11 kDa (the so-called N1 fragment) from the globular C-terminal part (the C1 fragment) which remains attached to the membrane via its GPI-anchor and is approximately 18 kDa in size (Altmeppen et al. 2011; Bremer et al. 2010). Given the importance of this thesis, the biological relevance of both the α-cleavage and, in particular, its resulting N1 fragment will be introduced in more detail below (see 2.3.2 onwards).

β-cleavage

Another processing event occurring on PrP is the β-cleavage, which is less prominent than α-cleavage under physiological conditions. It takes place at the end of the octameric repeat region (Q90 in the murine sequence), producing a soluble N2 and a membrane-bound C2 fragment of ~9 kDa and ~20 kDa, respectively. In fact, C2 fragments were found to be the main cleavage product of PrP in neuroblastoma cells under both prion infection and ROS-mediated stress conditions (Caughey et al. 1991), as well as in the brains of CJD patients (Chen et al. 1995; Jimenez-Huete et al. 1998). This indicates a rather pathophysiological relevance. In contrast to the C1 and N1 fragments derived from the α-cleavage, there has so far been no suggested physiological function for theC2/N2 fragments (Guillot-Sestier et al. 2009; Sunyach et al. 2007).

Membrane-proximate Shedding of PrP^C by the metalloprotease ADAM10

The third physiological cleavage of PrP^C, that has recently gained attention by our and other groups in the field, occurs in the close vicinity of the GPI-anchor and results in the release of the almost full-length (fl) and soluble protein from the plasma membrane. This cleavage is mediated by ADAM10 (*A disintegrin and metalloproteinase domain-containing protein 10*) (Altmeppen et al. 2012; Borchelt et al. 1993) and is termed `shedding`. The cleavage site (between Gly228 and Arg229 in the murine sequence) and the responsible protease were found in cells (Taylor et al. 2009) and mice (Altmeppen et al. 2011) and later confirmed *in vitro* (McDonald et al. 2014).

Interestingly, in addition to fl-PrP^C, ADAM10 is also capable of shedding the N-terminally truncated C1 fragment resulting from α-cleavage, which further expands the variety of PrP^C-derived proteolytic fragments (Linsenmeier et al. 2018; Wik et al. 2012).

γ-cleavage:

Recently, the fourth cleavage of PrP^C called γ-cleavage has been identified (Lewis et al. 2016). This cleavage releases an N-terminal fragment (N3) of ~20 kDa and leaves a small GPI-anchored C3 fragment of ~5 kDa at the membrane, indicating that the cleavage takes place in a region between amino acids 170 and 200 (Haigh and Collins 2016; Lewis et al. 2016). However, the responsible protease and the exact cleavage site remain to be identified (Taguchi et al. 2009). Interestingly, γ-cleavage seems to exclusively involve unglycosylated PrP^C, indicating that the glycosylation pattern of PrP^C has a strong impact on the activity of the responsible protease (Kojima, Konishi, and Akizawa 2014; Lewis et al. 2016). Moreover, the Golgi apparatus and the trans-Golgi network, as well as the endocytic recycling compartment, have been suggested as likely locations for this cleavage. While the prevalence and relevance of this cleavage in different species, tissues, and cell culture models require further exploration, the finding of increased C3 amounts in CJD brain samples might point towards a mainly pathophysiological role of this cleavage (Lewis et al. 2016).
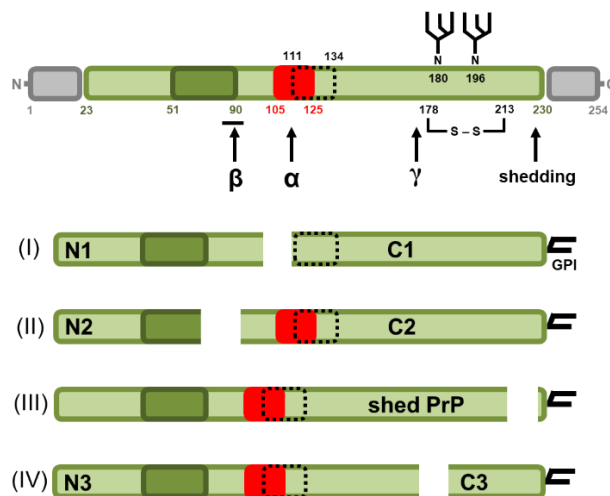
Figure 2: Schematic representation of murine PrP^C and its proteolytic processing. After removal of the N-terminal signal sequence (aa 1-22; grey box on the left) by signal peptidases at the ER membrane and the C-terminal signal sequence for the attachment of the GPI-anchor (aa 231-254; grey box on the right), the mature PrP^C contains an octameric repeat region (aa 51-90; dark green), a neurotoxic domain (aa 105-125; red box), a hydrophobic core (aa 111-134; dotted box), a disulfide bridge (between aa 178 and

213), and two variably occupied N-glycosylation sites (aa 180 and 196). The three most important cleavage events are indicated by arrows. (I) α-cleavage gives rise to a soluble N1 fragment of 11 kDa and a membrane-bound C1 fragment of 18 kDa. Of note, this cleavage destroys the neurotoxic domain and exposes the hydrophobic core as the new N-terminus of the resulting C1 fragment. (II) β-cleavage at the end of the octameric repeat region produces N2 (9 kDa) and C2 (20 kDa) fragments. (III) ADAM10-mediated shedding close to the GPI-anchor results in the release of nearly full-length PrP from the membrane. (IV) γ-cleavage resulting in a large N-terminal fragment (N3) of ~20 kDa and a small GPI-anchored C3 fragment of ~5 kDa. Modified from (Altmeppen et al. 2012).

1.3.2   The α-cleavage of PrP^C and its biological relevance

The α-cleavage is the main proteolytic processing event on PrP^C under physiological conditions. Depending on the cell type and brain region, 5-50% of total PrP^C molecules undergo α-cleavage, which therefore may be considered a major and irreversible post-translational modification of PrP^C (Chen et al. 1995; Shyng et al. 1993; Westergard, Turnbaugh, and Harris 2011).

Several functions of PrP^C have been attributed to the N-terminal part of the protein. For example, a variety of ligands was shown to bind to different motifs of this part (reviewed in (Beland and Roucou 2012)). Therefore, PrP^C α-cleavage can act as a regulator of these functions, highlighting its physiological importance.

One of the best characterized functions of PrP^c to date is a role in myelin maintenance, which seems to be substantially linked to its α-cleavage. A function of PrP^c in the myelin maintenance of peripheral nerves was reported; mice lacking PrP^c showed a chronic demyelinating polyneuropathy (CDP) at higher age (Baumann et al. 2007; Bremer et al. 2010; Shmerling et al. 1998). More recent data then showed that the flexible N-terminal part of PrP^C acts as a specific ligand for the G protein-coupled receptor Adgrg6, which promotes myelin homeostasis in the PNS (Küffer et al. 2016). Furthermore, α-cleavage was shown to be increased in brains of AD patients, with a significant positive correlation between the levels of α-cleavage and guanidine-extractable Aβ strongly supporting the hypothesis that PrP^C α-cleavage is an endogenous neuroprotective feedback mechanism in response to AD (Béland et al. 2014).

Importantly, the α-cleavage takes place within the neurotoxic domain (red box in Fig. 2) of PrP^C (amino acids 106-126 in human and 105-125 in murine sequence) which builds the structural prerequisite for the conformational conversion of PrP^C to PrP^{Sc} (Chen et al. 1995; Gasset et al. 1992; Prusiner 1998). In addition to this neurotoxic domain, studies in prion infected animals revealed that, after conversion of PrP^C to PrP^{Sc}, α-cleavage is completely impaired. A potential explanation is that steric hindrance in the misfolded, beta-sheet-rich PrP^{Sc} prevents the responsible

protease from getting access to the cleavage site. Recent reports using different experimental setups and prion strains show that transgenic mice expressing C1 in the absence of full-length PrP^C were not susceptible to prion infection did not accumulate PrP^{Sc}, and did not show any signs of neurodegeneration, thus C1 seems to be inconvertible to a PrP^{Sc} form and even acts as a dominant negative inhibitor of the prion conversion process (Lewis et al. 2009; Westergard et al. 2011).

1.3.3 Approaches to identify the responsible protease have failed so far

Despite many years of studies, there is still controversy regarding the identity of the protease(s) responsible for the α-cleavage, a so-called α-PrPase. Initial reports suggested an involvement of lysosomal serine proteases (Shyng et al. 1993) or a calpain-like activity (Barnewitz et al. 2006) for this cleavage *in vitro*, but *in vivo* data could not confirm any of these candidates (Barnewitz et al. 2006; Hachiya et al. 2011; Shyng et al. 1993).

Most of the current work on the identification of the protease(s) responsible for the α-cleavage of PrP^C focuses on ADAM10 and ADAM17 (Vincent et al. 2000, 2001). Interestingly, in the case of ADAM17, not only has its contribution to α-cleavage been suggested, but a regulatory mechanism has also been investigated in detail (reviewed in (Checler 2012)). However, a relevant involvement of ADAM17 could not be confirmed by other laboratories (Endres et al. 2009; Taylor et al. 2009). Recently, ADAM8 was identified as the functionally relevant α-PrPase in skeletal muscle, though it should be noted that the expression levels of both PrP^C and ADAM family proteases are much lower in muscles than in the brain (J Liang et al. 2012), meaning the involvement of ADAM8 in α-cleavage still remains controversial. It is likely that interspecies and inter-tissue differences exist (Klein and Bischoff 2011) and may explain discrepancies between experiments and publications. Of note, sequence differences at the cleavage site (H111/M112 in humans compared to H110/V111 in mice) may account for such interspecies differences regarding the α-cleavage with ADAM family proteases (Collins et al. 2009; Mohan et al. 2002).

1.3.4 The released N1 fragment and its (neuro)protective character

Despite all the uncertainty regarding the identity of the α-PrPase, several recent findings highlight the physiological importance of this cleavage event. Some neuroprotective functions initially attributed to the expression of PrP^C in general (Milhavet et al. 2000; Notari et al. 2004; Pushie and Vogel 2008; Watt et al. 2005) may, in part, be mediated by soluble N1. In fact, it has been shown that N1 has a neuroprotective effect by inducing anti-apoptotic signaling in neurons through the

p53 pathway both *in vivo* and *in vitro* (Guillot-Sestier et al. 2009) and it protects against oligomeric Aβ -mediated toxicity in cultured cells (M. V. Guillot-Sestier et al. 2012). The underlying mechanism still needs to be further investigated.

N1 has been shown to bind diverse membrane receptors and interact with a broad range of binding partners, contributing to cellular communication with its charged polybasic cluster region (for binding to glycosaminoglycans) and its copper-binding octameric repeat domain (Jones et al. 2004; Sunyach et al. 2003).

Moreover, N1 production was shown to interfere with the neurotoxicity of Aβ oligomers, the proposed neurotoxic entity in AD. Recently, two motifs (residues 23-27 and 95-110), both located within the N-terminus of PrP^C, have been reported to build a high-affinity platform for the binding of toxic Aβ oligomers (Chen, Yadav, and Surewicz 2010; Laurén, David A Gimbel, et al. 2009). Thus, in addition to the neuroprotective signaling, this effect might in part be achieved by soluble N1 blocking and sequestering Aβ oligomers in the extracellular space, thereby preventing binding of these toxic conformers to cell surface PrP^C and subsequent neurotoxic signaling pathways (M. V Guillot-Sestier et al. 2012). Interestingly, this blocking and neuroprotective function of N1 might not be limited exclusively to Aβ oligomers but could be a more general mechanism of protection against toxic, β-sheet-rich conformers found in different neurodegenerative proteinopathies (Resenberger et al. 2011). In fact, by releasing soluble N1 fragment, α-cleavage might have a dual protective function in this context first of all by releasing neuroprotective N1 in the extracellular matrix, the toxic oligomers can be blocked and sequester. Secondly, α-cleavage is reducing full-length PrP^C at the cell membrane which is required as a receptor, not only in prion disease (Brandner et al. 1996; Mallucci et al. 2003) but also in other neurodegenerative conditions (Chung et al. 2010; Gimbel et al. 2010; Laurén, David A Gimbel, et al. 2009; Resenberger et al. 2011). In line with this, expression of N-terminally truncated or deleted constructs that are unable to undergo α-cleavage leads to toxicity in transgenic mice (Li et al. 2007; Shmerling et al. 1998).

Taken together, the aforementioned neuroprotective aspects of the N1 fragment, it seemed reasonable and promising to study its biological roles and therapeutic potential in much more detail.

2 Materials and Methods

2.1 Materials

2.1.1 Instruments

Name	Company
7500 Fast Real-Time PCR system	Applied Biosystems
Analysis balance (MC1 Research RC210P)	Satorius
Centrifuge (F45-24-11)	Eppendorf
Chemi Doc MP imaging system	BioRad
Confocal microscope (TCS SP5)	Leica
Fine balance (CP3202S)	Satorius
Freezer (-80°C) (UF80-450S)	Colora Messtechnik GmbH
Hot plate stirrer (Ikamag RCT)	IKA
Incubator (Heraeus)	Thermo Scientific
Light microscope (DMD 108)	Zeiss
Magnetic stirrer (Variomag mono)	Thermo Electron Corporation
Microplate spectrophotometer (µQuant)	BioTek
Microscope (Eclipse TS 100)	Nikon
Microwave (R334-W)	Sharp
Gel-electrophoresis chamber	BioRad
Nanodrop ND 1000	Wilmington
Automated cell counter	Thermo Fisher Scientific
Odyssey Imaging System	LI-COR Biosciences
pH meter (CG 840)	Schott
Pipettes	Eppendorf
Table-top centrifuge (5415R)	Eppendorf
Thermocycler MyCycler PCR	BioRad
Gel documentation system	Analytik Jena US
NanoZoomer digital slide scanner	Hamamatsu

2.1.2 Consumables

Name	Company
6, 12, 24 and 96 well-plates	Thermo Scientific
Coverslips	Menzel
Disposable pipettes (2ml, 5ml, 10ml, 25ml)	BD Biosciences
Microscopy slides	Roth
Whatman paper	BioRad
Nitrocellulose membrane 0.2 µm	BioRad
Novex® Bis-Tris Gele (4-12 %)	Life Technologies
Parafilm	SPI Supplies
PCR tubes	Rapidozym

Name	Company
Sterile filter (0.22µm) for syringes	Roth
Cell strainer 70 µm	Falcon
Syringes (10 ml, 30 ml and 50 ml)	BD Biosciences
T25 and T75 cell culture flasks	Sarstedt

2.1.3 Chemical reagents and buffers

Name	Company
0.05% Trypsin-EDTA	Gibco
1 kb DNA plus ladder	Life Technologies
10x Fast Digest Green Buffer	New England Biolabs
10x T4 DNA Ligase Buffer	Thermo Scientific
10xDream*Taq* Buffer	Thermo Scientific
2-propanol	Roth
2X SYBR® Green PCR Master Mix	Applied Biosystems
Synthetic human Aβ42	Genic Bio
Acetic acid	Roth
Acrylamid solution (Rotiphorese 30%)	Roth
Agarose	Invitrogen
Ammonium persulfate (APS)	BioRad
Ampicillin (Amp)	Sigma-Aldrich
β-Mercaptoethanol	Thermo Scientific
Bovine serum albumin (BSA)	Roth
Bromophenol blue	Merck
DAPI Flouromount G	Southern Biotech
Dimethyl sulfoxide (DMSO)	Sigma-Aldrich
dNTP mix	Sigma-Aldrich
Dulbecco's Modified Eagle Media (DMEM) High Glucose (4.5g/l)	Life Technologies
Dulbecco's phosphate-buffere saline (PBS)	Gibco
EDTA (Ethylene diamine tetra-acetic acid)	Applichem
EDTA free protease inhibitor cocktail	Roche
Ethanol J.T.	Baker
Ethidium bromide	Roth
Fetal bovine serum (FBS)	PAA Laboratories
Glycerol	GE Healthcare
Instant milk powder	GranoVita
Opti-MEM	Life Technologies
PAGE Rule Prestained Protein Ladder (10-170kDa)	Fermentas
Paraformaldehyde (PFA)	Merck

Sodium azide	Sigma-Aldrich
Sodium chloride (NaCl)	Sigma-Aldrich
Sodium deoxycholate	Sigma-Aldrich
Sodium dodecyl sulfate (SDS)	Bio-Rad
Super Signal West Femto Substrate	Thermo Scientific
Super Signal West Pico Substrate	Thermo Scientific
Tetramethylethylenediamine (TEMED)	Roth
Triton X100	Applichem
Tween 20	Roth
TRIzol^R Reagent	Life Technologies

2.1.4 Commercial kits

Name	Company
GeneJet PCR purification Kit	Thermo Scientific
High Capacity cDNA Reverse Transcription Kit	Applied Biosystems
QIAprep® Midiprep Kit	Qiagen
QIAprep® Miniprep Kit	Qiagen
Large fragment DNA recovery Kit	Zymoclean^{TM}
QuicChange Lightning Site-Directed Mutagenesis Kit	Agilent Technologies
QuicChange II XL Site-Directed Mutagenesis Kit	Agilent Technologies
In-Fusion^{R}HD Cloning Kit	Clontech
Pierce Co-Immunoprecipitation (Co-IP) Kit	Thermo Scientific
PNGase F digestion Kit	Roche
Standard cDNA Synthesis Kit	Thermo Scientific

2.1.5 Software

Name	Company
LAS AF Lite	Leica
Office 2010	Microsoft
Prism 6	GraphPad
Quantity One	BioRad
NDP.View 2	Hamamatsu
QuantStudio^{TM} Design & Analysis	Applied Biosystems
Image Studio Lite Version 5.2	Li-Cor
Mendeley	Mendeley Ltd.

2.1.6 Media and buffers

Name	Recipe
RIPA buffer	50mM Tris Base, pH=8, 150mM NaCl, 1% NP40, 1mM EDTA, 0.1% SDS and 1% Na-deoxycholate
Laemmli Buffer (4x)	240mM Tris Base pH 6.8, 8% SDS, 40% glycerol, .2% bromophenol Blue, 5% β-mercaptoethanol, ,
MES/SDS Buffer (10X)	97.6 g MES, 60.6 g Tris Base, 10 g SDS, 3.6 g EDTA, in 1 litter ddH$_2$O
Resolving gel buffer	1.5M Tris Base pH= 8.8, 1% SDS, in 100 ml ddH$_2$O
Stacking gel buffer	0.5M Tris base pH= 6.8, in 100 ml ddH$_2$O
Running Buffer (10X)	0.25M Tris Base, 1.92M Glycine, 1% SDS, in 1 litter ddH$_2$O
Blotting Buffer (10X)	250mM Tris Base, 1.92M Glycine, in 1 litter ddH$_2$O
TBS-T(ween)	100mM Tris Base, 1.4M NaCl, pH= 7.4, 1% Tween-20, in 1 litter ddH$_2$O

2.1.7 Antibodies

Name	Catalog -Nr.	Company	Species	MW (kDa)	Dilution	Blocking buffer
CREB (86B10)	9104	Cell signalling	Mouse	43	1:1000	5% milk in TBST
P-CREB (Ser133)	9191	Cell signalling	Rabbit	43	1:1000	5% BSA in TBST
p44/42 MAPK (Erk1/2) (137F5)	4695	Cell signalling	Rabbit	42, 44	1:1000	5% BSA in TBST
P-p44/42 MAPK (Erk1/2) (Thr202/Tyr204)	9101	Cell signalling	Rabbit	42, 44	1:1000	5% BSA in TBST
HSP70 (D69)	4876	Cell signalling	Rabbit	70	1:1000	5% BSA in TBST
HSP90	4874	Cell signalling	Rabbit	90	1:1000	5% BSA in TBST
cPLA2	2832	Cell signalling	Rabbit	95	1:1000	5% BSA in TBST
P-Cpla2 (Ser505)	2831	Cell signalling	Rabbit	95	1:1000	5% BSA in TBST
p38 MAPK Antibody	9212	Cell signalling	Rabbit	43	1:1000	5% BSA in TBST
P-p38 MAPK (Thr180/Tyr182) (D3F9) XP Rabbit mAb	4511	Cell signalling	Rabbit	44	1:1000	5% BSA in TBST

eIF2a Antibody	9722	Cell signalling	Rabbit	38	1:1000	5% BSA in TBST
P-eIF2a (Ser51) Antibody	9721	Cell signalling	Rabbit	38	1:1000	5% BSA in TBST
Fyn Antibody	4023	Cell signalling	Rabbit	59	1:1000	5% BSA in TBST
P-Src Family (Tyr416) Antibody	2101	Cell signalling	Rabbit	60	1:1000	5% BSA in TBST
Akt (pan) (40D4) Mouse mAb	2920	Cell signalling	Mouse	60	1:2000	5% milk in TBST
P-Akt (Ser473) Antibody	9271	Cell signalling	Rabbit	60	1:1000	5% BSA in TBST
SAPK/JNK Antibody	9252	Cell signalling	Rabbit	46, 54	1:1000	5% BSA in TBST
P-SAPK/JNK (Thr183/Tyr185)	9255	Cell signalling	Mouse	46 , 54	1:2000	5% milk in TBST
POM1	-	Prof Dr. Aguzzi, Zürich, Switzerland	Mouse	17, 25-35	1:2000	1x Roti block in TBST
Pom2	-	Prof Dr Aguzzi, Zürich, Switzerland	Mouse	11, 25-35	1:2000	1x Roti block in TBST
6D11	808001	Biolegend	Mouse	11, 25-35	1:2000	1x Roti block in TBST
Anti mouse/rat beta amyloid (sAPP alpha)	826801	Biolegend	Rabbit	95	1:1000	1x Roti block in TBST
6E10	803002	Biolegend	Mouse	4-130	1:1000	1x Roti block in TBST
β-actin(C4)	MAB1501	Millipore	Mouse	43	1:3000	in 1x Roti block in TBST
β-catenin	9582s	Cell signalling	Rabbit	92	1:1000	in 1x Roti block
Synaptophysin	ab32594	abcam	Rabbit	-	1:200	1% BSA in PBST
Anti-MAP2 antibody, Mouse Monoclonal	M9942	Sigma-Aldrich	Mouse	-	1:500	1% BSA in PBST
IRDye 680 RD Donkey anti-Rabbit IgG	925-68073	LICOR	Anti-Rabbit	-	1:10000	in 1x Roti block

IRDye 800 CW Donkey anti-mouse IgG	925-32212	LICOR	Anti-Mouse	-	1:10000	in 1x Roti block
Anti Rabbit IgG HRP conjugate	W401B	Promega	Anti-Rabbit	-	1:5000	in 1x Roti block
Anti-mouse IgG HRP conjugate	W402B	Promega	Anti-Mouse	-	1:5000	in 1x Roti block
Donkey anti-Rabbit, Alexa Fluor 488	R37118	Invitrogen	Anti-Rabbit	-	1:5000	1% BSA in PBST
Goat anti-Mouse, Alexa Fluor 555	A-21127	Invitrogen	Anti-Mouse	-	1:500	1% BSA in PBST

2.1.8 Primers

Name	Primer Sequence	Application
F N1 STOP	CAACCTCAAGCATTAGGCAGGGGCTGCG	Mutagenesis at α-cleavage site
R N1 STOP	CGCAGCCCCTGCCTAATGCTTGAGGTTG	Mutagenesis at α-cleavage site
F1-Exone2	GAGCTGAAGCATTCTGCCTTCC	Forward primer for genotyping
R3-PrP	GATCTTCTCCCGTCGTAATAGGCCT	Reverse primer for genotyping
F-control PrP	ATGGCGAACCTTGGCTACTGGCT	Control Forward primer for genotyping
R-control PrP	CATCCCACGATCAGGAAGATGAGG	Control reverse primer for genotyping
R-HGC-Seq	TGTACATTTCCCAGGGCCCATCAGTGC	Reverse primer for sequencing the insert in HGC
F-XhoI-N1	GCTCTCTGGCTAACTCGAGAACCCACTGCTTACTG	Primers for taking out N1 cDNA from pcDNA3.1
R-XhoI-N1	CAGTAAGCAGTGGGTTCTCGAGTTAGCCAGAGAGC	Primers for taking out N1 cDNA from pcDNA3.1
F-BglII-N1	CTCAAGCATGTGGCAAGATCTGCGGCAGCTGGGG	Primers for taking out N1 cDNA from pcDNA3.1
R-BglII-N1	CCCCAGCTGCCGCAGATCTTGCCACATGCTTGAG	Primers for taking out N1 cDNA from pcDNA3.1
F-mRPL13	CGGAATGGCATGATACTGAAGCC	qPCR
R-mRPL13	TTGGTGTGGTATCTCACTGTAGG	qPCR
F-N terminus	ATGGCGAACCTTGGCTACTG	qPCR
R-N terminus	CTGAGGTGGGTAACGGTTGC	qPCR

2.2 Methods

2.2.1 Ethics Statement

All animal experiments in this study were carried out in accordance with the recommendations in the *Guide for the Care and Use of Laboratory Animals* of the German Animal Welfare Act on the protection of animals. Procedures were done in accordance with the guidelines of the animal facility of the University Medical Center Hamburg-Eppendorf and approved by the Committee on Ethics of the Freie und Hansestadt Hamburg (permit number 84/13).

2.2.2 Constructs used for *in vitro* studies

To generate the N1-coding plasmid, the pcDNA3.1(-)/Zeo expression vector containing the coding sequence of the mouse *Prnp* gene (generated by former lab student Dr. Clemens Falker) was used. A stop codon at amino acid (aa) 111 was inserted using the QuickChange Site-Directed Mutagenesis Kit (Agilent Technologies). To clone the construct expressing the N1-Fc fusion protein, the pFUSE-mIgG1-Fc1 vector with a CMV promotor and the CH2 and CH3 domains of the IgG heavy chain were purchased (InvivoGen). The sequence coding for aa 1-110 of mPrP was subcloned into the pFUSE vector in such a way that the Fc tag is linked to the C-terminus of the PrP-N1 sequence with a short hinge region in between. To generate the N1-Nb construct, the cDNA coding for aa 23-110 of mPrP was subcloned into the pCSE2.5 construct containing an IgKappa leader, a linkage region, a single chain variable domain, and a His/Myc tag at the very C-terminus (the Nb construct was provided by the group of Prof. Dr. Nolte, Immunology, UKE Hamburg).

2.2.3 Generation of TgN1 and TgN1-Fc mice

To generate transgenic mice overexpressing the N1 or N1-Fc constructs, the previously described half-genomic expression construct (mPrP-HGC;(Fischer et al. 1996)) was used. For TgN1 mice, a stop codon was inserted into the murine *Prnp* sequence coding for aa 111 in the mPrP-HGC using the QuickChange II XL Site-Directed Mutagenesis Kit. For TgN1-Fc mice, the N1-Fc sequence from the above mentioned pFUSE vector was subcloned into the mock HGC after introducing new restriction sites in both constructs using the QuickChange II XL Site-Directed Mutagenesis Kit. Before pronuclear injection of the final constructs into the embryos, N1mPrPHGC and N1FcmPrPHGC vectors were first cut with SalI and NotI to remove the pBlue script sequence. The pronuclear injections into C57BL/6J mice were kindly performed in the Transgenic Mouse Facility

(ZMNH, UKE, Hamburg). Positive heterozygous animals were subsequently selected by genotyping using genomic DNA obtained from tail biopsies. All primers used are listed in Table 2.1.8 above.

2.2.4   Preparation of murine brain homogenates

Fresh or frozen brain tissue from TgN1 or WT littermates was used to prepare 10% (w/v) homogenates on ice using RIPA buffer freshly supplemented with Complete EDTA-free protease inhibitors (PI) and phosphatase inhibitor (PhosStop) cocktails (Roche). Importantly, samples used for PK digestion for PrP^{Sc} detection in prion-infected samples were made in RIPA without PI and PhosStop. Samples were homogenized 30x using a Dounce homogenizer and incubated on ice for 15 min, shortly vortexed, and incubated for another 15 min prior to centrifugation at 12,000 g at 4°C for 10 min. Supernatants were either further processed for immediate SDS-PAGE or stored at -80°C. Total protein content was assessed by Bradford assay (BioRad) following the manufacturer`s instructions. Primary neuronal cultures

*Monocultures***:** Primary neurons were prepared from transgenic mice and WT littermates at postnatal day 0 to 1 (P0-P1). Briefly, after dissecting out the pups' brains, meninges were removed from both hemispheres. Brain tissues were then washed once with pre-cooled dissecting media (DM; 1x HBSS, 1% penicillin-streptomycin, 10mM Hepes, 0.6% glucose solution). The brains were cut into smaller pieces using sterile surgical scissors and the tissue pieces were transferred into a 60 mm dish with 4.5 mL DM plus 0.5 mL pre-warmed 2.5% Trypsin (Thermo Fisher Scientific) for incubation at 37°C for 15 min under mild horizontal agitation.

After Trypsin digestion, 100 µL per dish of sterile 1 mg/mL DNaseI was added into the dishes and gently swirled. Trypsin and DNaseI enzymatic activity were then quenched after 1 min with 5 mL of Glial Growth Medium (GGM; DMEM + 0,6% glucose solution, 1% penicillin-streptomycin, 10% FBS). The solutions were mixed very well by gently pipetting up and down 2-3 times (on-dish trituration), transferred into new 15 mL falcon tubes and centrifuged for 5 min at 1000 rpm at RT.

After carefully decanting the supernatant, the pellet was re-suspended in 5 ml Neuronal Maintenance Medium (NMM; 1% Glutamax with a final concentration of 2 mM, 2% B27 serum supplement, 1% penicillin-streptomycin, in 50 ml with Neurobasal medium). The trituration step

was carried out by gently pipetting the neurons up and down 20 times. After filtration through a 70 µm cell strainer, the neurons were seeded onto PLL-coated dishes (Poly-L-lysine hydrobromide, Sigma Aldrich). The media was changed after maximum 4 hours of incubation at 37°C and 5% CO_2. The next day, cells were treated with 10µM of the mitotic inhibitor fluorodeoxyuridine (FUdR, Sigma Aldrich) overnight in order to eliminate non-neuronal cells. On day 5 post dissection, neurons, and conditioned media were either harvested for analysis of protein expression or neurons were treated overnight with 5 µM proteasomal inhibitor (MG132), or left untreated in OptiMEM, followed by harvesting neuronal lysates and the respective conditioned media.

Co-culturing neurons on an astrocyte feeder layer: For morphological assessment, hippocampal neurons were co-cultured with hippocampal astrocytes following a previously published protocol (Kaech and Banker 2006). Astrocytes were prepared 3 weeks before the neuronal dissection day. For the preparation of the astrocytes, the hippocampi of four WT newborn mice (P0 to P1) were pooled together. After the first centrifugation step, the brain tissues were gently triturated with a 5 ml pipette using GGM. The dissociated cells were filtered through a 70 µm cell strainer, seeded into a T75 flask, and maintained up to 8 weeks in culture with weekly medium changes. One day before dissection of neurons, three wax dots were dropped per well in a 12-well plate which was irradiated with UV light for 20 min under the cell culture bench for sterilization. Approximately 80,000 astrocytes (assessed by cell counter (Thermo fisher)) were seeded between the wax dots in 1ml NMM. The next day, ~60,000 neurons were plated on 18 mm glass coverslips pre-coated with PLL. After 4 h to allow the neurons to adhere to the coverslips, the latter were carefully placed face-down on top of the wax dots in the plates containing astrocytes in order to keep the neurons incubated above the astrocyte feeder layer. The next day, the neurons were treated with 10 µM FUdR. Every three days, half of the NMM was exchanged with fresh media. On day 15 of co-culture, cells were isolated from the astrocyte by bringing the coverslips back in a new 24-well plate. Neurons were then treated with monomeric Aβ42 dissolved in DMSO (GenicBio Synthetic Peptide) with the final concentration of 5 µM for 12 hours.

2.2.5 Immunofluorescence staining of primary hippocampal neurons

After aspirating the media, coverslips were gently washed three times with cold PBS. The cells were then fixed with paraformaldehyde (PFA) solution (2 ml PBS, 1 ml 16% PFA and 1 ml 16%

Sucrose) for 10 min at RT on a platform shaker at 100 rpm. After three washes with PBS, permeabilization was performed using 0.25% Triton X100 in PBS for 10 min at RT. Following three additional washes with PBS, blocking (with 1% BSA + 0.25% Triton X100) was done for one hour at RT. Coverslips were then incubated with primary antibodies against Synaptophysin and MAP2 overnight at 4°C while gently shaking. The next day, coverslips were washed three times with PBS and incubated with fluorescently labeled secondary antibodies for one hour at RT in the dark.

2.2.6 Quantification of synaptic puncta density using SynPAnal software

Three single neurons per coverslip from each condition (WT and TgN1 derived neurons with or without Aβ treatment) were scanned by confocal scanning microscopy using a TCS SP5 system (Leica). The gain and zoom settings were kept constant for all images acquired from the same experimental trial. Thereafter, TIFF-format images with merged channels were analyzed to measure the synaptic punctae along defined dendritic stretches using SynPAnal software with a semi-automated punctae detection feature. After setting the thresholds for all three channels (DAPI in blue, MAP2 in red, and Synaptophysin in green), 3-5 dendritic segments from each investigated neuron were selected for the final measurements. Relative punctae density values were used for the quantifications according to a previously published protocol (Danielson and Lee 2014).

2.2.7 Cell culture, transfection and treatment of cells

Murine neuroblastoma (N2a) cells were maintained at 37°C with 5% CO_2 in Dulbecco's modified Eagle's medium (DMEM; Thermo Fisher Scientific) supplemented with 10% fetal bovine serum (FBS; Thermo Scientific). N2a PrP-/- (PrP-KO) were generated by CRISPR/Cas9 technology and provided by Dr. M. Willem (LMU, München). N2a cells were transfected by Lipofectamine 2000 (Thermo Fisher Scientific) following the manufacturer's instructions. Briefly, N2a cells at 70-90% confluency were treated with transfection mixture (4 µg of the desired plasmid, 10 µl of Lipofectamine reagent in the total volume of 500 µl OptiMEM) and incubated at RT under the cell culture bench for about 20 minutes. After changing the media of cells to 1 ml pre-warmed OptiMEM, cells were treated with the transfection mixture and incubated at 37°C for 4 to 6 hours. After this incubation time, media was changed again to fresh DMEM with 10% FBS and incubated overnight at 37°C. After 24 hours, the media was again changed to 1 ml of OptiMEM and incubated overnight at 37°C. The next day, cells and conditioned media were collected, processed (as

described below) and subsequently analyzed by biochemical assessment. Antibody treatments of N2a cells were performed by adding 4 µg of either POM1 or 6D11 to 1 ml media supernatant (freshly exchanged pre-warmed OptiMEM) for 18 hours.

2.2.8 Cell lysis, harvesting and TCA precipitation of conditioned media, SDS-PAGE and western blot analysis

N2a cells or primary neurons were washed with cold PBS, lysed using an appropriate amount of RIPA buffer supplemented with protease and phosphatase inhibitor, and incubated on ice for 15 min followed by centrifugation at 12,000 g for 10 min at 4°C. For SDS-PAGE, cell lysates were mixed with Laemmli buffer including 5% β-mercaptoethanol and denatured for 5 min at 95°C. For the analysis of proteins in the conditioned media (of N2a cells or primary neurons), experiments were carried out with freshly exchanged serum-free media (OptiMEM) overnight. Proteins in media were precipitated with trichloroacetic acid (TCA). In brief, supernatants were carefully collected, immediately incubated on ice and mixed with a concentrated protease inhibitors cocktail, and two mild centrifugation steps were carried out at 500 g and 5000 g in order to remove cellular debris. Next, 1/100 volume of 2% sodium deoxycholate (NaDOC) was added to each sample and samples were incubated on ice for 30 min. Afterwards, 1/10 volume of TCA was added to the mixture and again incubated for at least 30 min on ice. After centrifugation at 15,000 g for 15 min at 4°C, the supernatant was aspirated and the pellet was air-dried for maximum 5 min. The pellet was then completely resolved in 100 µL of 1x Laemmli buffer (with 5% of β-ME) and denatured for 5 min at 95°C.

For SDS-PAGE, denatured samples were loaded on either precast Any kD™ Mini-PROTEAN® TGX™ Precast Protein Gels (BioRad) or precast Nu-PAGE 4-12% Bis-Tris protein gels (Thermo Fisher). Afterwards, proteins were transferred to nitrocellulose membranes (BioRad) by the wet-blotting method and membranes were subsequently blocked for at least 30 min with either 1x RotiBlock (Carl Roth) or 5% BSA or 5% milk (all in TBS-T) and incubated overnight with the respective primary antibodies (diluted in the same blocking buffer) at 4°C on a shaking platform.

2.2.9 Co-immunoprecipitation assay

To assess the binding of the N1 fragment to synthetic Aβ$_{42}$, a co-immunoprecipitation assay was performed using the Pierce Co-Immunoprecipitation (Co-IP) kit (Thermo Scientific). Briefly, 50

µl of AminoLink Plus Coupling Resin were washed three times with 1X coupling buffer followed by centrifugation at 1000 g for 1 min. After removing the wash buffer, 10 µg of antibody (POM2, an antibody against PrP; or 6E10, an antibody against Aβ) were coupled to the resin in each reaction column and immediately after, 3µl of sodium cyanoborohydride solution was added to each column under a chemical hood, and incubated for 2 hours at RT on a rotator. After the incubation, resins were centrifuged at 1000 g for 1 min and the flow-through was discarded. After quenching the columns again, 3µl of sodium cyanoborohydride solution was again added and incubated for 15 min with gentle end-over-end mixing. The flow-through was discarded after another centrifugation step and resins were washed eight times with wash solution. Antibody-coupled resins were then incubated (at 4°C overnight with end-over-end mixing) with conditioned media of N2a cells pre-treated overnight with synthetic Aβ$_{42}$. The next day, bound antigens/complexes were eluted and resins with covalently-bound antibodies were washed and stored at 4°C to be reused. Eluates were then analyzed by western blot (described above).

2.2.10 RNA extraction, cDNA synthesis and qPCR

Mouse brain tissues from forebrain as well as cerebellum (about 100 mg) of adult mice were collected, homogenized with 1 ml TRIzol, and incubated for 5 minutes at RT. After centrifugation at 12,000 g for 10 min at 4°C, the upper phase was collected. Next, 200 µL of chloroform was added to each sample which was vigorously shaken by hand for 15 sec and then incubated at RT for about 2-3 min. After centrifugation of the mixture at 12,000 g for 15 min at 4° C, the upper aqueous phase was carefully collected. 500 µL of 100% isopropanol was added to the collected aqueous phase, which was then incubated for 10 min at RT. After another centrifugation step at 12,000g for 15 min, the supernatant was discarded and the RNA pellet was washed twice with 1 ml of cold 75% ethanol, vortexed, and centrifuged at 7,500 g for 5 min at 4° C. Next, the pellet was air-dried for 5-10 min, dissolved in double distilled water, and heated at 55°C for 10 min. Concentration and purity of extracted RNA were assessed by Nanodrop (Thermo Scientific) measurement. The cDNA was synthesized subsequently according to the manual`s instructions (Thermo Scientific).

Real-time quantitative polymerase chain reaction (RT-qPCR) was done using SYBR®Green kit (Thermo Scientific). All reagents were added according to the manufacturer's instructions. Samples

were loaded in triplicates. The relative expression levels of PrP were then calculated by the $2^{-\Delta\Delta Ct}$ method after referring to RPL13 as the reference gene.

2.2.11 Prion inoculation of mice

Intracerebral inoculations of TgN1 mice and WT littermate controls with Rocky Mountain Laboratory (RML) prions were performed under deep anesthesia with ketamine and xylazine hydrochloride. Briefly, 10 to 11 weeks-old TgN1 mice (n=10) and littermate controls (n=10) were inoculated with 30 µL of a 1% brain homogenate containing RML prions (RML 5.0 inoculum, corresponding to 3×10^5 LD50) into the caudaputamen. Additionally, mock inoculations were also performed with 30 µl of a 1% brain homogenate from uninfected CD1 mice (no prions) into age-matched TgN1 (n=5) and littermate controls (n=4). These animals were sacrificed at 241 days post inoculation (dpi) with no clinical signs.

After inoculation, a special observation was applied until initial recovery. Mice were then checked regularly and, following the appearance of characteristic clinical signs of prion disease (such as hind limbs clasping, weakness, and hunched back), observation was even increased to two times per day. All mice at the terminal disease stage were sacrificed and after dissecting out the brains, one hemisphere was frozen and analyzed biochemically while the other hemisphere was fixed in formalin and used for histopathological analysis.

2.2.12 PK digestion of brain homogenates

For assessment of PrP^{Sc} levels in prion-infected mouse brains, 10% homogenates (w/v) of the frontal brain were prepared in RIPA buffer without any protease inhibitors (as this would affect the enzymatic digestion by PK). Homogenates were prepared by 30 strokes on ice using a Dounce homogenizer. After centrifugation at 12,000 rpm for 10 min, the resulting supernatants were collected and 2 µL of each homogenate were digested with 20 µg/mL PK (Roche) in a total volume of 22 µl of RIPA buffer for 1 h at 37°C under mild agitation. Digestion was stopped by adding 6 µL of 4x Laemmli buffer (plus 5% β-ME) and the mixture was heated for 5 min at 95°C. Subsequently, SDS-PAGE and western blot analysis were performed with proper technical controls (i.e., PK-digested sample of a CD1 brain as well as a non-PK-digested RML-infected sample) as described above. All the work with prion-infected samples was done in our prion lab with Biosafety level 3.

2.2.13 Histological assessment of mouse brain sections

Morphological analysis was performed as described previously (Altmeppen et al., 2015). Briefly, brain tissues were dissected out and fixed by incubating in 4% PFA overnight at 4°C. In the case of prion- or CD1-inoculated animals maintained in the S2 animal facility, samples were initially inactivated for 1 h in 98-100% formic acid before exporting them from the respective facility. Afterwards samples were washed for several times with water to remove formic acid, and then samples were again incubated with 4% PFA overnight at 4°C. The next day samples were dehydrated and embedded in paraffin according to standard laboratory procedures. Brain sections with 4 μm thickness were cut and mounted on slides and then stained either with hematoxylin and eosin (HE) or stained according to standard procedures of immunohistochemistry using the Ventana Benchmark XT machine (Ventana). Briefly, for antigen retrieval sections were boiled in 10mM citrate buffer (pH 6.0) for between 30 to 60 min. All primary antibodies used in histology were prepared in 5% goat serum (Dianova), 45% Tris-buffered saline (TBS) pH 7.6, and 0.1% Triton X-100 in antibody diluent solution (Zytomed). Detection was performed by anti-rabbit or anti-goat histofine, Simple Stain MAX PO Universal immunoperoxidase polymer or Mouse Stain Kit (for detection of mouse antibodies on mouse sections). Secondary antibody polymers were purchased from Nichirei Biosciences. Detection of antibodies was performed with Ultra View Universal DAB Detection Kit. Of note, experimental groups were stained in one run to avoid variations between groups.

2.2.14 Statistical analysis

In this study, all statistical analysis of western blot results, morphological quantifications of dendritic spines and qRT-PCR results between experimental groups were performed using Student's t-test. For the incubation times after prion inoculation, the assessment was performed using log-rank (Mantel-Cox) test for two-group comparisons with consideration of statistical significance at p values <0.05 (*), <0.01 (**), and <0.001 (***).

2   Results

3.1   Generation of N1-overexpressing cells

For studying the neuroprotective effects of N1 *in vitro*, a cell line overexpressing the N1 fragment first needed to be generated. To do so, a N1 construct was generated by changing amino acid (aa) 111 (of the murine PrP sequence) from a valine (codon GTG) to a stop codon (TAG) using site-directed mutagenesis, resulting in the expression of a C-terminally truncated fragment consisting of the ER signal peptide (SP, aa 1-23) and the N1 coding region (aa 23-110). PrP^C knockout (KO) and wild-type (WT) neuroblastoma cells (N2a) were transiently transfected to overexpress N1. Western blot (WB) analyses were performed on cell lysates and on immunoprecipitated N1 from conditioned media to check whether or not transgenic N1 is expressed and secreted (Figure 3.1a).

In order to increase cellular secretion and facilitate later purification and detection, tagged N1 variants fused to either the Fc part of murine IgG1 (N1-Fc) or to a nanobody (N1-Nb) at the C-terminus were also generated. Of note, because the Fc domain of the IgG dimerizes, N1-Fc forms homodimers (Figure 3.1b). However, the denatured protein in WB runs at around 36 kDa, which corresponds to the expected molecular weight of monomeric N1-Fc.

In the case of the Nb tag, three different combinations of N1Nb fusion protein were generated using two different constructs but with the same CMV promoter: (i) with the original signal peptide (SP) of murine PrP in the vector pcDNA3.1; (ii) with a IgKappa leader sequence (instead of the murine SP) in a pCSE 2.5 vector; (iii) or with the same leader sequence and vector but with an additional C-terminus 6xHis-tag (N1-Nb +His). WB analysis of these N1Nb variants showed that secretion of N1-Nb with the IgGk leader sequence was stronger than with the original signal sequence of murine PrP^C (Figure 3.1c).

Interestingly, in both cases, with N1-Fc and N1-Nb, a relevant portion of the fusion proteins present with a band at ~11 kDa, thus likely corresponding to bona fide N1 fragment. This indicates that a fraction of the fusion proteins expressed in PrP^C-KO cells undergo an α- cleavage-like processing event resulting in the secretion of both, expected full-length fusion proteins as well as the cleaved fragments of N1 and the protein tags alone.
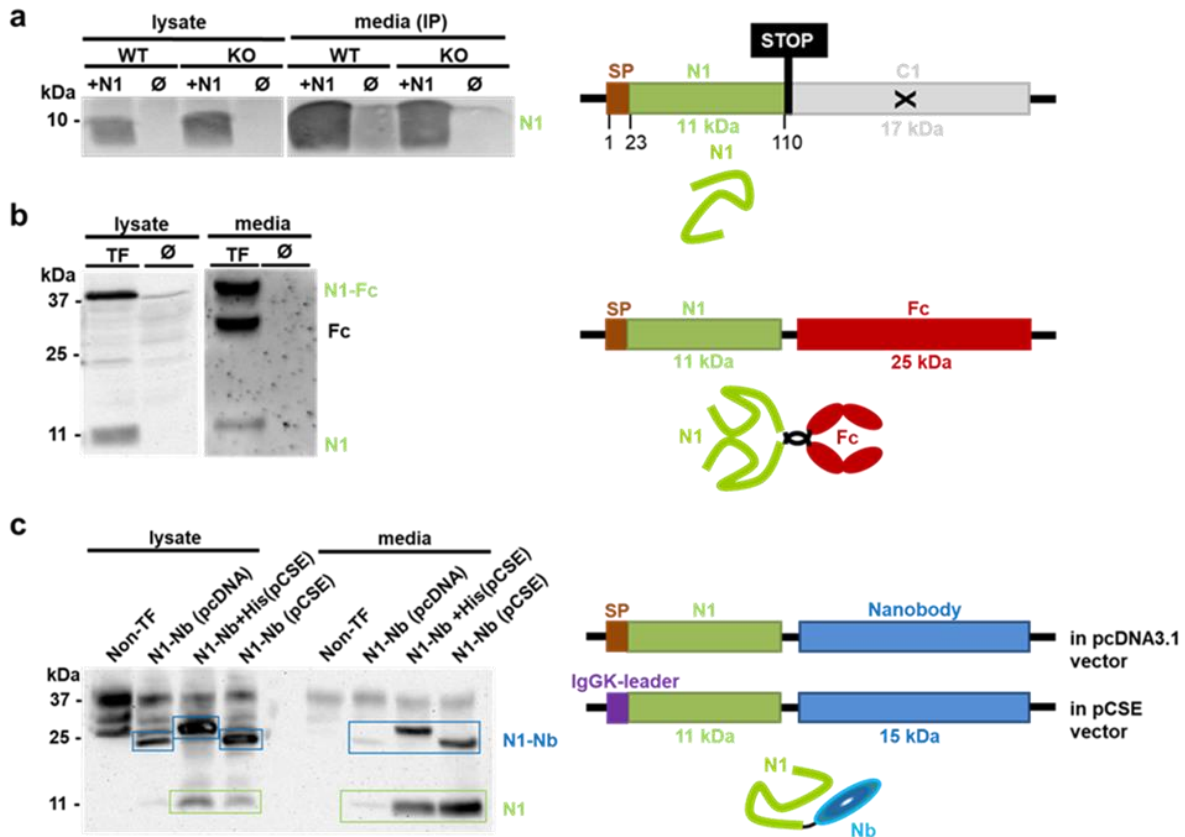
Figure 3.1: Design and expression of **N1 and N1 variants in PrP^C-depleted N2a cells.** (a) Expression of N1 (aa 1-110 of murine PrP) in transiently transfected WT and PrP-KO N2a cells revealed by WB analysis in cell lysates as well as in conditioned media after immunoprecipitation (IP) with thePOM2 antibody. (b) WB analysis of N1-Fc expression in PrP-KO N2a cells revealed high expression and secretion of the N1-Fc fusion protein as well as separated N1 and Fc fragments. (c) Comparison of expression and secretion of different N1-Nb constructs. Schematic representations of the cloning strategy/construct design of N1 variants are shown on the right side of each blot. The black stripe between N1 and the fusion tags is a 5GS linkage region. TF= transfected, Ø= Non-transfected, KO= PrP knockout, Nb= Nanobody, SP= signal peptide.

3.2 N1 binds Aβ and protects cells against Aβ toxicity

It has been shown that PrP^C acts as a receptor for toxic oligomers like Aβ in AD. Interestingly, N1 contains both of the PrP^C binding regions for Aβ (aa 23- 31 and 95-110 of murine PrP) (Laurén, David A. Gimbel, et al. 2009). An Aβ binding assay was performed to test whether the soluble N1 fragment in our cell model is able to bind synthetic Aβ$_{42}$. Interaction of N1 (transiently overexpressed in N2a PrP-KO cells) with Aβ was confirmed by incubating the media supernatants of N1-overexpressing cells with synthetic Aβ$_{42}$ overnight, followed by co-immunoprecipitation using antibodies against N1 (POM2) and Aβ (6E10) (Figure 3.2a). Both antibodies were able to

co-immunoprecipitate both N1 and $A\beta_{42}$, indicating that the N1 fragment is necessary and sufficient for binding to synthetic Aβ oligomers. Surprisingly, the signal for transgenic N1 in the lysates (but not in the supernatant) appeared as a conspicuous double band, which will be discussed in detail later.

It has also been described that cell surface PrP^C in Alzheimer`s disease and respective mouse models partially mediates the neurotoxicity of Aβ. In contrast, releasing N1 leads to antagonistic effects on the toxicity of Aβ: On the one hand, this decreases the amount of receptor for Aβ at the cell membrane (as N1 contains the Aβ binding sites of PrP^C); on the other hand, released N1 fragments have a neuroprotective effect against toxicity of Aβ in the extracellular space. Importantly, N1 is capable of noticeably suppressing the Aβ polymerization process (Nieznanski et al. 2012). Therefore, we assessed the neuroprotective potential of N1 variants against Aβ toxicity. After treatment with Aβ, N2a cells expressing N1 or N1-Fc showed reduced neurotoxicity compared to WT-PrP-expressing and PrP-KO N2a cells, based on immunofluorescent staining for cleaved (i.e. activated) caspase-3, an indicator of cell death (Abraham and Shaham 2004) (Figure 3.2b).
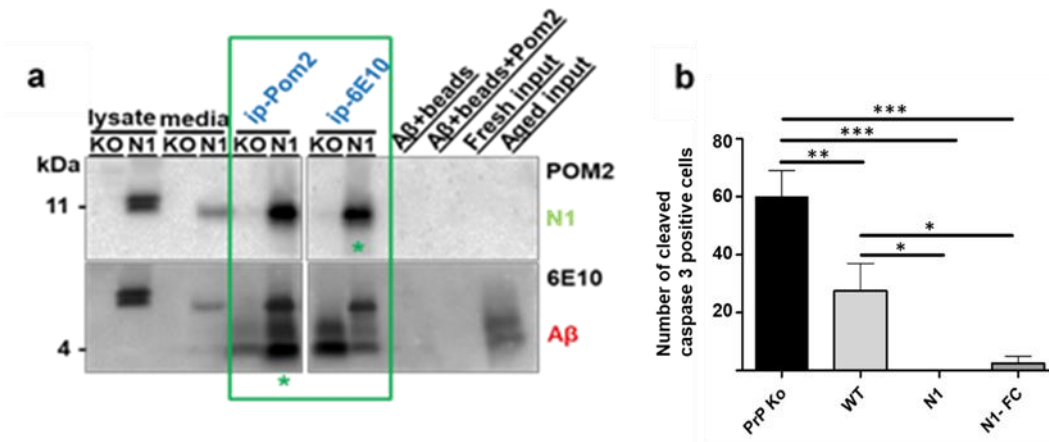

Figure 3.2: **Cell culture-based experiments on the N1/Aβ interaction and N1-mediated protection**. (a) Aβ binding assay was performed after incubating synthetic $A\beta_{42}$ with overnight conditioned media supernatants of N1-overexpressing versus PrP-KO N2a cells, demonstrating the N1/Aβ interaction (POM2: antibody against PrP/N1; 6E10: antibody against Aβ). the green asterisks refer to co-immunoprecipitated proteins (b) An Aβ toxicity assay was carried out after treating PrP-KO, WT, or N1/N1-Fc overexpressing N2a cells with synthetic $A\beta_{42}$. Read-out: Counting of cells stained positive for cleaved caspase 3 in immunocytochemistry.

3.3 Generation and characterization of TgN1 mice

One of the most important functions suggested for the N1 fragment of PrP^C is a neuroprotective action not only relevant in AD but also in other neurodegenerative conditions. Since the protease responsible for the α-cleavage of PrP^C has not been identified yet, to assess the role of N1 in prion diseases in detail, a transgenic mouse model (TgN1) stably overexpressing N1 was generated using the so called the half genomic PrP construct carrying the prion protein promoter (Fischer et al. 1996) on a wildtype (C57Bl/6) background (as endogenous expression of PrP^C is essential to study prion diseases (Bueler et al. 1993)). The construct was used for pronuclear injection of embryos at transgenic animal facility in ZMNH. Founders were then transferred to the UKE animal facility where a colony was established. General phenotypic characterization of these mice revealed no overt behavioral or phenotypic alterations based on body size and body weight (Figure 3.3a) compared to wildtype (WT) littermates. Copy number analysis of genomic DNA confirmed overexpression of the transgene in TgN1 mice (with a ΔΔCt value of -3.913 corresponding to a 15fold change). Transgenic overexpression was also confirmed by measuring mRNA levels in the cerebellum (TgN1: 2.34 ±0.38; WT set to 1.00 ±0.19; n=3; Figure 3.3b) and in the forebrain (TgN1: 3.41 ±0.58; WT set to 1.00 ±0.15; n=3;Figure 3.3c).
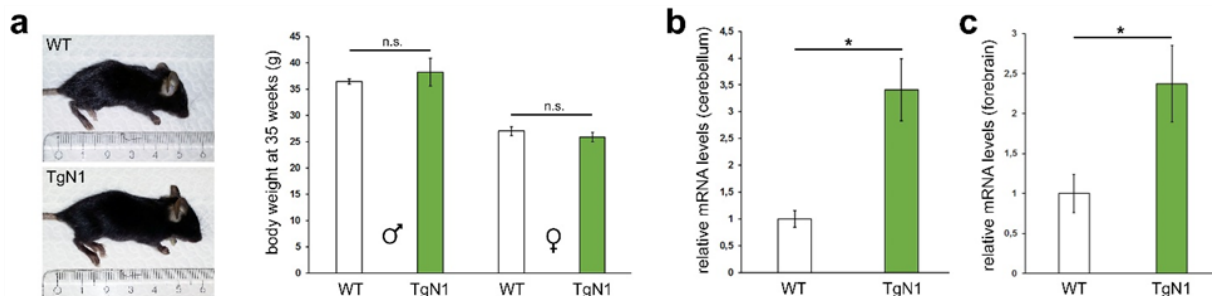

Figure 3.3: **Characterization of TgN1 mice**. (a) Body size (pictures on the left) and body weight measurements of male (♂) and female (♀) mice show no significant differences between age-matched TgN1 versus WT littermates (n=3). (b, c) RT-qPCR analysis in cerebellum (b) and forebrain homogenates (c) reveal higher PrP-N1 mRNA levels in TgN1 mice compared to WT control mice (n=3).

Furthermore, WB analysis of forebrain homogenates revealed a significant overexpression of N1 in both young TgN1 mice (8 weeks old mice, 3.8 ±0.14 for TgN1; WT set to 1.0 0 ±0.12; n=4; SEM; Figure 3.4a) and an even more pronounced overexpression in aged TgN1 mice (43 weeks: 5.2 ±0.44 for TgN1; WT set to 1.00 ±0.14; n=4; SEM; Figure 3.4b), whereas levels of full-length

(fl) PrP^C (which appears as a typical three banding pattern due to presence of un-, mono- and diglycosylated forms) and another PrP cleavage fragment of ~20 kDa (likely corresponding to N3 resulting from the recently described γ-cleavage (Lewis et al. 2016)) were both unchanged between genotypes (Figure 3.4 a&b). Of note, in contrast to endogenous N1 in WT brain homogenates, transgenic N1 appeared as a double band in the homogenates of TgN1 mice reminiscent of the finding in cell lysates (Figure 3.2a). This aspect will be further investigated and discussed below.
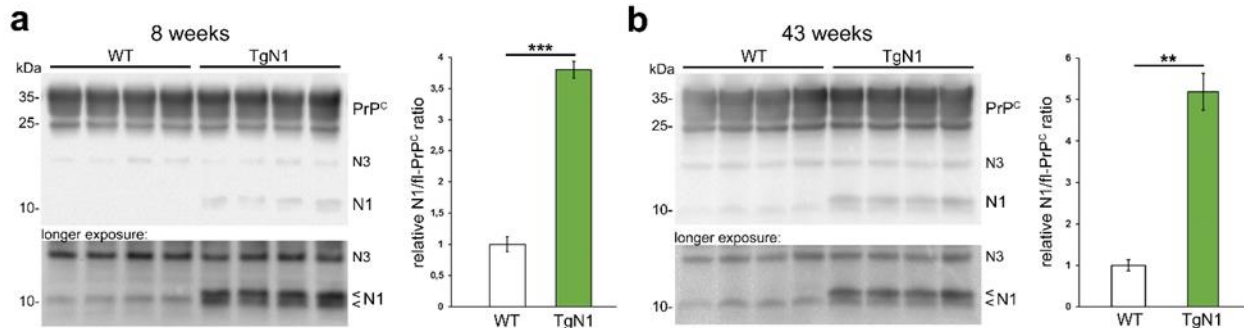

Figure 3.4: **Transgenic overexpression of N1 in TgN1 mouse brain homogenates:** Western blot analyses of forebrain samples of eight weeks-old mice (a; n=4; p=0.00001) and 43 weeks-old mice (b; n=4; p=0.0047) showing a higher N1 to fl-PrP ratio. POM2 antibody (directed against the N-terminal half of PrP^C) was used for detection. These data confirm the successful generation of transgenic mice overexpressing high levels of N1. The endogenous N3 fragment resulting from the recently described γ-cleavage of PrP^C is readily detectable in brain homogenates and, as fl-PrP^C, does not differ in amounts between both genotypes.

To further characterize the TgN1 mice under physiological conditions, signaling pathways known to be associated with PrP^C were investigated in forebrain homogenates of 43 weeks-old mice. Biochemical assessment of these samples revealed no alterations in the ratio of phosphorylated versus total levels of protein kinase B (Akt), eukaryotic initiation factor 2 (eIF2α), or Mitogen-activated protein kinase (MAP kinase) Erk1/2 (extracellular-signal-regulated kinases) and p38 (Figure 3.5).
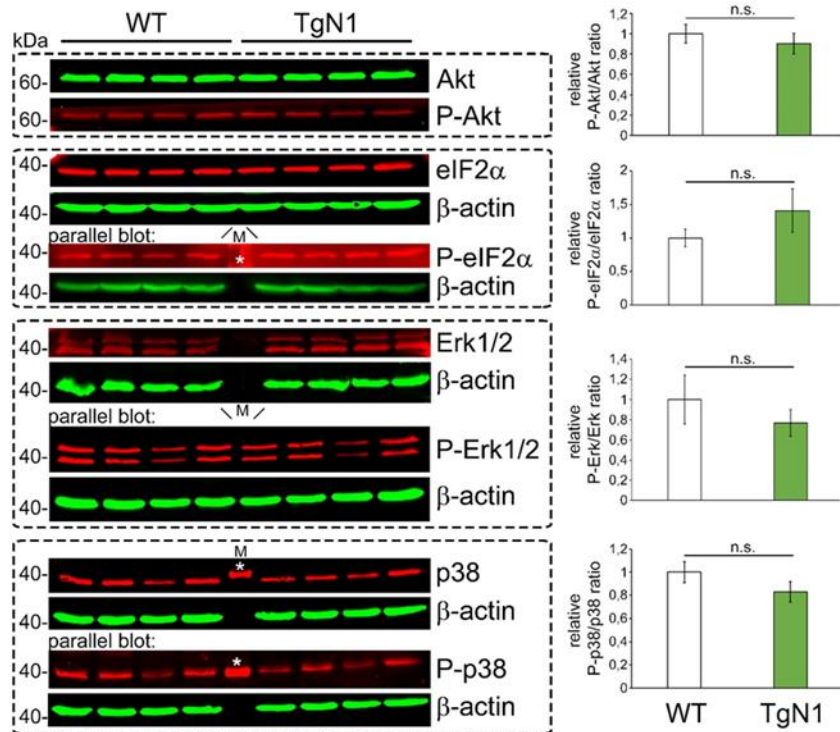
Figure 3.5: **No significant changes in candidate PrP-associated signaling pathways between TgN1 and WT mice**. Forebrain homogenates of 43 weeks-old mice were analyzed for the phosphorylation state of protein members of main signaling pathways related to the prion protein. No significant alterations between genotypes were observed for Akt, eIF2α, Erk1/2 and p38 under physiological conditions. Quantification of fluorescence signals (on the right) shows the direct ratio of phosphorylated (P) versus total levels for Akt which were detected on the same blot with antibodies from different species. When signals were detected on separate (replica) blots (eIF2α, Erk1/2 and p38), ratios were made after initial normalization to the corresponding β-actin signals. "M" indicates a molecular size marker lane in some of the blots located in the middle (which, in some cases highlighted by an asterisk, caused an unspecific signal in the red channel).

In addition, histological analysis showed no neuropathological alterations in the brains of eight weeks-old TgN1 mice compared to WT littermates in terms of overall brain morphology (HE staining), content and distribution of mature neurons (NeuN staining), and microglial activation (Iba1 staining) as shown here for cortical (Figure 3.6a) and cerebellar areas (Figure 3.6B). Similarly, no differences in the overall appearance of mature neurons (NeuN) or in the amount of Mib/Ki67-positive proliferating cells were found in the hippocampus (Figure 3.6c).
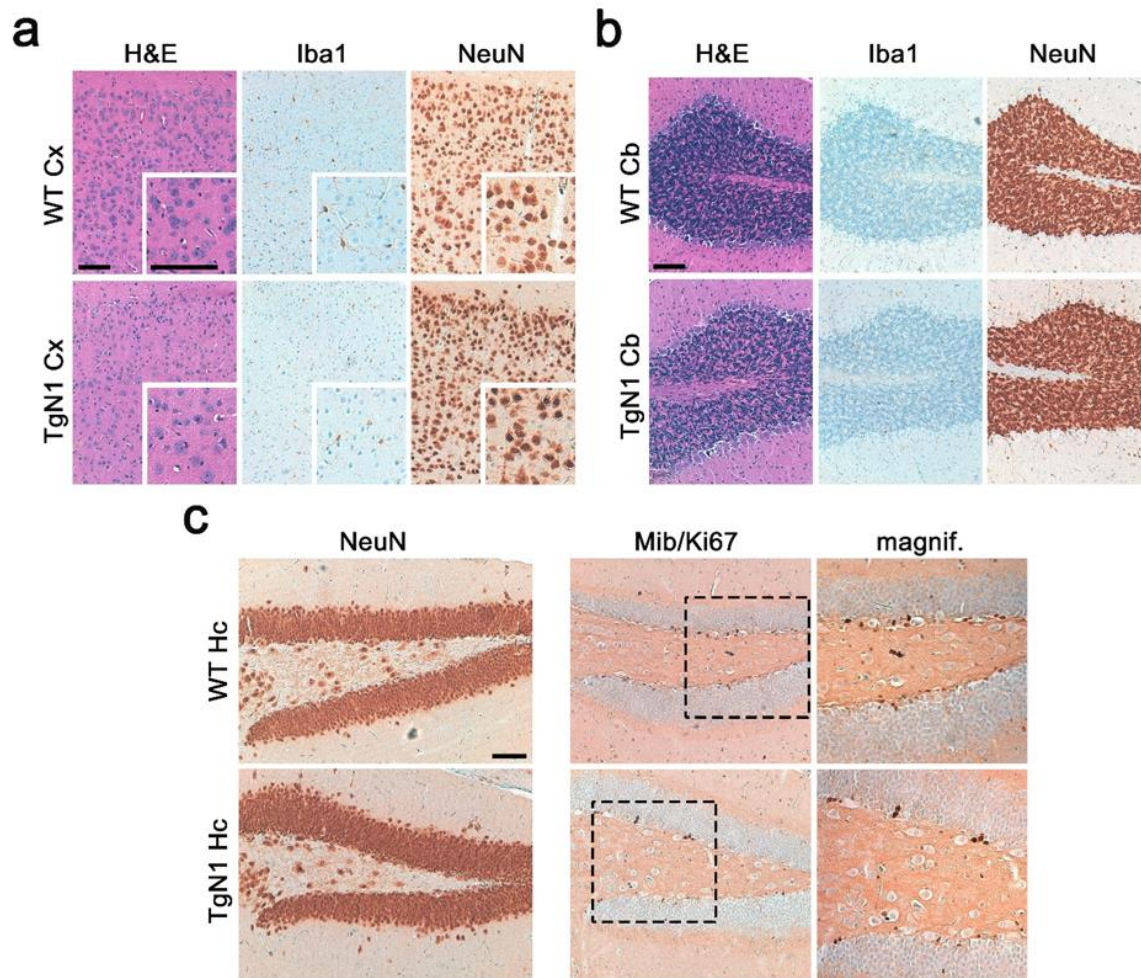
Figure 3.6: **No overt histological alterations in TgN1 mice**. (a, b) H&E staining and immunohistochemical analysis of microglia (Iba1) and neurons (NeuN) showed no obvious morphological alterations between eight weeks-old WT and TgN1 mice in cortical (Cx; in a) or cerebellar brain regions (Cb; in b). (c) Likewise, neuronal density (marker NeuN) and amounts of proliferating cells (assessed by the marker Mib/Ki67) were similar between both genotypes in the hippocampus (Hc). Scale bars = 100 µm.

3.4 Lack of protective effects against prions in TgN1 mice

After confirming expression of the N1 transgene, to study potentially neuroprotective effects of soluble N1 against prion disease, we performed intracerebral inoculations of mouse-adapted rocky mountains laboratories prions (RML) into six to eight weeks-old TgN1 mice and WT littermates, whereas negative controls of both genotypes were inoculated with a non-pathogenic control brain homogenate (CD1). Unexpectedly, mice of both genotypes showed equal incubation times and clinical signs typical for prion diseases and reached a terminal disease state at very similar time-

points (mean: TgN1+RML: 160 ±7 days; n=10; WT+RML: 159 ±9 days; n=9; SD), while the CD1 inoculated control group did not show any clinical signs until they were sacrificed at day 240 post inoculation (Figure 3.7a).

WB analysis was performed on the brain homogenates of terminal prion-diseased mice and CD1-inoculated control mice from both genotypes. Increased levels of total PrP species (including both PrP^C and PrP^{Sc}) and a shifted pattern of PrP glycoforms demonstrated the prion conversion in RML-infected mice of both genotypes compared to uninfected controls. Moreover, the appearance of SDS-stable oligomeric PrP conformations of higher molecular weight supported this finding (Figure 3.7b,c). Once more, a striking double band for N1 was apparent in the TgN1 brain samples, with the upper one running slightly higher than endogenous, proteolytically produced N1 in the WT mice (Figure 3.7b).
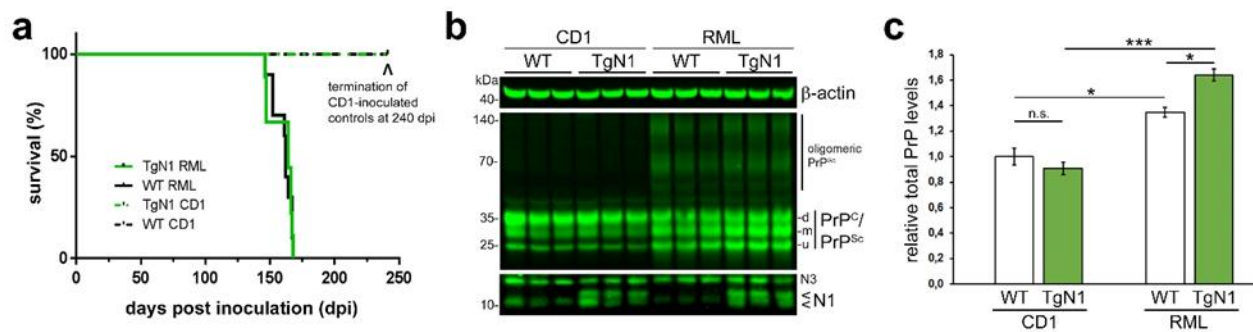

Figure 3.7: **Intracerebral prion inoculation of TgN1 and control mice**. (a) Kaplan-Meier survival curve of mice that underwent intracerebral inoculation with mouse-adapted RML prions. Similar incubation periods to terminal prion disease were detected for TgN1 (n=10) and WT littermates (n=9), whereas the mock-inoculated controls of each genotype (inoculated with CD1 brain homogenate) revealed no clinical signs until sacrification at 240 days post inoculation (n=4). (b) Western blot analysis of prion-infected versus non-infected forebrain homogenates from both genotypes showing an altered PrP glycosylation pattern, increased total PrP levels, and presence of oligomeric PrP^{Sc} forms in prion-infected samples compared to non-infected controls. (c) Quantification of as total PrP levels (i.e. PrP^C and PrP^{Sc}) with significant differences between infected samples from both genotypes (p=0.0167; n=3).

Noteworthy, slightly but significantly higher levels of total PrP were detected in infected TgN1 versus WT mice (TgN1+RML: 1.63 ±0.05; compared to WT+RML: 1.34 ±0.04; with non-infected WT +CD1 set to 1.00 ±0.07; n=3; SEM; Figure 3.7c). In line with this, digestion of brain homogenates with proteinase K (PK), which eliminates all available proteins in the sample except for the PK-resistant PrP^{Sc} molecules, showed higher PrP^{Sc} level in prion-infected TgN1 compared

to WT mice (TgN1+RML: 1.32 ±0.05; WT+RML set to 1.00 ±0.06; n=4; SEM; Figure 3.8). Thus, increased total PrP levels in TgN1 mice are likely due to slightly increased prion conversion in these animals.
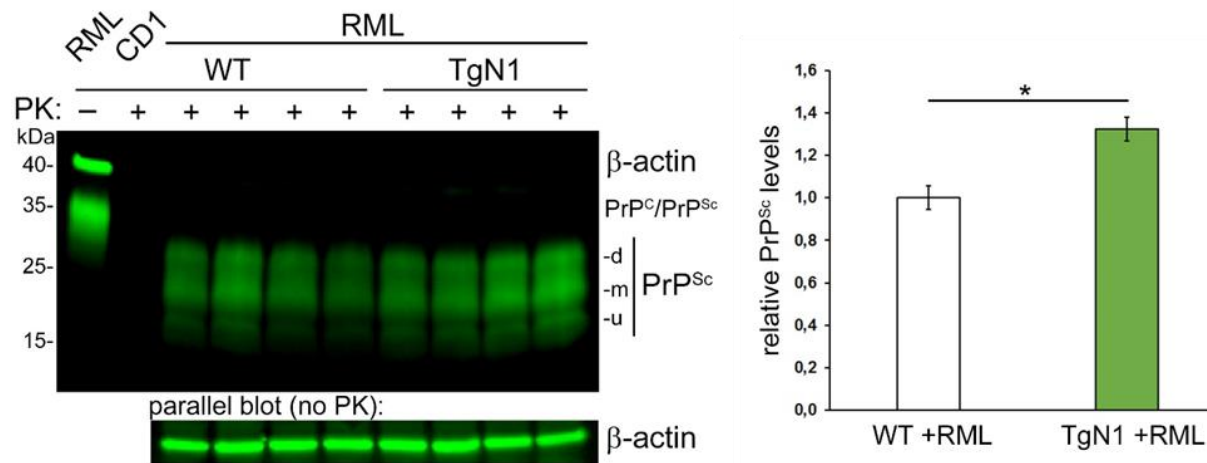

Figure 3.8: **Western blot analysis of PK-digested samples:** Brain homogenates of terminal prion-diseased mice of both genotypes were digested with proteinase K prior to analysis. Quantification was done by normalizing the PrP^{Sc} signals (probed with POM1 antibody) against actin from the parallel blot with non-PK-digested samples (n=4; p=0.0167). Technical controls (on the left) include a non-digested, RML-infected brain homogenate and a CD1-inoculated PK-digested brain sample. The shift in molecular weight of PrP (between the non-digested control and PK-digested samples) and the disappearance of the actin signal in all digested samples confirm successful enzymatic digestion.

Next, changes in the phosphorylation state of proteins from signaling pathways linked with PrP^{C} and shown to be affected in prion diseases were investigated in brain homogenates of WT and TgN1 mice inoculated with either infectious RML or non-pathogenic CD1 homogenates. For the MAP kinase Erk1/2 and the Akt kinase, there were no significant changes in phosphorylation state as a result of treatment or genotype (although Akt showed a tendency of activation upon prion infection). The Src kinase Fyn was significantly more phosphorylated in mice inoculated with RML prions (in both WT and TgN1 mice) compared to CD1 WT controls (Figure 3.9a). Of note, at terminal prion disease the MAP kinase p38 showed significantly higher phosphorylation/activation in TgN1 mice than in WT littermate controls (TgN1+RML: 2.49 ±0.26; WT+RML set to 1.00 ±0.07; n=4; SEM; Figure 3.9b). This difference between genotypes seems to specifically relate to the prion infection, as it was not detected under physiological conditions before (Figure 3.5)
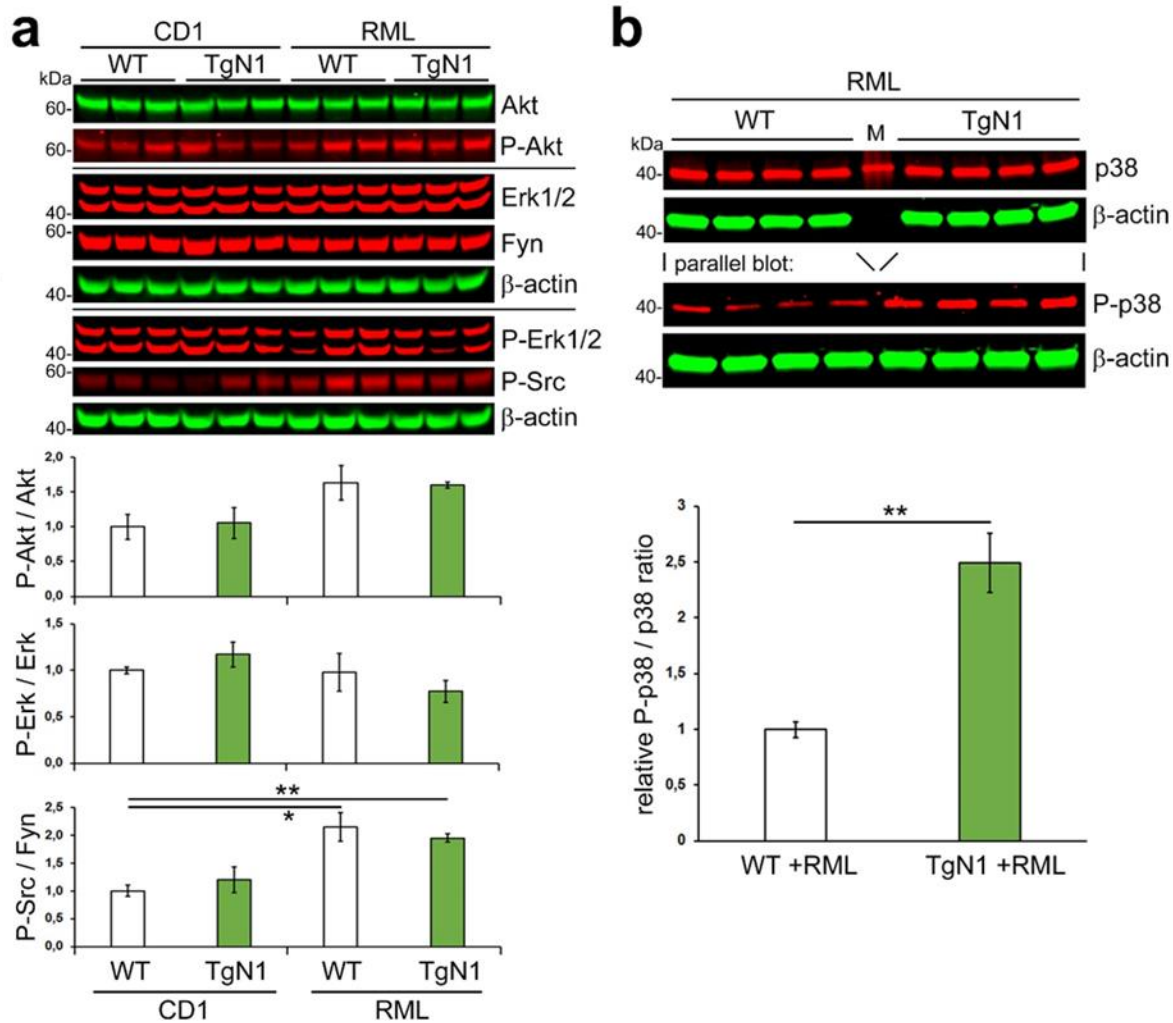
Figure 3.9: **Biochemical assessment of candidate signaling pathways associated with prion disease.** (a) No significant differences were detected in the phosphorylation state of Akt and Erk1/2 in prion-infected samples or between genotypes, whereas Src/Fyn was significantly more phosphorylated in prion-diseased animals of both genotypes (WT+CD1 vs. WT+RML: p=0.027; WT+CD1 vs. TgN1+RML: p=0.003; n=3). (b) The only signaling protein that showed a difference in activation between genotypes among the prion-inoculated animals was the MAP kinase p38, which was significantly more phosphorylated in TgN1 than in WT mice. (p=0.0032; n=4).

Next, neuropathological hallmarks of prion disease, such as astrogliosis, microglia activation, and spongiosis were investigated by (immuno)histological examination. In addition to the biochemical data presented above, these analyses also confirmed full establishment of prion disease in RML-infected mice compared to CD1-inoculated control mice, as they revealed prion-typical spongiform lesions in the brain parenchyma and strong activation/upregulation of both glial cell types in prion-

diseased mice. However, there were no overt differences between the two genotypes within the RML-infected animals (Figure 3.10).
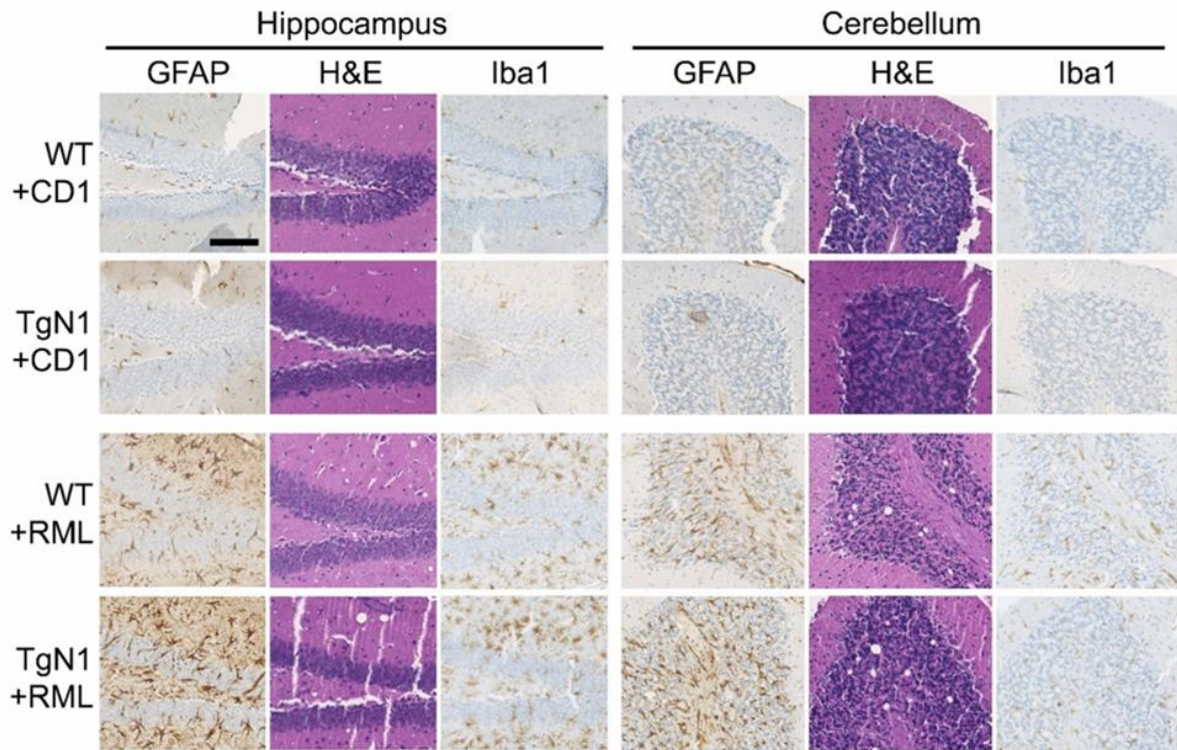

Figure 3.10: (Immuno-)histochemical assessment of spongiosis and glial activation in prion-infected versus CD1-inoculated control mice of both genotypes. In terminally diseased mice (+RML), astrocytes (marker: GFAP) and microglia (marker: Iba1) are highly upregulated in both TgN1 and WT mice compared to non-infected littermate controls (+CD1). Likewise, spongiosis (vacuoles detected in the H&E-stained sections) are only evident in prion-infected mice. Hippocampal and cerebellar areas are shown for representation. No overt alterations were observed between genotypes (n=4). Scale bar = 100 µm. Note that the tissue disruption apparent in some sections is due to technical issues during the staining process but does not affect the scientific conclusions.

In conclusion, contrasting our expectations, overexpression of N1 in the TgN1 mice did not show any protection against prion disease. In fact, PrP^{Sc} levels as well as p38 MAP kinase phosphorylation were even increased in terminally diseased TgN1 mice, although this moderate increase did not significantly alter the overall clinical course and incubation times compared to WT littermate controls. The likely reason for this lack of protection will be presented below (chapter 3.6).

3.5 Does overexpression of N1 protect neurons from the toxicity of Aβ?

It has been shown that the N1 fragment, upon release into the extracellular matrix, can bind with high affinity to Aβ oligomers (which are known to be the most toxic Aβ species), thereby blocking them and protecting neurons from Aβ-mediated toxicity (Resenberger et al. 2011). In this regard, the toxicity of Aβ oligomers, which first causes synaptic impairment followed by neuronal loss in neurodegenerative conditions, can be assessed at the synaptic level by quantification of the dendritic spines density (Fang et al. 2016). To study a potential neuroprotective effect of transgenic N1 overexpression against toxic Aβ entities by morphological means, low density cultures of primary neurons were prepared from TgN1 mice and WT littermates and co-cultured with a separately seeded astrocyte feeder layer to allow for extended culture time and promote neuronal maturation. Microscopic analysis of these neurons (Figure 3.11) did not show any differences in overall cellular or cytoskeletal morphology or density of dendritic spines (TgN1: 0.999 ±0.052; WT set to 1.00 ±0.092; SEM) between both genotypes when treated with solvent only (+mock; Figure 3.11a, c). Hence, overexpression of N1 in TgN1 does not cause any changes in these regards. However, after treatment with synthetic Aβ$_{42}$ (Figure 3.11b, c), dendritic spine density was significantly reduced compared to mock-treated neurons (with "WT+Aβ": 0.764 ±0.047 and "TgN1+Aβ": 0.665 ±0.055; SEM). However, no significant difference was detected between WT and TgN1 neurons treated with Aβ. This indicates that, similar to our findings in prion diseases mentioned above (chapter 3.4), transgenic overexpression of N1 does not confer protection against exogenously administered toxic proteopathic entities critically associated with neurodegenerative diseases.
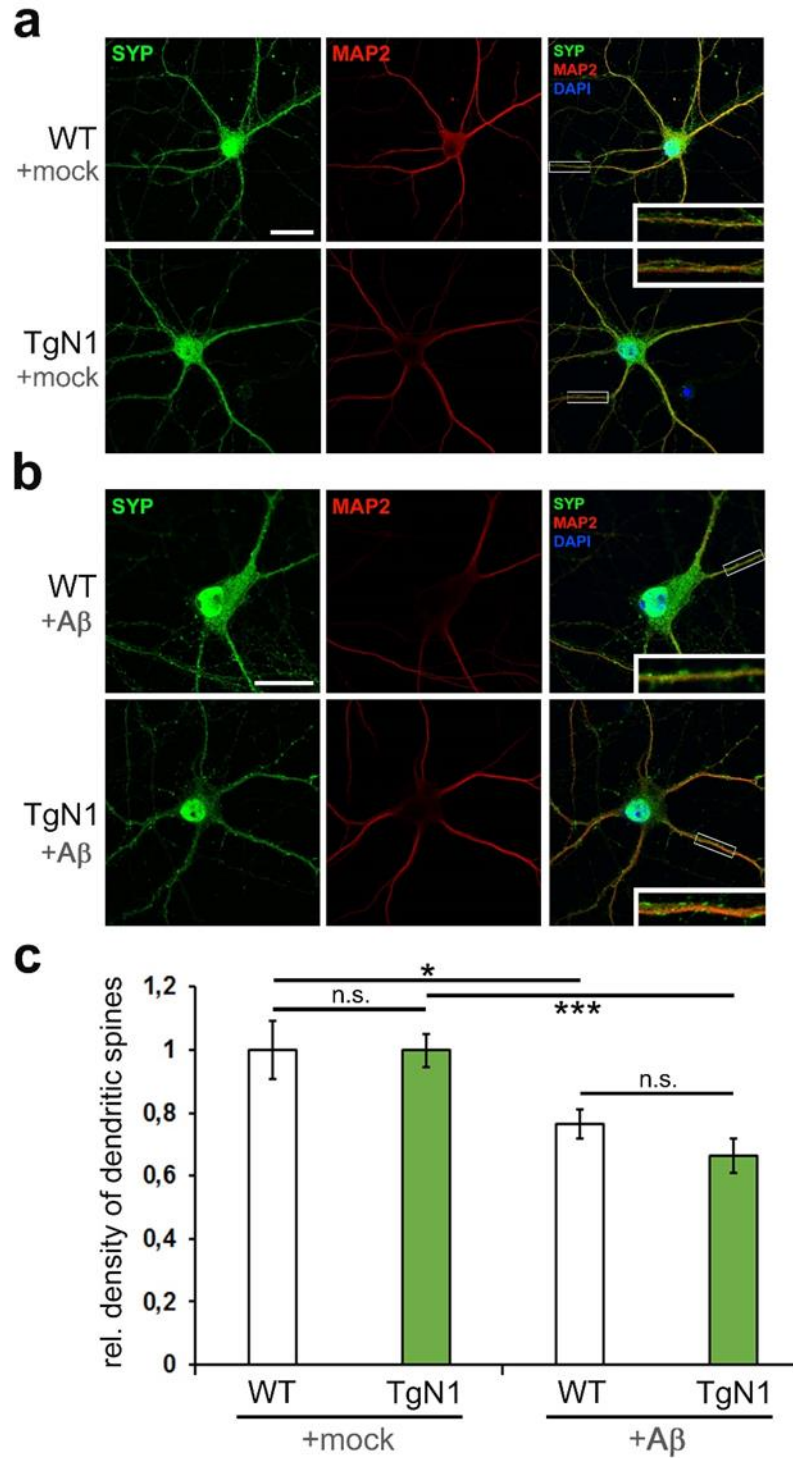
Figure 3.11: **Morphological assessment of primary neurons derived from TgN1 and control mice and analysis of Aβ toxicity.** (a, b) Representative images from primary neurons (co-cultured with an astrocyte feeder layer for two weeks prior to treatment) without (+mock; in a) and with overnight treatment with synthetic $A\beta_{42}$ (+Aβ; in b)revealed no difference in overall morphology and dendritic spines density between TgN1 and WT neurons. (c) Quantification of dendritic spine density using SynPanal software for primary neurons from both genotypes with and without $A\beta_{42}$ treatment. SYP = synaptophysin (green); MAP2 =

microtubule-associated protein 2 (red). (b, c) Treatment of neurons with toxic Aβ₄₂ resulted in a significant decrease in dendritic spine density compared to mock-treated controls (a, c) but no differences were found between treated neurons of both genotypes (b, c). Scale bar = 25 µm.

3.6 Impaired ER translocation of transgenic N1 results in its cytoplasmic retention

To our surprise, our protective strategy directed against proteopathic seeds by transgenic overexpression of N1 failed. But how can this lack of expected beneficial effects be explained? To answer this question, expression as well as the secretion levels of N1 was analysed in primary neurons isolated from both genotypes. WB analysis confirmed overexpression of the transgene and, again, presence of a double band in corresponding lysates of TgN1 neurons (Figure 3.12a), but surprisingly, no significant differences in the secreted levels of N1 in the conditioned media of TgN1 versus WT neurons were detected (TgN1: 0.75 ±0.17; WT set to 1.00 ±0.19; n=3; SEM; Figure 3.12). This indicated that transgenic N1 was not secreted but rather retained inside the cells and would be in strong agreement with recently published cell culture studies showing that proteins consisting exclusively of intrinsically disordered domains (IDDs), such as the N1 sequence, cannot efficiently translocate into the ER for secretion (Gonsberg et al. 2017; Heske et al. 2004; Miesbauer et al. 2009).

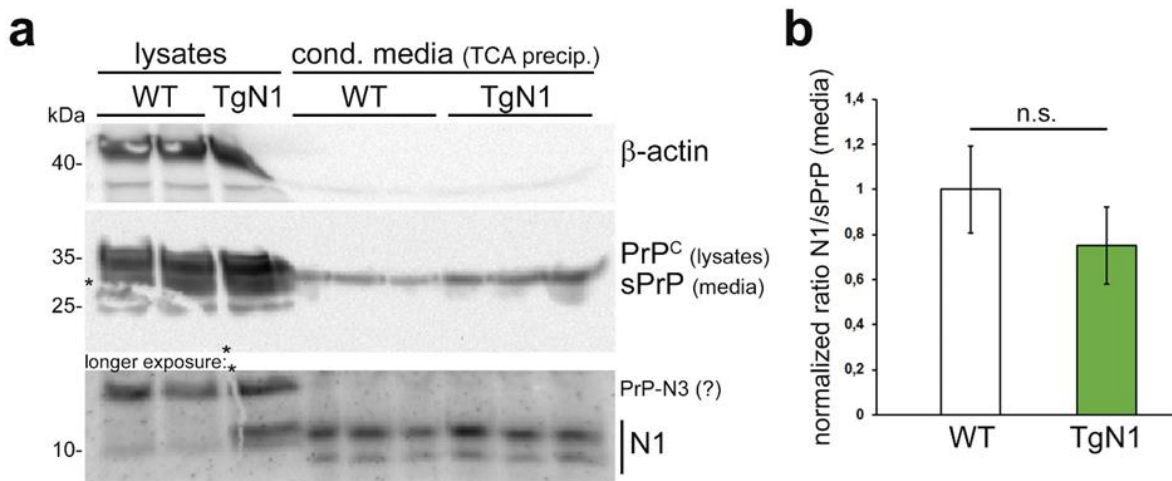Figure 3.12: **Transgenically expressed N1 is not secreted.** (a) Lysates and conditioned media of primary neurons (in mono-culture) from newborn WT and TgN1 mice (postnatal day 0 to 1) were biochemically analyzed for levels of N1 and PrP^C. While overexpression of N1 is confirmed in the lysates of TgN1 neurons, no increase in levels of secreted N1 is found in the respective media supernatants (n=3). Asterisks show

Based on these findings, we could expect transgenic N1 to be accumulated in the cytosol where it would eventually be degraded by the proteasome. To study this, we inhibited proteasomal degradation in primary neurons using MG132 and subsequently performed WB analyses (Figure 3.13). Indeed, this blockage of the proteasome (which was also confirmed by elevated levels of the cytosolic resident β-catenin) resulted in severe accumulation of N1, supporting the view that N1 is not transported into the ER but rather retained in the cytosol. Interestingly, this cytosolic accumulation of N1 likely explains the presence of the double band (also detected in various WB both in N1-transfected N2a cells (Figure 3.2a) and TgN1 mouse samples shown above (Figure 3.4a) with the lower band corresponding to bona fide N1 (~10 kDa), whereas the upper band represents N1 with uncleaved N-terminal ER-targeting signal peptide (N1-SP ~12 kDa). Lastly, TgN1 mice serve as the first *in Vivo* model for impaired ER translocation and secretion of IDDs, questions a relevant role of cytosolic prions in prion diseases, and highlight important aspects to be considered when investigating the α-cleavage of PrP^C and its fragment

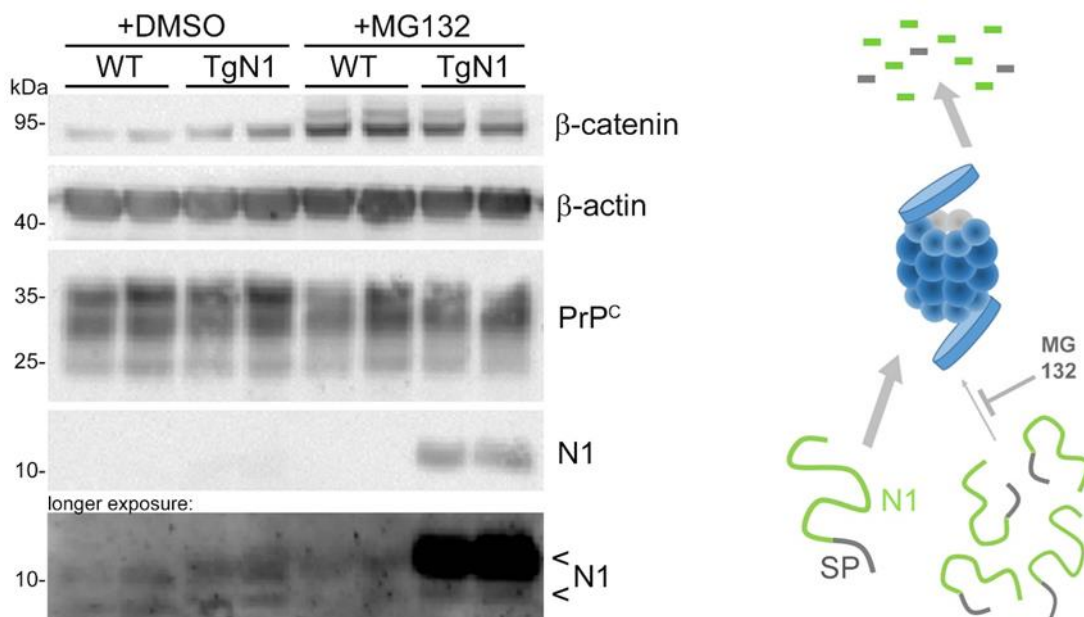Figure 3.13: **Proteasomal inhibition results in accumulation of N1 with uncleaved SP in the cytosol.** Primary neurons treated with proteasomal inhibitor (+MG132) or solvent only (+DMSO; as control) assessed by western blot analysis of lysates for expression levels of N1, PrP^C, β-catenin and β-actin. Note that, due to the low biostability of N1 leading to its fast degradation, detection of N1 occasionally needed longer

exposure. Blockage of the proteasomal degradation pathway resulted in a strong accumulation of N1 with an uncleaved signal peptide (SP) in the cytosol (diagram on the right; proteasome is depicted in blue).

3.7 Additional findings on N1 and the α-cleavage to be considered in future studies

Throughout this work on aspects related to N1 and the α-cleavage we also made observations that are of likely relevance for future studies on these topics and will briefly be presented here. For instance, a reliable detection of the N1 fragment in biochemical analyses has always been a challenging step for us and others in the field working on this small and unstructured soluble fragment. In fact, the reported (Yusa et al. 2012) low biostability and fast degradation of N1 upon release in biological samples make it difficult to work with it, to faithfully detect it and to study its physiological relevance, thus potentially providing a relevant hurdle for reproducibility between studies. To better understand the intricate nature of different N1 forms found in biochemical analyses presented here and elsewhere (Mange et al. 2004), we performed some experiments in murine neuroblastoma (N2a) cells. In WB analysis of cell lysates and conditioned media of cells, which had been frozen and thawed for a few times, N1 presented with several bands of slightly smaller molecular weight than the bona fide N1. By contrast, freshly prepared samples did not show such lower extra bands in our hands (e.g. Figure 3.2a for cells, Figure 3.4 for brain homogenates) and experiments of others (Beland et al. 2014; Miesbauer et al. 2009). This indicated that some (supposedly unspecific) proteolytic trimming events are taking place upon freezing and thawing.

We decided to further analyze this on endogenously produced N1 in the conditioned media of wild-type N2a cells. Interestingly, upon incubation of the culture media overnight with the 6D11 antibody directed against an epitope in the central part of fl-PrP^C (aa 93-110; which, upon α-cleavage, corresponds to the very C-terminal part of the N1 fragment), trimming of N1 to smaller fragments was completely blocked (Figure 3.14). In contrast, treatment with a negative control antibody (POM1 raised against the C-terminal half of PrP^C) did not interfere with this trimming process.

This finding revealed that, once N1 is released, it can be further cleaved and fragmented from its C-terminus, probably via unspecific cleavage by extracellular proteases. This may partially explain

the low biostability and fast degradation of N1. Of note, one of N1's described Aβ-binding sites is located exactly at very C-terminal end of N1 (aa 95-110(Laurén, David A Gimbel, et al. 2009)), and trimming may hence affect this interaction, highlighting the need of a C-terminal stabilizing modification when considering potential therapeutic options based on exogenous administration of N1 derivatives.
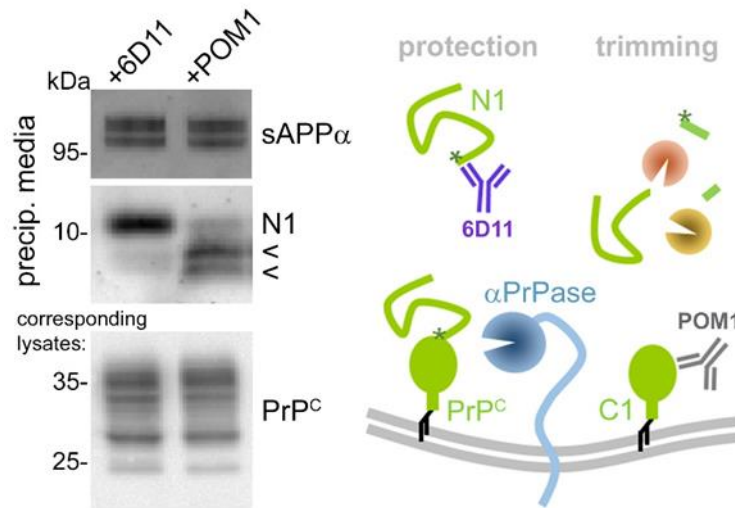

Figure 3.14: **Low biostability and fast degradation of N1 partially caused by C-terminal trimming events**. Western blot analysis of WT-N2a cells and conditioned media treated either with an antibody directed against the very C-terminus of N1 (6D11; epitope ranging from amino acid 93 to 109) or with an antibody against the globular C-terminal part of PrP^C (POM1). sAPPα, a fragment resulting from the non-amyloidogenic processing of APP, was detected as a loading control for media samples. N1 in media is detected as a clear single band at the expected size (~11 kDa) when cells were treated with 6D11, whereas in POM1-treated cells, fragmentation to lower molecular weight bands is observed. This clearly indicates a proteolytic trimming of N1 at its C-terminus once it is released from cells (scheme on the right).

Another characteristic of the α-cleavage that needs to be considered is the apparent tolerance of the responsible protease(s). Earlier studies have already pointed out that the relevant proteolytic entity is highly tolerant towards modifications at the cleavage site (Lutz et al. 2010; Oliveira-Martins et al. 2010), whereas one group suggested that the primary sequence around the cleavage site is of significant importance for the generation of N1 and C1 fragments and that a single amino acid substitution (H110Y) is sufficient to impair the cleavage (McDonald and Millhauser 2014). Therefore, we also mutated one amino acid at the suggested site (aa 110) from H to Y by site-directed mutagenesis. After transient transfection of N2a cells with either this PrP^C mutant (H110Y) or a WT-PrP^C construct, levels of the membrane-bound C1 fragment in the cell lysates

were assessed. For a clear detection of the C1 fragment, cell lysates were also digested with PNGase F in order to remove the N-linked glycans. In parallel, the N1 fragment was also detected in the corresponding conditioned media. In contrast to the study of McDonald et al, our WB analyses revealed no significant differences in the α-cleavage as assessed by the ratio of C1 to fl-PrP between the H110Y mutant and WT-PrP (WT set to 1, H110Y=1.16; SEM=0.12, n=3, *P=0.41*), thus rather confirming the earlier studies showing that α-cleavage is tolerant towards sequence modifications at the cleavage site (Figure 3.15).
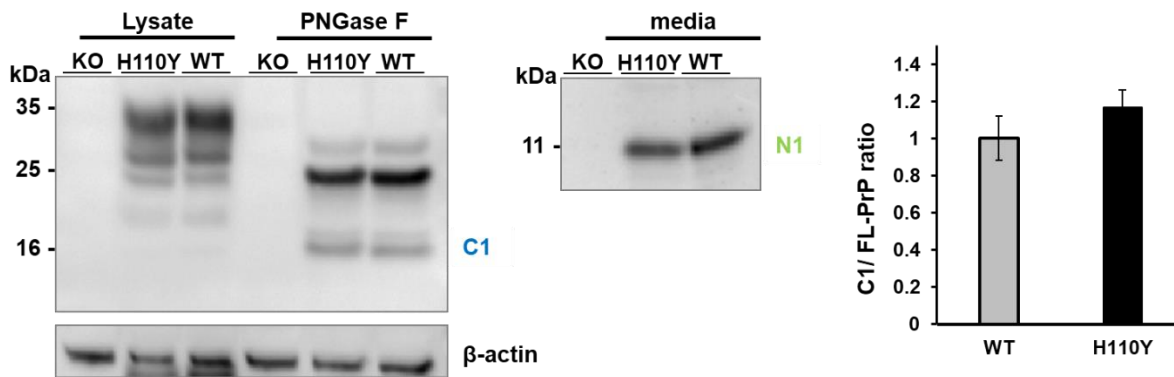

Figure 3.15: **The α-cleavage of PrP^C is tolerant towards modifications at the cleavage site**. Histidine at position 110 was substituted by tyrosine, as this modification (H110Y) was shown in one study to impair the α-cleavage. The blot (on the left) shows full-length PrP^C and its fragment (C1) before and after PNGase F digestion. Released N1 fragment was detected in the conditioned media (blot on the right). Quantification shows levels of the C1 fragment normalized to fl-PrP^C levels(n=3, *P=0.41*).

3.8 A promising solution: Successful generation of new transgenic mice expressing an N1-Fc fusion protein

The results obtained with our TgN1 mice represent the first *in vivo* proof of earlier studies showing that, for ER translocation to be successful and efficient, proteins need to present structural regions (such as α-helical domains) at one point in the growing peptide chain (Dirndorfer et al. 2013; Ziska et al. 2019). In the case of PrP^C, the structured C-terminal half fulfills these criteria (Heske et al. 2004), whereas expression of N1 alone, which lacks such elements, results in cytosolic accumulation as shown above (Figure 3.13).

Therefore, in order to study the neuroprotective effects of N1, an improved transgenic mouse model, which not only overexpresses but also secretes sufficient amounts of N1, was required and

had to take into account all considerations mentioned above. To overcome the lack of N1 secretion and to increase its biostability, we first carefully compared the expression of N1-fusion proteins in PrP-depleted N2a cells. As expected, in contrast to N1 alone, N1 fused either to the Fc region of an IgG (N1-Fc) or to a nanobody (N1-Nb) was efficiently secreted and readily detected in conditioned media (Figure 3.16). Of note, in addition to the respective full-length fusion proteins, we also detected signals at the expected size for N1 alone. This strongly suggests that α-cleavage or an α-cleavage-like proteolytic event can still take place, even if the C-terminal half of PrP^C is replaced by a completely different (though structured) protein. This finding further highlights the extreme tolerance of this cleavage event to significant modifications of the protein sequence described earlier (J B Oliveira-Martins et al. 2010).
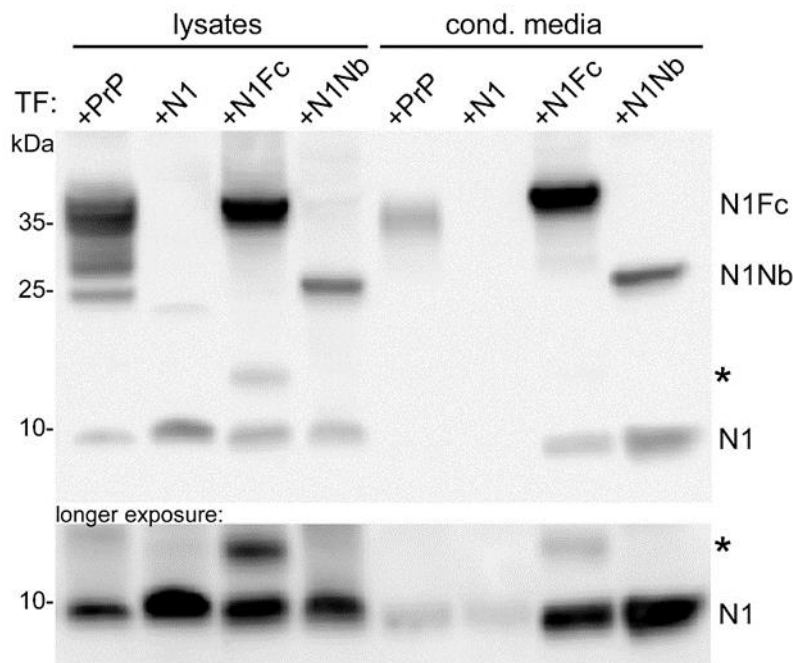
Figure 3.16: Western blot analysis of lysates and conditioned media of PrP-depleted N2a cells transfected with PrP, N1 or N1 fusion proteins. Expression levels of different N1 variants were analyzed upon transfection (TF) with constructs coding for full-length murine PrP (+PrP), N1 (+N1), or N1 fused either to an IgG Fc tag (+N1-Fc) or to a nanobody tag (+N1-Nb). In contrast to N1 alone (which rather accumulates inside the cells than being secreted), N1-Fc and N1-Nb are efficiently secreted into the media. Note that besides the full-length forms of both fusion proteins, an additional band corresponding to N1 was also observed. The asterisks indicate a band of unknown identity. Antibody used for detection: 6D11.

Lastly, the combination of N1 with Fc tag was considered to be a better option for generating the new mouse line, not only because of the higher expression/secretion of N1-Fc, but also because

future experiments may profit from the Fc tag for detection and purification, and the combination of a Fc tag with full-length PrP has been used before (Legname et al. 2002; Meier et al. 2003). In addition, by choosing a murine IgG Fc, we expected to minimize immunogenicity in mice. The new transgenic mice overexpressing N1 fused with a murine IgG1 Fc-tag (TgN1-Fc) were generated using the same half genomic PrP construct (used for TgN1 mice) after cloning the N1-Fc transgene into the construct.

TgN1Fc mice were generated by pronuclear injection of embryos at the transgenic animal facility at ZMNH. So far, these mice show no obvious phenotypic alteration and they breed normal. Initial biochemical characterization of mice was very recently performed by WB analysis of brain homogenates (Figure 3.17) showing successful expression of the fusion protein in TgN1-Fc mice.
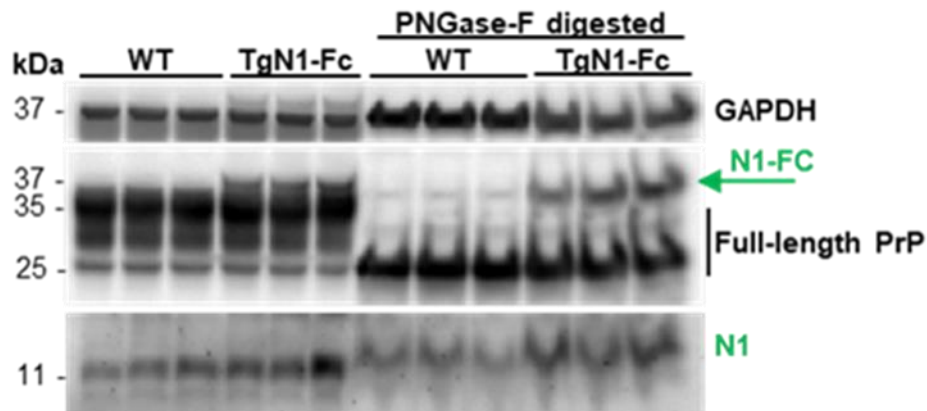
Figure 3.17: **Successful generation of N1-Fc-overexpressing (TgN1-Fc) mice**. Western blot analysis in forebrain homogenates from six weeks-old mice (n=3) indicating expression of the transgene in TgN1-Fc mice. Note that the N1-Fc fusion protein has almost the same molecular weight as di-glycosylated fl-PrP^C, thus causing the signals to partially overlap. Upon PNGase F digestion to remove glycans, the N1-Fc band (green arrow)becomes more clearly visible in TgN1-Fc mice.

4 Discussion

In my thesis, I aimed to investigating the protective effects of the prion protein N1 fragment against neurodegenerative diseases *in vivo*.

Under physiological conditions, the proteolytic α-cleavage is found to be the prominent processing event occurring on 5-50% of the PrP^C molecules depending on the cell type and brain region (Chen et al. 1995; Shyng et al. 1993), suggesting physiological relevance for this proteolytic cleavage and the resulting fragments. However, the protease responsible for this cleavage is still unknown. But it is known that α-cleavage is not dependent on cell membrane localization of PrP^C (Adrian R. Walmsley et al. 2009). In fact, this cleavage was suggested to take place in the late secretory pathway (A R Walmsley et al. 2009; Zhao et al. 2006), cleaving PrP^C in the middle of its amino acid sequence at position K110/H111 (Chen et al. 1995; Jimenez-Huete et al. 1998; Mange et al. 2004). As a consequence, the unstructured, flexible N-terminal half of the protein is released into the extracellular space and body fluids as a soluble N1 fragment, whereas the globular C-terminal part remains attached to the outer leaflet of the plasma membrane via its GPI-anchor (Figure 4.1).
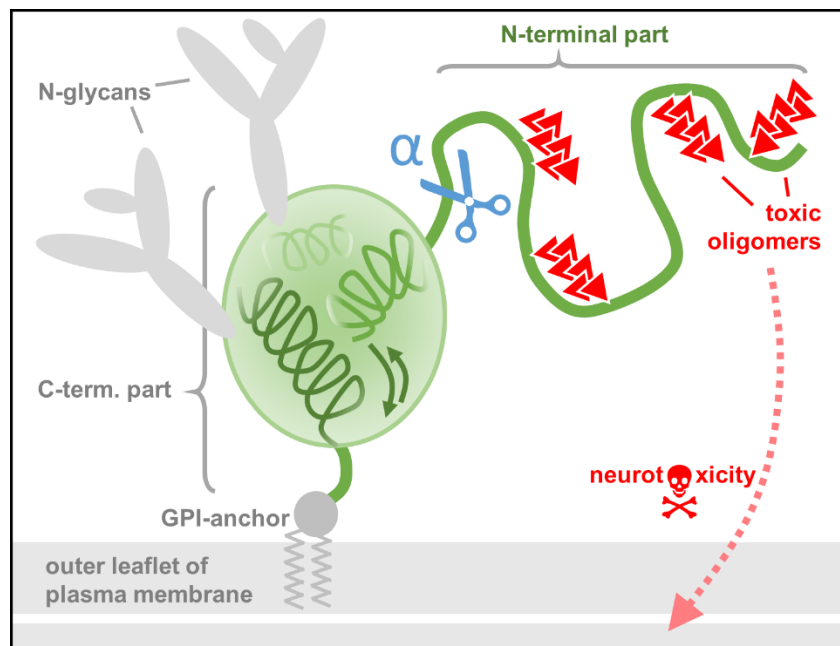
Figure 4.1: **Schematic representation of PrP^C**. The mature membrane-bound PrP^C is composed of two distinct structural parts. The C-terminal domain comprises three α-helices, a short β-sheet, up to two N-glycans and a GPI-anchor for anchorage to the outer leaflet of the plasma membrane. The unstructured and flexible N-terminal domain contains important binding sites for interaction with various molecules, such as toxic protein oligomers (red) found in neurodegenerative diseases. Having these binding sites, PrP^C can act as a receptor for toxic oligomers and triggers neurotoxic signaling events. A highly conserved proteolytic processing event, termed α-cleavage (blue) splits the two dissimilar halves of PrP^C resulting in C-terminal C1 fragment tethered to

outer leaflet of plasma membrane and the release of the flexible N1 fragment into the extracellular space, where it shows neuroprotective effects by blocking the toxic entities.

For the first time, Lauren *et al*. showed that PrP^C is a receptor for Aβ oligomers (the neurotoxic protein species involved in AD) and mediates the neurotoxicity of Aβ resulting in impaired hippocampal long term potentiation (Lauren et al. 2009). As such, the binding of Aβ oligomers to cell surface PrP^C provide important mechanistic insights into the pathophysiology of AD. In the present study, we could also confirm earlier in vitro studies showing the binding of Aβ to the N1 fragment, after Aβ treatment and immunoprecipitation of conditioned media from PrP-depleted N2a cells overexpressing N1. This supported the specific binding of synthetic Aβ$_{42}$ to the N1 fragment, which was produced in our cell culture model. However, there was also a weaker, probably non-specific band in PrP KO conditioned media after immunoprecipitation with Pom2 antibody (Figure 3.2a) which we believe is due to non-specific binding of Aβ to beads and tubes.

It was shown before in our group that the PrP^C-Aβ interaction always occurs in AD brains, whereas it was not seen in non-demented controls (Dohler et al. 2014). Importantly, both binding sites of PrP^C for Aβ oligomers are located within the N-terminal half (at amino acids 23-27 and 95-110) (Fluharty et al. 2013; Laurén, David A Gimbel, et al. 2009). In this regard, α-cleavage is expected to be protective, on the one hand by reducing membrane-bound full-length PrP (as the high affinity Aβ receptor at the neuronal surface) and, on the other hand, by releasing the soluble N1 fragment, which is capable of binding to the toxic Aβ oligomers in the extracellular space, thus preventing them from inducing neurotoxic signaling cascades in neurons (reviewed in (Altmeppen et al. 2013)). Interestingly, residues 23-31 of PrP^C are also a critical site for the initial binding of PrP^{Sc}, the pathogenic, misfolded form of the prion protein, and hence, are involved in the first steps in the templated conformational conversion underlying prion diseases (Turnbaugh et al. 2012). Consistent with this, Fang *et al*. showed that primary neurons from transgenic mice expressing N-terminally truncated forms of PrP^C (Δ23–31 and Δ23–111) are resistant to PrP^{Sc} toxicity, pinpointing an essential role for these residues in the pathogenesis of prion diseases (Fang et al. 2016). We therefore decided to investigate, whether the neuroprotective effect of N1, which has been mainly suggested in AD, also applies in prion diseases by interfering with the neurotoxicity and misfolding induced by critical seeds of PrP^{Sc}. We hypothesized that increased levels of N1 would interfere with prion conversion and prolong the incubation period of the disease and aimed for investigating this *in vivo*.

However, controversies regarding the identity of the endogenous α-PrPase responsible for the release of N1 impede the direct pharmaceutical targeting of this cleavage. Earlier studies suggested some members of the ADAM family of metalloproteases to be responsible for this cleavage, such as ADAM8 (which was proposed to be the α-PrPase at least in muscle tissue (Jingjing Liang et al. 2012) and ADAM10 (Cisse et al. 2005) and ADAM17 (also known as TACE) (Vincent et al. 2001). A later study in our group, while showing that ADAM10 is the sole sheddase of PrP challenged involvement of ADAM10 in the α-cleavage of PrP (Altmeppen et al. 2011). Therefore, with α-PrPase remaining unidentified it is difficult to manipulate levels and study the roles of released N1. To overcome this obstacle and to study in detail the potentially neuroprotective effects of N1 against toxicity of β-sheet rich oligomers in proteinopathies (such as Aβ$_{42}$ oligomers in AD and PrP^{Sc} in prion diseases), we aimed to overexpress N1 both *in vitro* and *in vivo.*

4.1   N1 and N1 fusion proteins can be expressed in N2a cells for *in vitro* study

In previous studies, the N1 fragment has been expressed with fusion tags, such as a GST tag (Guillot-Sestier et al. 2009). Alternatively, recombinant N1 protein has been used for *in vitro* experiments (Guillot-Sestier et al. 2009). In this thesis, I aimed to exclude any potential interference of a fusion tag with the bioactivity and structure of N1 *in vivo*, and to study a fragment most closely representing the natural form of N1 resulting from endogenous α-cleavage I therefore first cloned a construct coding for N1 alone without any additional tag. In addition, I generated other tagged N1 constructs with N1 fused to either an Fc part of a mouse IgG or to a nanobody tag, by using different cloning strategies in order to compare the expression and secretion levels of N1 versions in different experimental approaches. After transient transfection of PrP-depleted N2a cells with the N1-only construct, the level of expressed and secreted N1 was analyzed by western blot of cell lysates and of immunoprecipitated N1 from conditioned media. Although N1 appeared as a diffuse band (likely due to its described low biostability and fast degradation rate), this experiment showed that the construct was expressed and, importantly, indicated that N1 was also secreted by these neuronal cells (Figure 3.1a). The diffuse appearance of the band corresponding to N1 was improved later during this study by optimization in preparation, handling and analysis of the samples (i.e usage of 4-12 % gradient gels instead of commonly used hand-made 12 % continuous gels). These adjustments enabled us for a reliable and sensitive detection of the N1 fragment even in 50 µl of conditioned media without the need for an immunoprecipitation step.

The second fusion protein was produced using a Fc tag, a strategy that has been employed before by others in combination with the full-length PrP (Masel, Genoud, and Aguzzi 2004; Meier et al. 2003) and that is known for improving the secretion and biostability of a given protein while causing only low immunogenicity.

For expression of the N1 versions, the strong and commonly used CMV promotor was used in order to yield a robust overexpression of the transgenes. In the case of the N1-Nb constructs, two different ER signal peptides (SP) were used and the coding regions were cloned into different expression vectors. The reason for this was that the Nb coding sequence, which was initially cloned to be fused to the C-terminus of N1 in the pcDNA3.1 vector, resulted in very low expression level after transfection (Figure 3.1c). In contrast, the expression levels of either, N1 alone and Nb alone were comparably high. A possible explanation for this low expression of the fusion protein could be the relatively weak ER-targeting SP of murine PrP^C. Therefore, the N1 coding sequence was also cloned into a pCS3 vector placing it between the Nb sequence and the sequence of the Nb signal peptide Ig Kappa, which replaces the original murine SP with the more effective Nb signal peptide (Figure 3.1c).

Interestingly, upon expression in cells, a readily detectable portion of both N1-Nb and N1-Fc fusion proteins seem to undergo an α-cleavage-like event resulting in the appearance of three fragments: (i) the expected full-length fusion protein, (ii) a cleaved tag fragment, and (iii) a fragment likely corresponding to N1. This surprising observation may be considered as further evidence for the high tolerance of the α-cleavage towards even significant modifications at the cleavage site, which has been reported by others earlier (José B. Oliveira-Martins et al. 2010). Nevertheless, occurrence of α-cleavage on the overexpressed fusion proteins likely does not interfere with the overall experimental settings, as the major aim of this project was to increase levels of N1 in the extracellular space. Regarding the described high tolerance of the α-cleavage towards modifications (José B. Oliveira-Martins et al. 2010), we also showed that mutating an amino acid at the cleavage site does not stop and not even reduce the proteolytic processing rate (Figure 3.15 and Figure 4.2).
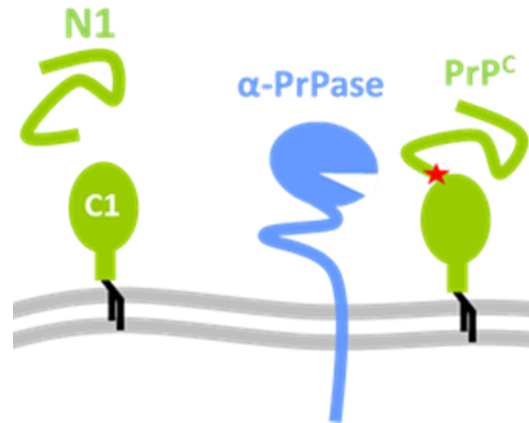
Figure 4.2: **High tolerance of α-PrPase towards modifications at the cleavage site**. In normal tissues and cells, PrP^C mainly cleaved at the 110/111 (of murine sequence)by an unknown protease(s). Inducing a mutation at the cleavage site did not affect the prevalence of the cleavage.

Detectable levels of N1 in the media of transfected N2a cells convinced us to continue using the "N1 alone strategy" for further experiments. In line with previous studies (Fluharty et al. 2013; Laurén, David A Gimbel, et al. 2009), our *in vitro* Aβ binding assay also confirmed the capability of N1 (expressed in n2a cells)to bind Aβ$_{42}$ oligomers (Figure 3.2a). Moreover, N1 overexpression was also neuroprotective in an Aβ neurotoxicity assay based on the assessment of activated, cleaved caspase 3 (Figure 3.2b), thus again confirming studies by others (Fluharty et al. 2013).

4.2 Generation of TgN1 mice for studying the protective effects of N1 in prion and Alzheimer's diseases

The need for a reliable mouse model for studying the neuroprotective potential of N1 against neurodegenerative diseases, such as prion diseases, and even against pathological conditions, like stroke, led us to generate TgN1 mice.. Different PrP KO mice lines have been generated in the past and all were resistant to prion diseases (Bueler et al. 1993; Steele, Lindquist, and Aguzzi 2007). This and several strong lines of evidence have shown that establishing prion disease requires expression of PrP^C at the cell surface of the host cells (Brandner et al. 1996; Chesebro et al. 2005), TgN1 mice were generated on a PrP WT background

The "half-genomic" mouse *Prnp* minigene containing the prion promoter and the *Prnp* open reading frame (Fischer et al. 1996) was used to generate TgN1 mice. The mice were successfully

generated (in the transgenic animal facility of the ZMNH/UKE) by pronuclear microinjection of embryos, resulting in a random integration of the transgene in variable copy numbers. Therefore, a pre-selection between different founders was required to select the ones with high expression. To do so, specific primers recognizing only the transgene but not the endogenous *Prnp* gene were required. This was especially difficult because the transgene has a sequence identical to the endogenous *Prnp* gene, but in the half-genomic construct, is lacking the introns. Profiting from this dissimilarity between gene and transgene, the primers for the genotyping were designed in a way to amplify a small part of exon 2 (i.e. the non-coding exon which is separated from coding exon 3 in the endogenous *Prnp* by a 6 kb intron (Westaway et al. 1994) until the middle of exon 3where the sequence coding for N1 ends. Using this strategy, the problem for genotyping was solved.

Two different founders (one with higher and the other with a mild expression of N1) were selected and maintained in two separate lines. As expected, transgenic N1 mice are viable, fertile and do not present any obvious phenotypical alteration even at very advanced age (some mice were maintained up to 72 weeks). This is particularly important, as some transgenic animals with mutations or truncated forms of PrP have been linked to neurodegenerative phenotypes (Hegde et al. 1999; Ma, Wollmann, and Lindquist 2002). Further characterization of TgN1 mice confirmed expression of the transgene at different levels, showing (i) higher copy numbers, (ii) increased levels of mRNA, and (iii) most importantly, increased protein levels of N1 in different brain regions (as it was shown in Figure 3.2, Figure 3.3 and Figure 3.4).

4.3   Unexpected outcomes from challenging TgN1 mice in disease conditions

While the natural transmission of most prion diseases occurs via peripheral infection, such as the oral route (Thackray, Klein, and Bujdoso 2003), the most efficient route for experimental initiation of CNS prion propagation and subsequent prion disease is by direct intracerebral inoculation with (host-adapted) prion strains (Bett et al. 2012). Notably, different prion strains represent different conformations of PrP^{Sc} which in turn result in differences in their biological properties such as incubation times (Safar et al. 1998; Tanaka et al. 2004). In the case of mouse-adapted RML prions, WT mice infected via intracerebral route show fully established prion disease and reach a terminal stage at about 150 days post inoculation (Altmeppen et al. 2015; Legname et al. 2005). Terminal

disease stage is defined by roughened fur, hind limbs clasping, hunched back, tail rigidity, weakness, ataxia and weight loss (Watts and Prusiner 2014).

Mice intracerebrally challenged with RML prions, showed no differences in the appearance of clinical signs of the disease compared to their WT littermate controls and reached a terminal stage of the disease at very similar time-points (Figure 3.7a and table 4.1). This result might, at first glance, indicate that overexpression of N1 in TgN1 mice is not protective against prion disease. But does this lack of protection really contradicting the beneficial effects of N1 against β-sheet rich oligomers or does it instead point towards a problem of our mouse model? This question was answered by investigating the secretion of N1 by primary neurons derived from TgN1 mice and their WT littermates. This analysis clearly showed that, while TgN1 neurons indeed express higher level of N1 (detected in lysates), there is no increased secretion into the culture media (Figure 3.12). Thus, transgenic N1 failed to traffic to the extracellular space where protective effects were expected to take place, and was instead retained in the cytosol (as will be discussed further in chapter 4.5).

Noteworthy, slightly yet significantly higher levels of total PrP (i.e. PrP^C and PrP^{Sc} including SDS-stable PrP^{Sc} oligomers of higher molecular weight) were detected in terminal prion-infected TgN1 mice compared to WT controls (Figure 3.8). In line with this, PK digestion of infected samples (which eliminates all proteins in the sample except for the PK-resistant PrP^{Sc} molecules) revealed increased PrP^{Sc} levels in prion-infected TgN1 mice (Figure 3.8). Thus, increased total PrP levels in TgN1 mice are likely due to slightly increased prion conversion in these animals.

Furthermore, assessment of candidate signaling pathways related to prion diseases showed higher levels of phosphorylated p38 MAP kinase in the brain samples of the prion-infected TgN1 mice. This could be due to higher levels of PrP^{Sc} in these animals (Fang et al. 2018; Puig et al. 2016). p38 MAPK is a stress-activated protein kinase, which is stimulated in different conditions of cellular stress (reviewed in (Cuadrado and Nebreda 2010), and has been implicated in a wide range of important functions, such as regulation of the cell cycle, induction of cell death, and cell differentiation. In the nervous system, p38 MAPK has been linked to neurodegenerative diseases by playing a role in neuronal damage and survival, as well as in synaptic plasticity (Corrêa and Eales 2012; Thomas and Huganir 2004)

4.4 Lack of N1-mediated protection against neurotoxicity of Aβ

Dendritic spines are very complex cellular structures and the contact sites for most excitatory synapses in the brain, which undergo continuous structural modification and remodeling during development, learning, and memory formation in response to a variety of stimuli (Fiala, Spacek, and Harris 2002; Herms and Dorostkar 2016; Siskova et al. 2013). Loss of dendritic spines precedes neuronal death, making dendritic spines an important locus in neurodegenerative diseases such as AD. (Herms and Dorostkar 2016). The existing literature states that N1 fragment in the extracellular space binds selectively and with high affinity to transient Aβ species (which is forming during the polymerization of this peptide into fibrils) and it thereby inhibits the polymerization process of Aβ (Fluharty et al. 2013). In this study, the neuroprotective effects of N1 against Aβ-mediated toxicity were assessed using a novel low-density co-culture of hippocampal neurons with a separate astrocyte feeder layer that recapitulates Aβ-induced synaptotoxicity and retraction of dendritic spines. Our results show that, while Aβ treatment of primary neurons does induce retraction of dendritic spines, there is no significant difference detectable between WT and TgN1 neurons treated with Aβ (Figure 3.11).

Our transgenic overexpression of N1 showed no protection, not only in prion diseased mice, but also against Aβ-mediated dendritic spine loss in primary neurons. It is noteworthy to state, that both experiments were conducted before the key experiment clarifying that transgenic N1 is not secreted. The failure of N1 to be secreted explains the lack of protective effect observed. A cell biological explanation of our "failed strategy" will be discussed in the following chapter. The existing literature states that N1 fragment in the extracellular space binds selectively and with high affinity to transient Aβ species (which form during the polymerization of Aβ into fibrils) and thereby inhibits the polymerization process of Aβ (Fluharty et al. 2013).

Nevertheless, we were able to establish the previously published neuron-astrocyte co-culture system (Kaech and Banker 2006) and used it in our study to confirm that quantitative analysis of dendritic spines can be used as a reliable method for studying neurotoxicity of Aβ at the synaptic level. The advantages of these low density cultures for morphological analysis of neurons are, that neurons can fully grow without overlapping each other, thus facilitating the visualization of single neurons. Moreover, co-culturing of neurons with astrocytes on a separated layer (without any physical interaction) provides neurons with important factors for growth and differentiation

helping them to mature and develop their morphology. This protocol also allows to keep neurons in culture for extended time periods (compared to neuronal monocultures). This is because astrocytes have important roles in the intercellular communication and development, support, and maintenance of the central nervous system, with functions including the secretion of growth factors and uptake of transmitters (Allen 2014; Clarke and Barres 2013; Perea, Navarrete, and Araque 2009).

The lack of protection in TgN1 mice is in contrary to what we saw initially in cell culture experiments. In fact, our *in vitro* experiments initially confirmed the binding of N1 to Aβ and also showed the neuroprotection of N1 against Aβ toxicity. However, we think the sufficient secretion levels of N1 in N2a cells could be due to transient transfection and strong CMV promoter, which may cause a unphysiologically high level of secretion of the transgene. After facing this problem with TgN1 mice, we immediately reacted by generating a second mice line overexpressing N1, but this time as a fusion protein using a Fc tag. The second line of transgenic mice can be used to answer the initial questions mentioned above, namely: Does overexpression of N1 change the disease course, PrP^{Sc} formation, propagation, and neurotoxicity of prion diseases? Does overexpression of N1 protect neurons from the neurotoxicity of Aβ?

4.5 Cytoplasmic retention of N1 due to impaired ER translocation

As pointed out above, further investigations revealed that the transgenic N1 is not secreted but retained inside the cell. This finding is in strong agreement with cell culture studies which showed that, during translation, those proteins lacking any structured domains, such as α-helices, and instead consisting solely of intrinsically disordered domains (IDDs), cannot efficiently translocate into the ER and, hence, cannot enter the secretory pathway in the first place (Figure 4.3) (Gonsberg et al. 2017; Heske et al. 2004; Miesbauer et al. 2009). Instead, such proteins are retained in the cytoplasm where they are subject to proteasomal degradation (Ma and Lindquist 2001). In the case of full-length PrP^C, the globular C-terminal half with its α-helices fulfills these criteria of structured domains. By contrast, in the case of N1 alone, structural elements are missing completely. Accordingly, N1 bands detected in conditioned media of primary neurons from both genotypes solely correspond to endogenous proteolytically generated N1 with no increased levels found for TgN1 neurons (Figure 3.12).

Figure 4.3: **Accumulation of N1 fragment with un-cleaved SP in cytosol**. Structural elements, such as α-helical domains, have to be present in the nascent chain for an efficient ER translocation of a given peptide by Sec61. Despite having a SP, the N1 fragment lacks any structured domain. Consequently, it retains in the cytosol. By contrast, the, addition of any alpha helical element to N1 will increase its translocational rate.

Cytosolic forms of PrP has been described (Mironov Jr. et al. 2003; Stewart and Harris 2003). These aberrant forms of PrP may result from pathogenic mutations, retrotranslocation from the ER in cellular stress conditions, or from inefficient ER translocation. Aggregation-prone cytPrP is constantly cleared by the proteasome, but if, this degradation system is impaired, the cytoplasmic accumulation of CytPrP occurs (Ashok and Hegde 2009; Ma et al. 2002; Orsi et al. 2006). Fittingly, upon proteasomal inhibition, we also observed drastic accumulation of N1. It has been shown in some studies that cytosolic PrP accumulates in cells upon treatment with proteasome inhibitors. This observation initially suggested that some molecules are retrotranslocated into the cytoplasm from the ER lumen as part of normal ER quality control mechanisms (Ma and Lindquist 2001; Ma et al. 2002; Yedidia et al. 2001). However, another study showed that cytosolic PrP molecules are untranslocated molecules that have never entered into the ER. It was even shown that this form of PrP contains an uncleaved N-terminal SP (Drisaldi et al. 2003). This is in line with our observation in this study that N1 accumulates in cytosol with an uncleaved SP in TgN1 primary neurons. This uncleaved SP form of N1 also explains the appearance of an additional band with slightly higher molecular weight than the bona fide N1.

4.6   Conclusion & future directions

There is no doubt that some of the suggested functions for PrP^C are mediated by the flexible N-terminal fragment, N1. Among them, neuroprotection of N1 against β-sheet rich oligomers like Aβ, seems to be a potential therapeutic strategy against neurodegenerative proteinopathies. However, it remained to be determined whether N1 indeed acts protective against toxicity and propagation of prions *in vivo*. Using our TgN1 mice model, this issue could not be answered due to the above mentioned, cytosolic retention of N1. Given that the proteasomal degradation is involved in PrP^{Sc} degradation, it is plausible that the massive overproduction and accumulation of cytosolic N1 reduces the efficiency of the proteasome to degrade PrP^{Sc}. In addition, activation of the MAP kinase p38 has been linked to the toxic signaling underlying prion diseases. Hence, it is likely that the increase in p38 phosphorylation in our TgN1 mice at the terminal stage of prion disease is a consequence of the elevated PrP^{Sc} levels.

Our TgN1 mice did not exhibit a neuroprotective effect against Aβ and could therefore prion diseases and AD. Nevertheless, it is still a valid model for studying the impaired translocation while having an ER-targeting signal constituting the first *in vivo* proof of what has previously been studied *in vitro*. For this, we are starting a new project in collaboration with experts at the University of Bochum to further investigate this matter.

The addition of a strong secretion tag seemed to be a promising strategy in generating a transgenicmice model that can secret the soluble N1. In fact, our preliminary data from characterization of TgN1Fc mice confirm that. These mice will soon be used for several studies on neurodegenerative diseases including prion diseases and AD as well as for hypoxic conditions like stroke. For the latter goal, we have already started a collaboration with the institute of Neurology at the UKE, in order to induce strokes in TgN1Fc mice. As overexpression of PrP has been shown to reduce the infarction area after stroke.

5 Summary

The highly conserved and constitutively active endogenous α-cleavage of the prion protein has so far mostly been linked to protective effects. As a soluble factor, the released unstructured N1 fragment acts beneficially in several ways. For instance, it reduces hypoxia-induced neuronal damage and is involved in myelin maintenance. Many studies have shown that N1 is able to block toxic oligomers, such as Aβ which is abundantly produced in Alzheimer`s disease, and interferes with their synaptic impairment and neurotoxicity.

However, for prion diseases, a potentially protective role of N1 by a similar mechanism neutralizing PrP^{Sc} oligomers and interfering with prion conversion has not been studied yet. Since the protease responsible for the α-cleavage has not been identified, pharmacological targeting of this entity is not yet possible. We therefore directly addressed this issue *in vivo* by generating transgenic mice (TgN1) overexpressing N1 on a wild-type background and challenging them with prions. Despite moderate differences in PrP^{Sc} formation and p38 activation, incubation times and disease duration were similar between TgN1 mice and wild-type littermate controls. Biochemical and morphological assessment of brain samples, primary neurons, and cell culture models then revealed that our direct "protective" strategy failed due to cytosolic accumulation and lack of secretion of the transgenic N1. Nevertheless, this work provides the first *in vivo* proof of the recently described impaired translocation of intrinsically disordered peptides into the endoplasmic reticulum. Moreover, it demonstrates the effects of cytosolic accumulation of N1 with uncleaved signal peptide, addresses proteasomal degradation, questions the general relevance of cytosolic prions in prion diseases, and highlights important aspects to be considered when investigating the α-cleavage of PrP^{C} or devising N1-based therapeutic approaches. To study the potential neuroprotective effect of N1 in the future, a second transgenic mouse model overexpressing N1 fused to a Fc tag was generated and its initial characterization will be provided here.

6 References

Abraham, Mary C. and Shai Shaham. 2004. "Death without Caspases, Caspases without Death." *Trends in Cell Biology*.

Adle-Biassette, Homa, Catherine Verney, Katell Peoc'h, Marie Christine Dauge, Férechté Razavi, Laurence Choudat, Pierre Gressens, Herbert Budka, and Dominique Henin. 2006. "Immunohistochemical Expression of Prion Protein (PrPC) in the Human Forebrain during Development." *Journal of Neuropathology and Experimental Neurology*.

Aguzzi, A. and A. M. Calella. 2009. "Prions: Protein Aggregation and Infectious Diseases." *Physiol Rev* 89(4):1105–52.

Aguzzi, A. and M. Heikenwalder. 2006. "Pathogenesis of Prion Diseases: Current Status and Future Outlook." *Nat Rev Microbiol* 4(10):765–75.

Allen, Nicola J. 2014. "Astrocyte Regulation of Synaptic Behavior." *Annual Review of Cell and Developmental Biology*.

Altmeppen, Hermann C., Johannes Prox, Susanne Krasemann, Berta Puig, Katharina Kruszewski, Frank Dohler, Christian Bernreuther, Ana Hoxha, Luise Linsenmeier, Beata Sikorska, Pawel P. Liberski, Udo Bartsch, Paul Saftig, Markus Glatze, and Markus Glatzel. 2015. "The Sheddase ADAM10 Is a Potent Modulator of Prion Disease." *ELife* 4.

Altmeppen, Hermann C., Johannes Prox, Berta Puig, Frank Dohler, Clemens Falker, Susanne Krasemann, and Markus Glatzel. 2013. "Roles of Endoproteolytic α-Cleavage and Shedding of the Prion Protein in Neurodegeneration." *FEBS Journal* 280(18):4338–47.

Altmeppen, Hermann C., Johannes Prox, Berta Puig, Mark A. Kluth, Christian Bernreuther, Dana Thurm, Ellen Jorissen, Bettina Petrowitz, Udo Bartsch, Bart De Strooper, Paul Saftig, and Markus Glatzel. 2011. "Lack of A-Disintegrin-and-Metalloproteinase ADAM10 Leads to Intracellular Accumulation and Loss of Shedding of the Cellular Prion Protein in Vivo." *Molecular Neurodegeneration* 6(1):36.

Altmeppen, Hermann C., Berta Puig, Frank Dohler, Dana K. Thurm, Clemens Falker, Susanne Krasemann, and Markus Glatzel. 2012. "Proteolytic Processing of the Prion Protein in Health and Disease." *American Journal of Neurodegenerative Disease* 1(1):15–31.

Alzheimer's, Association. 2016. "2016 Alzheimer's Disease Facts and Figures." *Alzheimers Dement* 12(4):459–509.

Anantharam, Vellareddy, Arthi Kanthasamy, Christopher J. Choi, Dustin P. Martin, Calivarathan Latchoumycandane, Jüergen A. Richt, and Anumantha G. Kanthasamy. 2008. "Opposing Roles of Prion Protein in Oxidative Stress- and ER Stress-Induced Apoptotic Signaling." *Free Radical Biology and Medicine*.

Ashok, A. and R. S. Hegde. 2009. "Selective Processing and Metabolism of Disease-Causing Mutant Prion Proteins." *PLoS Pathog* 5(6):e1000479.

Bakkebo, M. K., S. Mouillet-Richard, A. Espenes, W. Goldmann, J. Tatzelt, and M. A. Tranulis. 2015. "The Cellular Prion Protein: A Player in Immunological Quiescence." *Front Immunol* 6:450.

Barnewitz, K., M. Maringer, G. Mitteregger, A. Giese, U. Bertsch, and H. A. Kretzschmar. 2006. "Unaltered Prion Protein Cleavage in Plasminogen-Deficient Mice." *Neuroreport* 17(5):527–30.

Basler, K., B. Oesch, M. Scott, D. Westaway, M. Wälchli, D. F. F. Groth, M. P. P. McKinley, S. B. B. Prusiner, and C. Weissmann. 1986. "Scrapie and Cellular PrP Isoforms Are Encoded by the Same Chromosomal Gene." *Cell* 46(3):417–28.

Baumann, F., M. Tolnay, C. Brabeck, J. Pahnke, U. Kloz, H. H. Niemann, M. Heikenwalder, T. Rulicke, A. Burkle, and A. Aguzzi. 2007. "Lethal Recessive Myelin Toxicity of Prion Protein Lacking Its Central Domain." *Embo J* 26(2):538–47.

Beck, E., P. M. Daniel, D. M. Asher, D. C. Gajdusek, and C. J. Gibbs. 1973. "Experimental Kuru in the Chimpanzee. A Neuropathological Study." *Brain* 96:441–62.

Beland, M., M. Bedard, G. Tremblay, P. Lavigne, and X. Roucou. 2014. "Abeta Induces Its Own Prion Protein N-Terminal Fragment (PrPN1)-Mediated Neutralization in Amorphous

Aggregates." *Neurobiol Aging* 35(7):1537–48.

Beland, M. and X. Roucou. 2012. "The Prion Protein Unstructured N-Terminal Region Is a Broad-Spectrum Molecular Sensor with Diverse and Contrasting Potential Functions." *J Neurochem* 120(6):853–68.

Béland, Maxime, Mikaël Bédard, Guillaume Tremblay, Pierre Lavigne, and Xavier Roucou. 2014. "Aβ Induces Its Own Prion Protein N-Terminal Fragment (PrPN1)–Mediated Neutralization in Amorphous Aggregates." *Neurobiology of Aging* 35(7):1537–48.

Belay, E. D. 1999. "Transmissible Spongiform Encephalopathies in Humans." *Annu Rev Microbiol* 53:283–314.

Bendheim, P. E., H. R. Brown, R. D. Rudelli, L. J. Scala, N. L. Goller, G. Y. Wen, R. J. Kascsak, N. R. Cashman, and D. C. Bolton. 1992. "Nearly Ubiquitous Tissue Distribution of the Scrapie Agent Precursor Protein." *Neurology* 42(1):149–149.

Beraldo, Flavio H., Camila P. Arantes, Tiago G. Santos, Cleiton F. Machado, Martin Roffe, Gláucia N. Hajj, Kil S. Lee, Ana C. Magalhães, Fabiana A. Caetano, Gabriel. L. Mancini, Marilene H. Lopes, Tatiana A. Américo, Margaret H. Magdesian, Stephen S. G. Ferguson, Rafael Linden, Marco A. M. Prado, and Vilma R. Martins. 2011. "Metabotropic Glutamate Receptors Transduce Signals for Neurite Outgrowth after Binding of the Prion Protein to Laminin Γ1 Chain." *The FASEB Journal* 25(1):265–79.

Bertuchi, Fernanda R., Dominique M. G. Bourgeon, Michele C. Landemberger, Vilma R. Martins, and Giselle Cerchiaro. 2012. "PrPC Displays an Essential Protective Role from Oxidative Stress in an Astrocyte Cell Line Derived from PrPC Knockout Mice." *Biochemical and Biophysical Research Communications* 418(1):27–32.

Bett, Cyrus, Shivanjali Joshi-Barr, Melanie Lucero, Margarita Trejo, Pawel Liberski, Jeffery W. Kelly, Eliezer Masliah, and Christina J. Sigurdson. 2012. "Biochemical Properties of Highly Neuroinvasive Prion Strains." *PLoS Pathogens*.

Borchelt, D. R., M. Rogers, N. Stahl, G. Telling, and S. B. Prusiner. 1993. "Release of the Cellular Prion Protein from Cultured Cells after Loss of Its Glycoinositol Phospholipid Anchor."

Glycobiology 3(4):319–29.

Brandner, S., S. Isenmann, A. Raeber, M. Fischer, A. Sailer, Y. Kobayashi, S. Marino, C. Weissmann, and A. Aguzzi. 1996. "Normal Host Prion Protein Necessary for Scrapie-Induced Neurotoxicity." *Nature* 379(6563):339–43.

Bremer, J., F. Baumann, C. Tiberi, C. Wessig, H. Fischer, P. Schwarz, A. D. Steele, K. V Toyka, K. A. Nave, J. Weis, and A. Aguzzi. 2010. "Axonal Prion Protein Is Required for Peripheral Myelin Maintenance." *Nat Neurosci* 13(3):310–18.

Bribián, Ana, Xavier Fontana, Franc Llorens, Rosalina Gavín, Manuel Reina, José Manuel García-Verdugo, Juan María Torres, Fernando de Castro, and José Antoniol del Río. 2012. "Role of the Cellular Prion Protein in Oligodendrocyte Precursor Cell Proliferation and Differentiation in the Developing and Adult Mouse CNS." *PLoS ONE*.

Brown, D. R. and C. M. Mohn. 1999. "Astrocytic Glutamate Uptake and Prion Protein Expression." *Glia* 1(25):3.

Brown, D. R., W. J. Schulz-Schaeffer, B. Schmidt, and H. A. Kretzschmar. 1997. "Prion Protein-Deficient Cells Show Altered Response to Oxidative Stress Due to Decreased SOD-1 Activity." *Exp Neurol* 146(1):104–12.

Budka, H. 2003. "Neuropathology of Prion Diseases." *Br Med Bull* 66:121–30.

Bueler, H., A. Aguzzi, A. Sailer, R. A. Greiner, P. Autenried, M. Aguet, and C. Weissmann. 1993. "Mice Devoid of PrP Are Resistant to Scrapie." *Cell* 73(7):1339–47.

Büeler, H., A. Aguzzi, A. Sailer, R. A. Greiner, P. Autenried, M. Aguet, C. Weissmann, H. Bueler, A. Aguzzi, A. Sailer, R. A. Greiner, P. Autenried, M. Aguet, and C. Weissmann. 1993. "Mice Devoid of PrP Are Resistant to Scrapie." *Cell* 73(7):1339–47.

Büeler, Hansruedi, Marek Fischer, Yolande Lang, Horst Bluethmann, Hans Peter Lipp, Stephen J. Dearmond, Stanley B. Prusiner, Michel Aguet, and Charles Weissmann. 1992. "Normal Development and Behaviour of Mice Lacking the Neuronal Cell-Surface PrP Protein." *Nature* 356(6370):577–82.

Caetano, F. A., M. H. Lopes, G. N. Hajj, C. F. Machado, C. Pinto Arantes, A. C. Magalhaes, P. Vieira Mde, T. A. Americo, A. R. Massensini, S. A. Priola, I. Vorberg, M. V Gomez, R. Linden, V. F. Prado, V. R. Martins, and M. A. Prado. 2008. "Endocytosis of Prion Protein Is Required for ERK1/2 Signaling Induced by Stress-Inducible Protein 1." *J Neurosci* 28(26):6691–6702.

Caughey, B., G. J. Raymond, D. Ernst, and R. E. Race. 1991. "N-Terminal Truncation of the Scrapie-Associated Form of PrP by Lysosomal Protease(s): Implications Regarding the Site of Conversion of PrP to the Protease-Resistant State." *J Virol* 65(12):6597–6603.

Checler, F. 2012. "Two-Steps Control of Cellular Prion Physiology by the Extracellular Regulated Kinase-1 (ERK1)." *Prion* 6(1):23–25.

Chen, S. G., D. B. Teplow, P. Parchi, J. K. Teller, P. Gambetti, and L. Autilio-Gambetti. 1995. "Truncated Forms of the Human Prion Protein in Normal Brain and in Prion Diseases." *The Journal of Biological Chemistry* 270(32):19173–80.

Chen, S., S. P. Yadav, and W. K. Surewicz. 2010. "Interaction between Human Prion Protein and Amyloid-Beta (Abeta) Oligomers: Role OF N-Terminal Residues." *J Biol Chem* 285(34):26377–83.

Chesebro, B., M. Trifilo, R. Race, K. Meade-White, C. Teng, R. LaCasse, L. Raymond, C. Favara, G. Baron, S. Priola, B. Caughey, E. Masliah, and M. Oldstone. 2005. "Anchorless Prion Protein Results in Infectious Amyloid Disease without Clinical Scrapie." *Science* 308(5727):1435–39.

Chung, E., Y. Ji, Y. Sun, R. J. Kascsak, R. B. Kascsak, P. D. Mehta, S. M. Strittmatter, and T. Wisniewski. 2010. "Anti-PrPC Monoclonal Antibody Infusion as a Novel Treatment for Cognitive Deficits in an Alzheimer's Disease Model Mouse." *BMC Neurosci* 11:130.

Cisse, M. A., C. Sunyach, S. Lefranc-Jullien, R. Postina, B. Vincent, and F. Checler. 2005. "The Disintegrin ADAM9 Indirectly Contributes to the Physiological Processing of Cellular Prion by Modulating ADAM10 Activity." *J Biol Chem* 280(49):40624–31.

Clarke, Laura E. and Ben A. Barres. 2013. "Emerging Roles of Astrocytes in Neural Circuit

Development." *Nature Reviews Neuroscience*.

Cohen, F. E. and S. B. Prusiner. 1998. "Pathologic Conformations of Prion Proteins." *Annu Rev Biochem* 67:793–819.

Cohen, Fred E., Keh Ming Pan, Ziwei Huang, Michael Baldwin, Robert J. Fletterick, and Stanley B. Prusiner. 1994. *Structural Clues to Prion Replication*. Vol. 264.

Collinge, J. and A. R. Clarke. 2007. "A General Model of Prion Strains and Their Pathogenicity." *Science* 318(5852):930–36.

Collins, S. J., C. L. Haigh, V. A. Lewis, L. J. Vella, C. L. Masters, A. F. Hill, V. A. Lawson, and S. J. Collins. 2009. "PrPC-Related Signal Transduction Is Influenced by Copper, Membrane Integrity and the Alpha Cleavage Site." *Cell Research* 19(9):1062–78.

Corrêa, Sônia A. L. and Katherine L. Eales. 2012. "The Role of P38 MAPK and Its Substrates in Neuronal Plasticity and Neurodegenerative Disease." *Journal of Signal Transduction*.

Cuadrado, Ana and Angel R. Nebreda. 2010. "Mechanisms and Functions of P38 MAPK Signalling." *Biochemical Journal*.

D'Souza-Schorey, Crislyn, Elly van Donselaar, Victor W. Hsu, Chunzhi Yang, Philip D. Stahl, and Peter J. Peters. 1998. "ARF6 Targets Recycling Vesicles to the Plasma Membrane: Insights from an Ultrastructural Investigation." *The Journal of Cell Biology* 140(3):603–16.

Danielson, E. and S. H. Lee. 2014. "SynPAnal: Software for Rapid Quantification of the Density and Intensity of Protein Puncta from Fluorescence Microscopy Images of Neurons." *PLoS ONE* 9(12):e115298.

Deleault, N. R., B. T. Harris, J. R. Rees, and S. Supattapone. 2007. "Formation of Native Prions from Minimal Components in Vitro." *Proc Natl Acad Sci U S A* 104(23):9741–46.

Dirndorfer, Daniela, Ralf P. Seidel, Guy Nimrod, Margit Miesbauer, Nir Ben-Tal, Martin Engelhard, Richard Zimmermann, Konstanze F. Winklhofer, and Joŗg Tatzelt. 2013. "The α-Helical Structure of Prodomains Promotes Translocation of Intrinsically Disordered Neuropeptide Hormones into the Endoplasmic Reticulum." *Journal of Biological Chemistry*.

Dohler, Frank, Diego Sepulveda-Falla, Susanne Krasemann, Hermann Altmeppen, Hartmut Schlüter, Diana Hildebrand, Inga Zerr, Jakob Matschke, and Markus Glatzel. 2014. "High Molecular Mass Assemblies of Amyloid-β Oligomers Bind Prion Protein in Patients with Alzheimer's Disease." *Brain*.

Drisaldi, Bettina, Richard S. Stewart, Cheryl Adles, Leanne R. Stewart, Elena Quaglio, Emiliano Biasini, Luana Fioriti, Roberto Chiesa, and David A. Harris. 2003. "Mutant PrP Is Delayed in Its Exit from the Endoplasmic Reticulum, but Neither Wild-Type nor Mutant PrP Undergoes Retrotranslocation Prior to Proteasomal Degradation." *Journal of Biological Chemistry* 278(24):21732–43.

Dupiereux, Ingrid, Nandini Falisse-Poirrier, Willy Zorzi, Nicole T. Watt, Olivier Thellin, Danièle Zorzi, Olivier Pierard, Nigel M. Hooper, Ernst Heinen, and Benaïssa Elmoualij. 2008. "Protective Effect of Prion Protein via the N-Terminal Region in Mediating a Protective Effect on Paraquat-Induced Oxidative Injury in Neuronal Cells." *Journal of Neuroscience Research*.

Durig, J., A. Giese, W. Schulz-Schaeffer, C. Rosenthal, U. Schmucker, J. Bieschke, U. Duhrsen, and H. A. Kretzschmar. 2000. "Differential Constitutive and Activation-Dependent Expression of Prion Protein in Human Peripheral Blood Leucocytes." *Br J Haematol* 108(3):488–95.

Endres, K., G. Mitteregger, E. Kojro, H. Kretzschmar, and F. Fahrenholz. 2009. "Influence of ADAM10 on Prion Protein Processing and Scrapie Infectiosity in Vivo." *Neurobiol Dis* 36(2):233–41.

Fang, C., B. Wu, N. T. T. Le, T. Imberdis, R. C. C. Mercer, and D. A. Harris. 2018. "Prions Activate a P38 MAPK Synaptotoxic Signaling Pathway." *PLoS Pathog* 14(9):e1007283.

Fang, Cheng, Thibaut Imberdis, Maria Carmen Garza, Holger Wille, and David A. Harris. 2016. "A Neuronal Culture System to Detect Prion Synaptotoxicity" edited by J. Bartz. *PLoS Pathog* 12(5):e1005623.

Fiala, J. C., J. Spacek, and K. M. Harris. 2002. "Dendritic Spine Pathology: Cause or Consequence of Neurological Disorders?" *Brain Res Brain Res Rev* 39(1):29–54.

Fischer, Marek, T. Rülicke, Alex Raeber, A. Sailer, Markus Moser, B. Oesch, S. Brandner, A. Aguzzi, C. Weissmann, Thomas Rulicke1, Alex Raeber, Andreas Sailer2, Markus Moser, Bruno Oesch3, Sebastian Brandner4, Adriano Aguzzi4, Charles Weissmann5, T. Rülicke, Alex Raeber, A. Sailer, Markus Moser, B. Oesch, S. Brandner, A. Aguzzi, and C. Weissmann. 1996. "Prion Protein (PrP) with Amino-Proximal Deletions Restoring Susceptibility of PrP Knockout Mice to Scrapie." *Embo J* 15(6):1255–64.

Fluharty, Brian R., Emiliano Biasini, Matteo Stravalaci, Alessandra Sclip, Luisa Diomede, Claudia Balducci, Pietro La Vitola, Massimo Messa, Laura Colombo, Gianluigi Forloni, Tiziana Borsello, Marco Gobbi, and David A. Harris. 2013. "An N-Terminal Fragment of the Prion Protein Binds to Amyloid-β Oligomers and Inhibits Their Neurotoxicity in Vivo." *Journal of Biological Chemistry* 288(11):7857–66.

Gabriel, J. M., B. Oesch, H. Kretzschmar, M. Scott, and S. B. Prusiner. 1992. "Molecular Cloning of a Candidate Chicken Prion Protein." *Proceedings of the National Academy of Sciences* 89(19):9097–9101.

Gajdusek, D. C., C. J. Gibbs, and M. Alpers. 1966. "Experimental Transmission of a Kuru-like Syndrome to Chimpanzees." *Nature* 209:794–96.

Gasperini, Lisa, Elisa Meneghetti, Beatrice Pastore, Federico Benetti, and Giuseppe Legname. 2014. "Prion Protein and Copper Cooperatively Protect Neurons by Modulating NMDA Receptor Through S-Nitrosylation." *Antioxidants & Redox Signaling*.

Gasset, M., M. A. Baldwin, D. H. Lloyd, J. M. Gabriel, D. M. Holtzman, F. Cohen, R. Fletterick, and S. B. Prusiner. 1992. "Predicted Alpha-Helical Regions of the Prion Protein When Synthesized as Peptides Form Amyloid." *Proc Natl Acad Sci U S A* 89(22):10940–44.

Ghosh, R. N., W. G. Mallet, T. T. Soe, T. E. McGraw, and F. R. Maxfield. 1998. "An Endocytosed TGN38 Chimeric Protein Is Delivered to the TGN after Trafficking through the Endocytic Recycling Compartment in CHO Cells." *The Journal of Cell Biology* 142(4):923–36.

Gimbel, D. A., H. B. Nygaard, E. E. Coffey, E. C. Gunther, J. Lauren, Z. A. Gimbel, and S. M. Strittmatter. 2010. "Memory Impairment in Transgenic Alzheimer Mice Requires Cellular Prion Protein." *J Neurosci* 30(18):6367–74.

Goldfarb, L. G., R. B. Petersen, M. Tabaton, P. Brown, A. C. LeBlanc, P. Montagna, P. Cortelli, J. Julien, C. Vital, W. W. Pendelbury, and et al. 1992. "Fatal Familial Insomnia and Familial Creutzfeldt-Jakob Disease: Disease Phenotype Determined by a DNA Polymorphism." *Science* 258(5083):806–8.

Gonsberg, A., S. Jung, S. Ulbrich, A. Origi, A. Ziska, M. Baier, H. G. Koch, R. Zimmermann, K. F. Winklhofer, and J. Tatzelt. 2017. "The Sec61/SecY Complex Is Inherently Deficient in Translocating Intrinsically Disordered Proteins." *J Biol Chem*.

Gorodinsky, A. and D. A. Harris. 1995. "Glycolipid-Anchored Proteins in Neuroblastoma Cells Form Detergent- Resistant Complexes without Caveolin." *Journal of Cell Biology*.

Graner, E., A. F. Mercadante, S. M. Zanata, O. V Forlenza, A. L. Cabral, S. S. Veiga, M. A. Juliano, R. Roesler, R. Walz, A. Minetti, I. Izquierdo, V. R. Martins, and R. R. Brentani. 2000. "Cellular Prion Protein Binds Laminin and Mediates Neuritogenesis." *Brain Res Mol Brain Res* 76(1):85–92.

Griffiths, H. H., I. J. Whitehouse, H. Baybutt, D. Brown, K. A. Kellett, C. D. Jackson, A. J. Turner, P. Piccardo, J. C. Manson, and N. M. Hooper. 2011. "Prion Protein Interacts with BACE1 Protein and Differentially Regulates Its Activity toward Wild Type and Swedish Mutant Amyloid Precursor Protein." *J Biol Chem* 286(38):33489–500.

Guillot-Sestier, M. V, C. Sunyach, C. Druon, S. Scarzello, and F. Checler. 2009. "The Alpha-Secretase-Derived N-Terminal Product of Cellular Prion, N1, Displays Neuroprotective Function in Vitro and in Vivo." *J Biol Chem* 284(51):35973–86.

Guillot-Sestier, M. V, C. Sunyach, S. T. Ferreira, M. P. Marzolo, C. Bauer, A. Thevenet, and F. Checler. 2012. "Alpha-Secretase-Derived Fragment of Cellular Prion, N1, Protects against Monomeric and Oligomeric Amyloid Beta (Abeta)-Associated Cell Death." *J Biol Chem* 287(7):5021–32.

Guillot-Sestier, Marie Victoire, Claire Sunyach, Sergio T. Ferreira, Maria Paz Marzolo, Charlotte Bauer, Aurélie Thevenet, and Frédéric Checler. 2012. "α-Secretase-Derived Fragment of Cellular Prion, N1, Protects against Monomeric and Oligomeric Amyloid β(Aβ)-Associated Cell Death." *Journal of Biological Chemistry*.

Hachiya, N., Y. Komata, S. Harguem, K. Nishijima, and K. Kaneko. 2011. "Possible Involvement of Calpain-like Activity in Normal Processing of Cellular Prion Protein." *Neurosci Lett* 490(2):150–55.

Haddon, D. J., M. R. Hughes, F. Antignano, D. Westaway, N. R. Cashman, and K. M. McNagny. 2009. "Prion Protein Expression and Release by Mast Cells after Activation." *J Infect Dis* 200(5):827–31.

Haigh, C. L. and S. J. Collins. 2016. "Endoproteolytic Cleavage as a Molecular Switch Regulating and Diversifying Prion Protein Function." *Neural Regen Res* 11(2):238–39.

Haire, L. F., S. M. Whyte, N. Vasisht, A. C. Gill, C. Verma, E. J. Dodson, G. G. Dodson, and P. M. Bayley. 2004. "The Crystal Structure of the Globular Domain of Sheep Prion Protein." *J Mol Biol* 336(5):1175–83.

Halliday, Mark and Giovanna R. Mallucci. 2014. "Targeting the Unfolded Protein Response in Neurodegeneration: A New Approach to Therapy." *Neuropharmacology*.

Haraguchi, T., S. Fisher, S. Olofsson, T. Endo, D. Groth, A. Tarentino, D. R. Borchelt, D. Teplow, L. Hood, and A. Burlingame. 1989. "Asparagine-Linked Glycosylation of the Scrapie and Cellular Prion Proteins." *Archives of Biochemistry and Biophysics* 274(1):1–13.

Hartmann, Camila Arantes, Vilma Regina Martins, and Flavia Regina Souza Lima. 2013. "High Levels of Cellular Prion Protein Improve Astrocyte Development." *FEBS Letters*.

Hegde, R. S., P. Tremblay, D. Groth, S. J. DeArmond, S. B. Prusiner, and V. R. Lingappa. 1999. "Transmissible and Genetic Prion Diseases Share a Common Pathway of Neurodegeneration ." *Nature* 402(6763):822–26.

Herms, Jochen and Mario M. Dorostkar. 2016. "Dendritic Spine Pathology in Neurodegenerative Diseases." *Annual Review of Pathology: Mechanisms of Disease* 11(1):221–50.

Heske, Johanna, Ulrich Heller, Konstanze F. Winklhofer, J. Tatzelt, and Jö Rg Tatzelt. 2004. "The C-Terminal Globular Domain of the Prion Protein Is Necessary and Sufficient for Import into the Endoplasmic Reticulum." *J Biol Chem* 279(7):5435–43.

Hornshaw, M. P., J. R. McDermott, and J. M. Candy. 1995. "Copper Binding to the N-Terminal Tandem Repeat Regions of Mammalian and Avian Prion Protein." *Biochem Biophys Res Commun* 207(2):621–29.

Hornshaw, M. P., J. R. McDermott, J. M. Candy, and J. H. Lakey. 1995. "Copper Binding to the N-Terminal Tandem Repeat Region of Mammalian and Avian Prion Protein: Structural Studies Using Synthetic Peptides." *Biochem Biophys Res Commun* 214(3):993–99.

Hsiao, Karen, Harry F. Baker, Tim J. Crow, Mark Poulter, Frank Owen, Joseph D. Terwilliger, David Westaway, Jurg Ott, and Stanley B. Prusiner. 1989. "Linkage of a Prion Protein Missense Variant to Gerstmann-Sträussler Syndrome." *Nature*.

Imran, M. and S. Mahmood. 2011a. "An Overview of Animal Prion Diseases." *Virol J* 8:493.

Imran, M. and S. Mahmood. 2011b. "An Overview of Human Prion Diseases." *Virol J* 8:559.

Jeffrey, M., I. A. Goodbrand, and C. M. Goodsir. 1995. "Pathology of the Transmissible Spongiform Encephalopathies with Special Emphasis on Ultrastructure." *Micron* 26(3):277–98.

Jimenez-Huete, A., P. M. Lievens, R. Vidal, P. Piccardo, B. Ghetti, F. Tagliavini, B. Frangione, and F. Prelli. 1998. "Endogenous Proteolytic Cleavage of Normal and Disease-Associated Isoforms of the Human Prion Protein in Neural and Non-Neural Tissues." *Am J Pathol* 153(5):1561–72.

Jones, C. E., S. R. Abdelraheim, D. R. Brown, and J. H. Viles. 2004. "Preferential Cu2+ Coordination by His96 and His111 Induces Beta-Sheet Formation in the Unstructured Amyloidogenic Region of the Prion Protein." *J Biol Chem* 279(31):32018–27.

Kaech, Stefanie and Gary Banker. 2006. "Culturing Hippocampal Neurons." *Nature Protocols*.

Kim, Boe Hyun, Hyoung Gon Lee, Jin Kyu Choi, Jae Il Kim, Eun Kyoung Choi, Richard I. Carp, and Yong Sun Kim. 2004. "The Cellular Prion Protein (PrPC) Prevents Apoptotic Neuronal Cell Death and Mitochondrial Dysfunction Induced by Serum Deprivation." *Molecular Brain Research*.

Kim, J. H. and E. E. Manuelidis. 1986. "Serial Ultrastructural Study of Experimental Creutzfeldt-Jacob Disease in Guinea Pigs." *Acta Neuropathol Berl* 69(1–2):81–90.

Klein, T. and R. Bischoff. 2011. "Active Metalloproteases of the A Disintegrin and Metalloprotease (ADAM) Family: Biological Function and Structure." *J Proteome Res* 10(1):17–33.

Kojima, A., M. Konishi, and T. Akizawa. 2014. "Prion Fragment Peptides Are Digested with Membrane Type Matrix Metalloproteinases and Acquire Enzyme Resistance through Cu(2)(+)-Binding." *Biomolecules* 4(2):510–26.

Küffer, Alexander, Asvin K. K. Lakkaraju, Amit Mogha, Sarah C. Petersen, Kristina Airich, Cédric Doucerain, Rajlakshmi Marpakwar, Pamela Bakirci, Assunta Senatore, Arnaud Monnard, Carmen Schiavi, Mario Nuvolone, Bianka Grosshans, Simone Hornemann, Frederic Bassilana, Kelly R. Monk, Adriano Aguzzi, A. Kuffer, Asvin K. K. Lakkaraju, Amit Mogha, Sarah C. Petersen, Kristina Airich, Cédric Doucerain, Rajlakshmi Marpakwar, Pamela Bakirci, Assunta Senatore, Arnaud Monnard, Carmen Schiavi, Mario Nuvolone, Bianka Grosshans, Simone Hornemann, Frederic Bassilana, Kelly R. Monk, and Adriano Aguzzi. 2016. "The Prion Protein Is an Agonistic Ligand of the G Protein-Coupled Receptor Adgrg6." *Nature* 536(7617):464–68.

Kuwahara, C., A. M. Takeuchi, T. Nishimura, K. Haraguchi, A. Kubosaki, Y. Matsumoto, K. Saeki, Y. Matsumoto, T. Yokoyama, S. Itohara, and T. Onodera. 1999. "Prions Prevent Neuronal Cell-Line Death [4]." *Nature*.

Lainé, Jeanne, Marie Elizabeth Marc, Man Sun Sy, and Herbert Axelrad. 2001. "Cellular and Subcellular Morphological Localization of Normal Prion Protein in Rodent Cerebellum." *European Journal of Neuroscience*.

Lauren, J., David A. Gimbel, Haakon B. Nygaard, John W. Gilbert, Stephen M. Strittmatter, Juha Laurén, David A. Gimbel, Haakon B. Nygaard, John W. Gilbert, and Stephen M. Strittmatter. 2009. "Cellular Prion Protein Mediates Impairment of Synaptic Plasticity by Amyloid-Beta Oligomers." *Nature* 457(7233):1128–32.

Laurén, Juha, David A Gimbel, Haakon B. Nygaard, John W. Gilbert, and Stephen M. Strittmatter.

2009. "Cellular Prion Protein Mediates Impairment of Synaptic Plasticity by Amyloid-Beta Oligomers." *Nature* 457(7233):1128–32.

Laurén, Juha, David A. Gimbel, Haakon B. Nygaard, John W. Gilbert, and Stephen M. Strittmatter. 2009. "Cellular Prion Protein Mediates Impairment of Synaptic Plasticity by Amyloid-B Oligomers." *Nature*.

Legname, G., H. O. Nguyen, I. V Baskakov, F. E. Cohen, S. J. Dearmond, and S. B. Prusiner. 2005. "Strain-Specified Characteristics of Mouse Synthetic Prions." *Proc Natl Acad Sci U S A* 102(6):2168–73.

Legname, Giuseppe, Peter Nelken, Zhengyu Guan, Zoltan F. Kanyo, Stephen J. DeArmond, and Stanley B. Prusiner. 2002. "Prion and Doppel Proteins Bind to Granule Cells of the Cerebellum." *Proceedings of the National Academy of Sciences* 99(25):16285–90.

Lewis, V., A. F. Hill, C. L. Haigh, G. M. Klug, C. L. Masters, V. A. Lawson, and S. J. Collins. 2009. "Increased Proportions of C1 Truncated Prion Protein Protect against Cellular M1000 Prion Infection." *J Neuropathol Exp Neurol* 68(10):1125–35.

Lewis, V., V. A. Johanssen, P. J. Crouch, G. M. Klug, N. M. Hooper, and S. J. Collins. 2016. "Prion Protein 'Gamma-Cleavage': Characterizing a Novel Endoproteolytic Processing Event." *Cell Mol Life Sci* 73(3):667–83.

Li, A., S. J. Barmada, K. A. Roth, and D. A. Harris. 2007. "N-Terminally Deleted Forms of the Prion Protein Activate Both Bax-Dependent and Bax-Independent Neurotoxic Pathways." *J Neurosci* 27(4):852–59.

Liang, J, W. Wang, D. Sorensen, S. Medina, S. Ilchenko, J. Kiselar, W. K. Surewicz, S. A. Booth, and Q. Kong. 2012. "Cellular Prion Protein Regulates Its Own Alpha-Cleavage through ADAM8 in Skeletal Muscle." *J Biol Chem* 287(20):16510–20.

Liang, Jingjing, Wei Wang, Debra Sorensen, Sarah Medina, Sergei Ilchenko, Janna Kiselar, Witold K. Surewicz, Stephanie A. Booth, and Qingzhong Kong. 2012. "Cellular Prion Protein Regulates Its Ownα-Cleavage through ADAM8 in Skeletal Muscle." *Journal of Biological Chemistry*.

Lima, F. R., C. P. Arantes, A. G. Muras, R. Nomizo, R. R. Brentani, and V. R. Martins. 2007. "Cellular Prion Protein Expression in Astrocytes Modulates Neuronal Survival and Differentiation." *J Neurochem* 103(6):2164–76.

Linsenmeier, Luise, Behnam Mohammadi, Sebastian Wetzel, Berta Puig, Walker S. Jackson, Alexander Hartmann, Keiji Uchiyama, Suehiro Sakaguchi, Kristina Endres, Jörg Tatzelt, Paul Saftig, Markus Glatzel, and Hermann C. Altmeppen. 2018. "Structural and Mechanistic Aspects Influencing the ADAM10-Mediated Shedding of the Prion Protein." *Molecular Neurodegeneration*.

Llorens, Franc, Patricia Carulla, Ana Villa, Juan M. Torres, Puri Fortes, Isidre Ferrer, and José A. Del Río. 2013. "PrP C Regulates Epidermal Growth Factor Receptor Function and Cell Shape Dynamics in Neuro2a Cells." *Journal of Neurochemistry*.

Lopes, M. H., G. N. Hajj, A. G. Muras, G. L. Mancini, R. M. Castro, K. C. Ribeiro, R. R. Brentani, R. Linden, and V. R. Martins. 2005. "Interaction of Cellular Prion and Stress-Inducible Protein 1 Promotes Neuritogenesis and Neuroprotection by Distinct Signaling Pathways." *J Neurosci* 25(49):11330–39.

Loubet, Damien, Caroline Dakowski, Mathéa Pietri, Elodie Pradines, Sophie Bernard, Jacques Callebert, Hector Ardila-Osorio, Sophie Mouillet-Richard, Jean-Marie Launay, Odile Kellermann, and Benoit Schneider. 2012. "Neuritogenesis: The Prion Protein Controls B1 Integrin Signaling Activity." *The FASEB Journal*.

Ma, J. and S. Lindquist. 2001. "Wild-Type PrP and a Mutant Associated with Prion Disease Are Subject to Retrograde Transport and Proteasome Degradation." *Proceedings of the National Academy of Sciences*.

Ma, J., R. Wollmann, and S. Lindquist. 2002. "Neurotoxicity and Neurodegeneration When PrP Accumulates in the Cytosol." *Science* 298:1781–85.

Madore, N. 2002. "Functionally Different GPI Proteins Are Organized in Different Domains on the Neuronal Surface." *The EMBO Journal*.

Mallucci, G., A. Dickinson, J. Linehan, P. C. Klohn, S. Brandner, and J. Collinge. 2003. "Depleting

Neuronal PrP in Prion Infection Prevents Disease and Reverses Spongiosis." *Science* 302(5646):871–74.

Mange, A., F. Beranger, K. Peoc'h, T. Onodera, Y. Frobert, and S. Lehmann. 2004. "Alpha- and Beta- Cleavages of the Amino-Terminus of the Cellular Prion Protein." *Biol Cell* 96(2):125–32.

Manson, J. C., A. R. Clarke, M. L. Hooper, L. Aitchison, I. McConnell, and J. Hope. 1994. "129/Ola Mice Carrying a Null Mutation in PrP That Abolishes MRNA Production Are Developmentally Normal." *Molecular Neurobiology* 8(2–3):121–27.

Masel, J., N. Genoud, and A. Aguzzi. 2004. "Efficient Inhibition of Prion Replication by PrP-Fc2 Suggests That the Prion Is a PrP(Sc) Oligomer." *J Mol Biol* in press(5):1243–51.

Masters, C. L., D. C. Gajdusek, and C. J. Gibbs. 1981. "Creutzfeldt-Jakob Disease Virus Isolations from the Gerstmann-Straussler Syndrome with an Analysis of the Various Forms of Amyloid Plaque Deposition in the Virus-Induced Spongiform Encephalopathies." *Brain* 104:559–88.

McDonald, A. J., J. P. Dibble, E. G. Evans, and G. L. Millhauser. 2014. "A New Paradigm for Enzymatic Control of Alpha-Cleavage and Beta-Cleavage of the Prion Protein." *J Biol Chem* 289(2):803–13.

McDonald, Alex J. and Glenn L. Millhauser. 2014. "PrP Overdrive: Does Inhibition of α-Cleavage Contribute to PrP(C) Toxicity and Prion Disease?" *Prion* 8(2).

Meier, P., N. Genoud, M. Prinz, M. Maissen, T. Rulicke, A. Zurbriggen, A. J. Raeber, and A. Aguzzi. 2003. "Soluble Dimeric Prion Protein Binds PrP(Sc) in Vivo and Antagonizes Prion Disease." *Cell* 113(1):49–60.

Miesbauer, Margit, Natalie V. Pfeiffer, Angelika S. Rambold, Veronika Müller, Sophia Kiachopoulos, Konstanze F. Winklhofer, and Jörg Tatzelt. 2009. "α-Helical Domains Promote Translocation of Intinsically Disordered Polypeptides into the Endoplasmic Reticulum." *Journal of Biological Chemistry*.

Milhavet, O., H. E. McMahon, W. Rachidi, N. Nishida, S. Katamine, A. Mange, M. Arlotto, D. Casanova, J. Riondel, A. Favier, and S. Lehmann. 2000. "Prion Infection Impairs the Cellular

Response to Oxidative Stress." *Proc Natl Acad Sci U S A* 97(25):13937–42.

Millhauser, Glenn L. 2007. "Copper and the Prion Protein: Methods, Structures, Function, and Disease." *Annual Review of Physical Chemistry* 58(1):299–320.

Mironov Jr., A., D. Latawiec, H. Wille, E. Bouzamondo-Bernstein, G. Legname, R. A. Williamson, D. Burton, S. J. DeArmond, S. B. Prusiner, and P. J. Peters. 2003. "Cytosolic Prion Protein in Neurons." *J Neurosci* 23(18):7183–93.

Mohan, M. J., T. Seaton, J. Mitchell, A. Howe, K. Blackburn, W. Burkhart, M. Moyer, I. Patel, G. M. Waitt, J. D. Becherer, M. L. Moss, and M. E. Milla. 2002. "The Tumor Necrosis Factor-Alpha Converting Enzyme (TACE): A Unique Metalloproteinase with Highly Defined Substrate Selectivity." *Biochemistry* 41(30):9462–69.

Moore, Richard C., Inyoul Y. Lee, Gregory L. Silverman, Paul M. Harrison, Robert Strome, Cornelia Heinrich, Amila Karunaratne, Stephen H. Pasternak, M. Azha. A. Chishti, Yan Liang, Peter Mastrangelo, Kai Wang, Arian F. .. Smit, Shigeru Katamine, George A. Carlson, Fred E. Cohen, Stanley B. Prusiner, David W. Melton, Patrick Tremblay, Leroy E. Hood, and David Westaway. 1999. "Ataxia in Prion Protein (PrP)-Deficient Mice Is Associated with Upregulation of the Novel PrP-like Protein Doppel [In Process Citation]." *J Mol Biol* 292(4):797–817.

Moser, M., R. J. Colello, U. Pott, and B. Oesch. 1995. "Developmental Expression of the Prion Protein Gene in Glial Cells." *Neuron* 14(3):509–17.

Naslavsky, Naava, Ronit Stein, Anat Yanai, Gilgi Friedlander, and Albert Taraboulos. 1997. "Characterization of Detergent-Insoluble Complexes Containing the Cellular Prion Protein and Its Scrapie Isoform." *Journal of Biological Chemistry*.

Nieznanski, Krzysztof, Jin Kyu Choi, Shugui Chen, Krystyna Surewicz, and Witold K. Surewicz. 2012. "Soluble Prion Protein Inhibits Amyloid-?? (A??) Fibrillization and Toxicity." *Journal of Biological Chemistry* 287(40):33104–8.

Notari, S., S. Capellari, A. Giese, I. Westner, A. Baruzzi, B. Ghetti, P. Gambetti, H. A. Kretzschmar, and P. Parchi. 2004. "Effects of Different Experimental Conditions on the

PrPSc Core Generated by Protease Digestion: Implications for Strain Typing and Molecular Classification of CJD." *J Biol Chem* 279(16):16797–804.

O'Connor, TP, JS Duerr, and D. Bentley. 1990. "Pioneer Growth Cone Steering Decisions Mediated by Single Filopodial Contacts in Situ." *The Journal of Neuroscience*.

Oliveira-Martins, J B, S. Yusa, A. M. Calella, C. Bridel, F. Baumann, P. Dametto, and A. Aguzzi. 2010. "Unexpected Tolerance of Alpha-Cleavage of the Prion Protein to Sequence Variations." *PLoS ONE* 5(2):e9107.

Oliveira-Martins, José B., Sei Ichi Yusa, Anna Maria Calella, Claire Bridel, Frank Baumann, Paolo Dametto, and Adriano Aguzzi. 2010. "Unexpected Tolerance of α-Cleavage of the Prion Protein to Sequence Variations." *PLoS ONE* 5(2).

Orsi, Andrea, Luana Fioriti, Roberto Chiesa, and Roberto Sitia. 2006. "Conditions of Endoplasmic Reticulum Stress Favor the Accumulation of Cytosolic Prion Protein." *Journal of Biological Chemistry*.

Pan, K. M., M. Baldwin, J. Nguyen, M. Gasset, A. Serban, D. Groth, I. Mehlhorn, Z. Huang, R. J. Fletterick, F. E. Cohen, and et al. 1993. "Conversion of Alpha-Helices into Beta-Sheets Features in the Formation of the Scrapie Prion Proteins." *Proc.Natl.Acad.Sci.U.S.A.* 90(23):10962–66.

Parkin, E. T., N. T. Watt, I. Hussain, E. A. Eckman, C. B. Eckman, J. C. Manson, H. N. Baybutt, A. J. Turner, and N. M. Hooper. 2007. "Cellular Prion Protein Regulates Beta-Secretase Cleavage of the Alzheimer's Amyloid Precursor Protein." *Proc Natl Acad Sci U S A* 104(26):11062–67.

Perea, Gertrudis, Marta Navarrete, and Alfonso Araque. 2009. "Tripartite Synapses: Astrocytes Process and Control Synaptic Information." *Trends in Neurosciences*.

Prince M, Wimo A, Guerchet M, et al. 2015. *World Alzheimer Report 2015: The Global Impact of Dementia | Alzheimer's Disease International*.

Prusiner, S. B. 1998. "The Prion Diseases." *Brain Pathol* 8(3):499–513.

Prusiner, S. B. 2004. "Prion Biology and Diseases." *Prion Biology and Diseases.* (Ed.2).

Prusiner, Stanley B., Michael R. Scott, Stephen J. DeArmond, and Fred E. Cohen. 1998. "Prion Protein Biology." *Cell* 93(3):337–48.

Puig, Berta, Hermann C. Altmeppen, Sarah Ulbrich, Luise Linsenmeier, Susanne Krasemann, Karima Chakroun, Claudia Y. Acevedo-Morantes, Holger Wille, Jörg Tatzelt, and Markus Glatzel. 2016. "Secretory Pathway Retention of Mutant Prion Protein Induces P38-MAPK Activation and Lethal Disease in Mice." *Scientific Reports*.

Pushie, M. J. and H. J. Vogel. 2008. "Modeling by Assembly and Molecular Dynamics Simulations of the Low Cu2+ Occupancy Form of the Mammalian Prion Protein Octarepeat Region: Gaining Insight into Cu2+-Mediated Beta-Cleavage." *Biophys J* 95(11):5084–91.

Rachidi, W, D. Vilette, P. Guiraud, M. Arlotto, J. Riondel, H. Laude, S. Lehmann, and A. Favier. 2003. "Expression of Prion Protein Increases Cellular Copper Binding and Antioxidant Enzyme Activities but Not Copper Delivery." *J Biol Chem* 278(11):9064–72.

Rachidi, Walid, Didier Vilette, Pascale Guiraud, Marie Arlotto, Jacqueline Riondel, Hubert Laude, Sylvain Lehmann, and Alain Favier. 2003. "Expression of Prion Protein Increases Cellular Copper Binding and Antioxidant Enzyme Activities but Not Copper Delivery." *Journal of Biological Chemistry*.

Resenberger, U. K., A. Harmeier, A. C. Woerner, J. L. Goodman, V. Muller, R. Krishnan, R. M. Vabulas, H. A. Kretzschmar, S. Lindquist, F. U. Hartl, G. Multhaup, K. F. Winklhofer, and J. Tatzelt. 2011. "The Cellular Prion Protein Mediates Neurotoxic Signalling of Beta-Sheet-Rich Conformers Independent of Prion Replication." *Embo J* 30(10):2057–70.

Riek, R., S. Hornemann, G. Wider, M. Billeter, R. Glockshuber, and K. Wuthrich. 1996. "NMR Structure of the Mouse Prion Protein Domain PrP(121-321)." *Nature* 382(6587):180–82.

Safar, J., H. Wille, V. Itri, D. Groth, H. Serban, M. Torchia, F. E. Cohen, and S. B. Prusiner. 1998. "Eight Prion Strains Have PrP(Sc) Molecules with Different Conformations ." *Nat Med* 4(10):1157–65.

Santuccione, A., V. Sytnyk, I. Leshchyns'ka, and M. Schachner. 2005. "Prion Protein Recruits Its

Neuronal Receptor NCAM to Lipid Rafts to Activate P59fyn and to Enhance Neurite Outgrowth." *J Cell Biol* 169(2):341–54.

Saunders, Samuel E., Shannon L. Bartelt-Hunt, and Jason C. Bartz. 2008. "Prions in the Environment: Occurrence, Fate and Mitigation." *Prion* 2(4):162–69.

Schätzl, Hermann M., Maria Da Costa, Leslie Taylor, Fred E. Cohen, and Stanley B. Prusiner. 1995. "Prion Protein Gene Variation Among Primates." *Journal of Molecular Biology*.

Scheltens, Philip, Kaj Blennow, Monique M. B. Breteler, Bart de Strooper, Giovanni B. Frisoni, Stephen Salloway, and Wiesje M. aria Van der Flier. 2016. "Alzheimer's Disease (Seminar)." *Lancet (London, England)*.

Scott-McKean, Jonah J., Krystyna Surewicz, Jin Kyu Choi, Vernon A. Ruffin, Ahlam I. Salameh, Krzysztof Nieznanski, Alberto C. S. Costa, and Witold K. Surewicz. 2016. "Soluble Prion Protein and Its N-Terminal Fragment Prevent Impairment of Synaptic Plasticity by Aβ Oligomers: Implications for Novel Therapeutic Strategy in Alzheimer's Disease." *Neurobiology of Disease* 91:124–31.

Selkoe, Dennis J. and John Hardy. 2016. "The Amyloid Hypothesis of Alzheimer's Disease at 25 Years." *EMBO Molecular Medicine*.

Shmerling, D., I. Hegyi, M. Fischer, T. Blattler, S. Brandner, J. Gotz, T. Rulicke, E. Flechsig, A. Cozzio, C. von Mering, C. Hangartner, A. Aguzzi, and C. Weissmann. 1998. "Expression of Amino-Terminally Truncated PrP in the Mouse Leading to Ataxia and Specific Cerebellar Lesions." *Cell* 93(2):203–14.

Shyng, S. L., M. T. Huber, and D. A. Harris. 1993. "A Prion Protein Cycles between the Cell Surface and an Endocytic Compartment in Cultured Neuroblastoma Cells." *Journal of Biological Chemistry*.

Shyng, Show Ling, John E. Heuser, and David A. Harris. 1994. "A Glycolipid-Anchored Prion Protein Is Endocytosed via Clathrin-Coated Pits." *Journal of Cell Biology*.

Shyu, W. C., S. Z. Lin, M. F. Chiang, D. C. Ding, K. W. Li, S. F. Chen, H. I. Yang, and H. Li. 2005. "Overexpression of PrPC by Adenovirus-Mediated Gene Targeting Reduces Ischemic

Injury in a Stroke Rat Model." *J Neurosci* 25(39):8967–77.

Siskova, Z., R. A. Reynolds, V. O'Connor, and V. H. Perry. 2013. "Brain Region Specific Pre-Synaptic and Post-Synaptic Degeneration Are Early Components of Neuropathology in Prion Disease." *PLoS ONE* 8(1):e55004.

Small, Scott A. and Karen Duff. 2008. "Linking Aβ and Tau in Late-Onset Alzheimer's Disease: A Dual Pathway Hypothesis." *Neuron*.

Spudich, A., R. Frigg, E. Kilic, U. Kilic, B. Oesch, A. Raeber, C. L. Bassetti, and D. M. Hermann. 2005. "Aggravation of Ischemic Brain Injury by Prion Protein Deficiency: Role of ERK-1/-2 and STAT-1." *Neurobiol Dis* 20(2):442–49.

Stahl, Neil, David R. Borchelt, Karen Hsiao, and Stanley B. Prusiner. 1987. "Scrapie Prion Protein Contains a Phosphatidylinositol Glycolipid." *Cell*.

Steele, A. D., S. Lindquist, and A. Aguzzi. 2007. "The Prion Protein Knockout Mouse: A Phenotype under Challenge." *Prion* 1(2):83–93.

Stewart, Richard S. and David A. Harris. 2003. "Mutational Analysis of Topological Determinants in Prion Protein (PrP) and Measurement of Transmembrane and Cytosolic PrP during Prion Infection." *The Journal of Biological Chemistry* 278(46):45960–68.

Sunyach, C., M. A. Cisse, C. A. da Costa, B. Vincent, and F. Checler. 2007. "The C-Terminal Products of Cellular Prion Protein Processing, C1 and C2, Exert Distinct Influence on P53-Dependent Staurosporine-Induced Caspase-3 Activation." *J Biol Chem* 282(3):1956–63.

Sunyach, Claire, Angela Jen, Juelin Deng, Kathleen T. Fitzgerald, Yveline Frobert, Jacques Grassi, Mary W. McCaffrey, and Roger Morris. 2003. "The Mechanism of Internalization of Glycosylphosphatidylinositol-anchored Prion Protein." *The EMBO Journal* 22(14):3591–3601.

Taguchi, Y., Z. D. Shi, B. Ruddy, D. W. Dorward, L. Greene, and G. S. Baron. 2009. "Specific Biarsenical Labeling of Cell Surface Proteins Allows Fluorescent- and Biotin-Tagging of Amyloid Precursor Protein and Prion Proteins." *Mol Biol Cell* 20(1):233–44.

Takada, Leonel T., Mee-ohk Kim, Ross W. Cleveland, Katherine Wong, Sven A. Forner, Jamie C. Fong, and Michael D. Geschwind. 2016. "Genetic Prion Disease : Experience of a Rapidly Progressive Dementia Center in the United States and a Review of the Literature." 36–69.

Tanaka, M., P. Chien, N. Naber, R. Cooke, and J. S. Weissman. 2004. "Conformational Variations in an Infectious Protein Determine Prion Strain Differences." *Nature* 428(6980):323–28.

Taylor, D. M. 2000. "Inactivation of Transmissible Degenerative Encephalopathy Agents: A Review ." *Vet J* 159(1):10–17.

Taylor, D. R., E. T. Parkin, S. L. Cocklin, J. R. Ault, A. E. Ashcroft, A. J. Turner, and N. M. Hooper. 2009. "Role of ADAMs in the Ectodomain Shedding and Conformational Conversion of the Prion Protein." *J Biol Chem* 284(34):22590–600.

Thackray, A. M., M. A. Klein, and R. Bujdoso. 2003. "Subclinical Prion Disease Induced by Oral Inoculation." *Journal of Virology*.

Thomas, Gareth M. and Richard L. Huganir. 2004. "MAPK Cascade Signalling and Synaptic Plasticity." *Nature Reviews Neuroscience*.

TURK, Eric, David B. TEPLOW, Leroy E. HOOD, and Stanley B. PRUSINER. 1988. "Purification and Properties of the Cellular and Scrapie Hamster Prion Proteins." *European Journal of Biochemistry*.

Turnbaugh, J. A., U. Unterberger, P. Saa, T. Massignan, B. R. Fluharty, F. P. Bowman, M. B. Miller, S. Supattapone, E. Biasini, and D. A. Harris. 2012. "The N-Terminal, Polybasic Region of PrP(C) Dictates the Efficiency of Prion Propagation by Binding to PrP(Sc)." *J Neurosci* 32(26):8817–30.

Vey, M., S. Pilkuhn, H. Wille, R. Nixon, S. J. DeArmond, E. J. Smart, R. G. W. Anderson, A. Taraboulos, and S. B. Prusiner. 1996. "Subcellular Colocalization of the Cellular and Scrapie Prion Proteins in Caveolae-like Membranous Domains." *Proc Natl Acad Sci U S A* 93(25):14945–49.

Vincent, B., E. Paitel, Y. Frobert, S. Lehmann, J. Grassi, and F. Checler. 2000. "Phorbol Ester-Regulated Cleavage of Normal Prion Protein in HEK293 Human Cells and Murine Neurons."

J Biol Chem 275(45):35612-6.

Vincent, B., E. Paitel, P. Saftig, Y. Frobert, D. Hartmann, B. De Strooper, J. Grassi, E. Lopez-Perez, and F. Checler. 2001. "The Disintegrins ADAM10 and TACE Contribute to the Constitutive and Phorbol Ester-Regulated Normal Cleavage of the Cellular Prion Protein." *J Biol Chem* 276(41):37743–46.

Walmsley, A R, N. T. Watt, D. R. Taylor, W. S. Perera, and N. M. Hooper. 2009. "Alpha-Cleavage of the Prion Protein Occurs in a Late Compartment of the Secretory Pathway and Is Independent of Lipid Rafts." *Mol Cell Neurosci* 40(2):242–48.

Walmsley, Adrian R., Nicole T. Watt, David R. Taylor, W. Sumudhu S. Perera, and Nigel M. Hooper. 2009. "α-Cleavage of the Prion Protein Occurs in a Late Compartment of the Secretory Pathway and Is Independent of Lipid Rafts." *Molecular and Cellular Neuroscience*.

Watt, N. T., D. R. Taylor, A. Gillott, D. A. Thomas, W. S. Perera, and N. M. Hooper. 2005. "Reactive Oxygen Species-Mediated Beta-Cleavage of the Prion Protein in the Cellular Response to Oxidative Stress." *J Biol Chem* 280(43):35914–21.

Watt, Nicole T., Michael N. Routledge, Christopher P. Wild, and Nigel M. Hooper. 2007. "Cellular Prion Protein Protects against Reactive-Oxygen-Species-Induced DNA Damage." *Free Radical Biology and Medicine*.

Watts, J. C. and S. B. Prusiner. 2014. "Mouse Models for Studying the Formation and Propagation of Prions." *J Biol Chem* 289(29):19841–49.

Watts, Joel C. and David Westaway. 2007. "The Prion Protein Family: Diversity, Rivalry, and Dysfunction." *Biochimica et Biophysica Acta - Molecular Basis of Disease*.

Weise, Jens, Olaf Crome, Raoul Sandau, Walter Schulz-Schaeffer, Mathias Bähr, and Inga Zerr. 2004. "Upregulation of Cellular Prion Protein (PrP c) after Focal Cerebral Ischemia and Influence of Lesion Severity." *Neuroscience Letters*.

Weise, Jens, Raoul Sandau, Sönke Schwarting, Olaf Crome, Arne Wrede, Walter Schulz-Schaeffer, Inga Zerr, and Mathias Bähr. 2006. "Deletion of Cellular Prion Protein Results in Reduced Akt Activation, Enhanced Postischemic Caspase-3 Activation, and Exacerbation of

Ischemic Brain Injury." *Stroke*.

Westaway, D., C. Cooper, S. Turner, M. Da Costa, G. A. Carlson, and S. B. Prusiner. 1994. "Structure and Polymorphism of the Mouse Prion Protein Gene." *Proc Natl Acad Sci U S A* 91(14):6418–22.

Westaway, David, Patricia A. Goodman, Carol A. Mirenda, Michael P. McKinley, George A. Carlson, and Stanley B. Prusiner. 1987. "Distinct Prion Proteins in Short and Long Scrapie Incubation Period Mice." *Cell*.

Westergard, Laura, Jessie A. Turnbaugh, and David A. Harris. 2011. "A Naturally Occurring C-Terminal Fragment of the Prion Protein (PrP) Delays Disease and Acts as a Dominant-Negative Inhibitor of PrPSc Formation." *The Journal of Biological Chemistry* 286(51):44234–42.

Wik, L., M. Klingeborn, H. Willander, and T. Linne. 2012. "Separate Mechanisms Act Concurrently to Shed and Release the Prion Protein from the Cell." *Prion* 6(5):498–509.

Williams, W. M., E. R. Stadtman, and J. Moskovitz. 2004. "Ageing and Exposure to Oxidative Stress in Vivo Differentially Affect Cellular Levels of PrP in Mouse Cerebral Microvessels and Brain Parenchyma." *Neuropathol Appl Neurobiol* 30(2):161–68.

Wu, Guoying, Kenta Nakajima, Natsumi Takeyama, Masayoshi Yukawa, Yojiro Taniuchi, Akikazu Sakudo, and Takashi Onodera. 2008. "Species-Specific Anti-Apoptotic Activity of Cellular Prion Protein in a Mouse PrP-Deficient Neuronal Cell Line Transfected with Mouse, Hamster, and Bovine Prnp." *Neuroscience Letters* 446(1):11–15.

Yedidia, Y., L. Horonchik, S. Tzaban, A. Yanai, and A. Taraboulos. 2001. "Proteasomes and Ubiquitin Are Involved in the Turnover of the Wild-Type Prion Protein." *EMBO Journal*.

You, H., S. Tsutsui, S. Hameed, T. J. Kannanayakal, L. Chen, P. Xia, J. D. Engbers, S. A. Lipton, P. K. Stys, and G. W. Zamponi. 2012. "Abeta Neurotoxicity Depends on Interactions between Copper Ions, Prion Protein, and N-Methyl-D-Aspartate Receptors." *Proc Natl Acad Sci U S A* 109(5):1737–42.

Yusa, S., J. B. Oliveira-Martins, Y. Sugita-Konishi, and Y. Kikuchi. 2012. "Cellular Prion Protein:

From Physiology to Pathology." *Viruses* 4(11):3109–31.

Zahn, R., A. Liu, T. Luhrs, R. Riek, C. von Schroetter, F. Lopez Garcia, M. Billeter, L. Calzolai, G. Wider, and K. Wuthrich. 2000. "NMR Solution Structure of the Human Prion Protein." *Proc Natl Acad Sci U S A* 97(1):145–50.

Zanata, S. M., M. H. Lopes, A. F. Mercadante, G. N. Hajj, L. B. Chiarini, R. Nomizo, A. R. Freitas, A. L. Cabral, K. S. Lee, M. A. Juliano, E. De Oliveira, S. G. Jachieri, A. Burlingame, L. Huang, R. Linden, R. R. Brentani, and V. R. Martins. 2002. "Stress-Inducible Protein 1 Is a Cell Surface Ligand for Cellular Prion That Triggers Neuroprotection." *Embo J* 21(13):3307–16.

Zeng, F., N. T. Watt, A. R. Walmsley, and N. M. Hooper. 2003. "Tethering the N-Terminus of the Prion Protein Compromises the Cellular Response to Oxidative Stress." *J Neurochem* 84(3):480–90.

Zhao, H., M. Klingeborn, M. Simonsson, and T. Linne. 2006. "Proteolytic Cleavage and Shedding of the Bovine Prion Protein in Two Cell Culture Systems." *Virus Res* 115(1):43–55.

Ziska, Anke, Jörg Tatzelt, Johanna Dudek, Adrienne W. Paton, James C. Paton, Richard Zimmermann, and Sarah Haßdenteufel. 2019. "The Signal Peptide plus a Cluster of Positive Charges in Prion Protein Dictate Chaperone-Mediated Sec61 Channel Gating." *Biology Open*.

7 Abbreviations:

aa	Amino acid
AD	Alzheimer's disease
ADAM	A disintegrin and metalloproteinase
APP	Amyloid precursor protein
Aβ	Amyloid β
BBB	Blood–brain barrier
BSE	Bovine spongiform encephalitis
cDNA	Complementary DNA
CDP	Chronic demyelinating polyneuropathy
CJD	Creutzfeldt-Jakob disease
Co-IP	Co-Immunoprecipitation
C-terminus	Carboxy terminus
DM	Dissecting Medum
DNA	Deoxyribonucleic acid
dpi	days post inoculation
EDTA	Ethylene diamine tetra-acetic acid
eIF2α	Eukaryotic initiation factor 2
ER	Endoplasmic reticulum
Erk1/2	Extracellular-signal-regulated kinases

FBS	Fetal bovine serum
FFI	Fatal familial insomnia
Fyn	Tyrosine-protein kinase
GGM	Glial Growth Medium
GPI	Glycophosphatidylinositol
GPR126	G-protein coupled receptor 126
GSS	Gerstmann-Sträussler-Scheinker syndrome
HE	Hematoxylin and eosin
HGC	Half-Genomic Construct
HPrDs	Human prion diseases
IDDs	intrinsically disordered domains
IP	Immunoprecipitation
MAP kinase	Mitogen-activated protein kinase
mGluRs	Metabotropic glutamate receptors
mRNA	Messenger RNA
N1	N-terminal part of prion protein amino acid 23-110
N1-Fc	N1 fused to the Fc region of an IgG
N1-Nb	N1 fused to a nanobody
N2a	Neuroblastoma cells
NaDOC	Sdium deoxycholate
Nb	Nanobody

NCAM	Neural cell adhesion molecule
NMM	Neuronal Maintenance Medium
PBS	Phosphate buffered saline
PI	Protease inhibitors
PK	Proteinase K
PrDs	Prion diseases
PrP	Prion protein
PrP^c	Cellular form of Prion protein
PrP^{Sc}	Scrapie prion protein
RML	Rocky Mountains laboratories prions
RT	Room tempreture
RT-qPCR	Real-time quantitative polymerase chain reaction
SP	Signal peptide
TBS	Tris-buffered saline
TCA	Trichloroacetic acid precipitation
TSE	Transmissible spongiform encephalopathies
WB	Western blot
WT	wild-type
β-ME	β-mercapto-ethanol

ACKNOWLEDGEMENTS